U.S. DEPARTMENT OF THE INTERIOR
BUREAU OF LAND MANAGEMENT
WINNEMUCCA DISTRICT OFFICE

March 2022

Night Sky Baseline Report for the Gerlach Geothermal Exploration Project

TABLE OF CONTENTS

Chapter Page

TABLES

Page

FIGURES

Page

APPENDIXES

Page

ACRONYMS AND ABBREVIATIONS

Acronym	Full Phrase
ALAN	artificial light at night
AOI	area of interest
Mag arcsec^2	luminosity of a celestial object relative to its distance
Black Rock NCA	Black Rock Desert-High Rock Canyon National Conservation Area
BLM	Bureau of Land Management
EA	environmental assessment
EMPSi	Environmental Management and Planning Solutions Inc.
KOP	key observation point
IBA	important bird area
LED	light-emitting diode
nWcm^{-2}sr^{-1}	nano-watts per square centimeter per steradian
Ormat	Ormat Nevada Inc.
VIIRS	Visible Infrared Imaging Radiometer Suite instrument
WDO	Winnemucca District Office
WRC	Western Research Company Inc.
WSA	wilderness study area
ZARI	zenith angle radiance index

This page intentionally left blank.

Section 1. Introduction

ORNI 26 LLC, a subsidiary of Ormat Nevada Inc. (Ormat), is proposing to construct, operate, and maintain the Gerlach Geothermal Exploration Project in Washoe County, Nevada. The proposed geothermal exploration area of interest (AOI) is located less than 1 mile northwest of Gerlach. The geothermal exploration operations plan submitted to the Bureau of Land Management (BLM) Winnemucca District Office (WDO) proposes 20 geothermal exploration wells.[1] The BLM is preparing an environmental assessment (EA) to evaluate the environmental effects of the proposed geothermal exploration project. The BLM intends for this night skies baseline report to achieve the following:

- Document the baseline night sky conditions in the study area
- Evaluate the contributions of the night sky to wildlife, wilderness characteristics, and regional socioeconomic conditions
- Consider the potential influence of the proposed geothermal exploration activity on baseline night sky conditions
- Compare the artificial light at night (ALAN) from the proposed geothermal exploration project to other regional sources of ALAN
- Consider best management practices that could be incorporated into the proposed project design or operations that would reduce the potential environmental impacts of the ALAN

This baseline report will accompany and inform the EA. The BLM does not have any policies related to managing the night sky resource. This report will enable the BLM to determine the nature and extent of any changes to existing night sky conditions in and near the study area (see **Section 1.2** for study area details). In conjunction with the EA, this report will assist the BLM decision-maker in determining whether there is a need for any environmental protection measures to avoid, minimize, or mitigate adverse impacts from the proposed project on night skies and the associated resources that benefit from night skies.

1.1 INITIAL PUBLIC OUTREACH

In November–December 2020, the BLM WDO held a 60-day pre-scoping public comment period to get public input on the proposed project. Materials released to the public in 2020 indicated the proposed project would entail geothermal development and include a geothermal power plant, aboveground pipelines, and a transmission line. Many concerns expressed by the public were related to geothermal development. Public concerns include the potential for a short- and long-term reduction in the quality of the night sky conditions in Gerlach and the surrounding areas. Commenters stated that the area's night sky is world-renowned and contributes to the regional economy and environmental quality.

[1] The draft exploration operations plan proposed 21 geothermal exploration wells; the final plan proposes 20 wells. Simulations and models were based on the number and location of geothermal exploration wells proposed in the draft exploration operations plan. Anticipated artificial light conditions are expected to be essentially identical under both scenarios.

Following the pre-scoping period, ORNI 26 LLC withdrew its plan of development and submitted a plan of operations for geothermal exploration. The proposed geothermal exploration does not include a power plant, transmission line, or geothermal pipelines.

1.2 Study Area Overview

The study area includes the proposed project AOI, the communities of Empire and Gerlach, and the portion of the WDO that extends northward along the Granite Range from Gerlach to the Massacre Rim Wilderness Study Area (WSA) and east to the Jackson Mountains. The study area is largely encompassed by the Black Rock Desert-High Rock Canyon Emigrant Trails National Conservation Area (Black Rock NCA), which includes the Black Rock Desert (see **Figure 1**). The study area is in the northern Basin and Range physiographic province, which is characterized by elongated, generally north-to-south-trending mountain ranges separated by broad open basins. Existing sources of ALAN include highways, the communities of Empire and Gerlach, Hycroft Mine, and the Burning Man event that takes place annually in the Black Rock Desert from late-August to early September.

1.3 Night Skies and Artificial Light at Night

The night sky refers to the darkness of space and the visibility of stars, planets, and other objects in space. Night skies contribute to amateur and professional astronomy, human and wildlife health, outdoor recreation experiences, and socioeconomic conditions. Increasingly, the night sky is considered a natural resource because it is integral to many natural processes (NPS 2021). The night sky is also a cultural resource because of the connections that people and cultures have made to the night sky. The stars, moon, and constellations contribute directly to the Indigenous traditions and knowledge systems for many cultures worldwide (Hamacher et al. 2020). Historically, the night sky has shaped cultural beliefs and civilizations, while providing inspiration for art and a source of interest for scientists and casual observers (NPS 2021).

ALAN is any light source that is produced by electricity or other means for human activity. Wildfires, moonlight, and lightning are not considered artificial. ALAN is necessary to conduct many activities safely and efficiently at night. Sources of ALAN are a consequence of modern civilization and can be found as a component of nearly all types of building exteriors, transportation systems, street lighting, industrial activity, construction, and recreational activities. Limiting human activities to daytime hours would result in a significant loss of productivity (Narisada and Schreuder 2004).

Over-illumination and light trespass, which contribute to light pollution and the loss of night skies, are an issue of growing concern. Studies estimate that ALAN has increased as much as 6 percent worldwide since the 1950s; light pollution now affects 23 percent of the global land surface (Challeat et al. 2021). Between 2012 and 2016, the brightness of continuously illuminated areas increased by 2.2 percent per year (Kyba et al. 2017). Light pollution from ALAN can diminish the night sky resource and disrupt amateur and professional astronomy, lead to human health impacts, disturb wildlife, and affect the characteristics of places being managed for specific natural and cultural resource values.

Sky glow from ALAN is the primary cause of diminishing night skies. Sky glow is light projected upward, which then reflects back to the earth as scattered light. Where aerosol concentrations are higher, such as over cities, horizontally and vertically refracting ALAN creates a noticeable glow. Studies suggest that sky glow from cities may impact night sky observers as far away as 65 miles from the source. Falchi et al. (2016) found that sky glow is regularly visible to over 80 percent of the world's population.

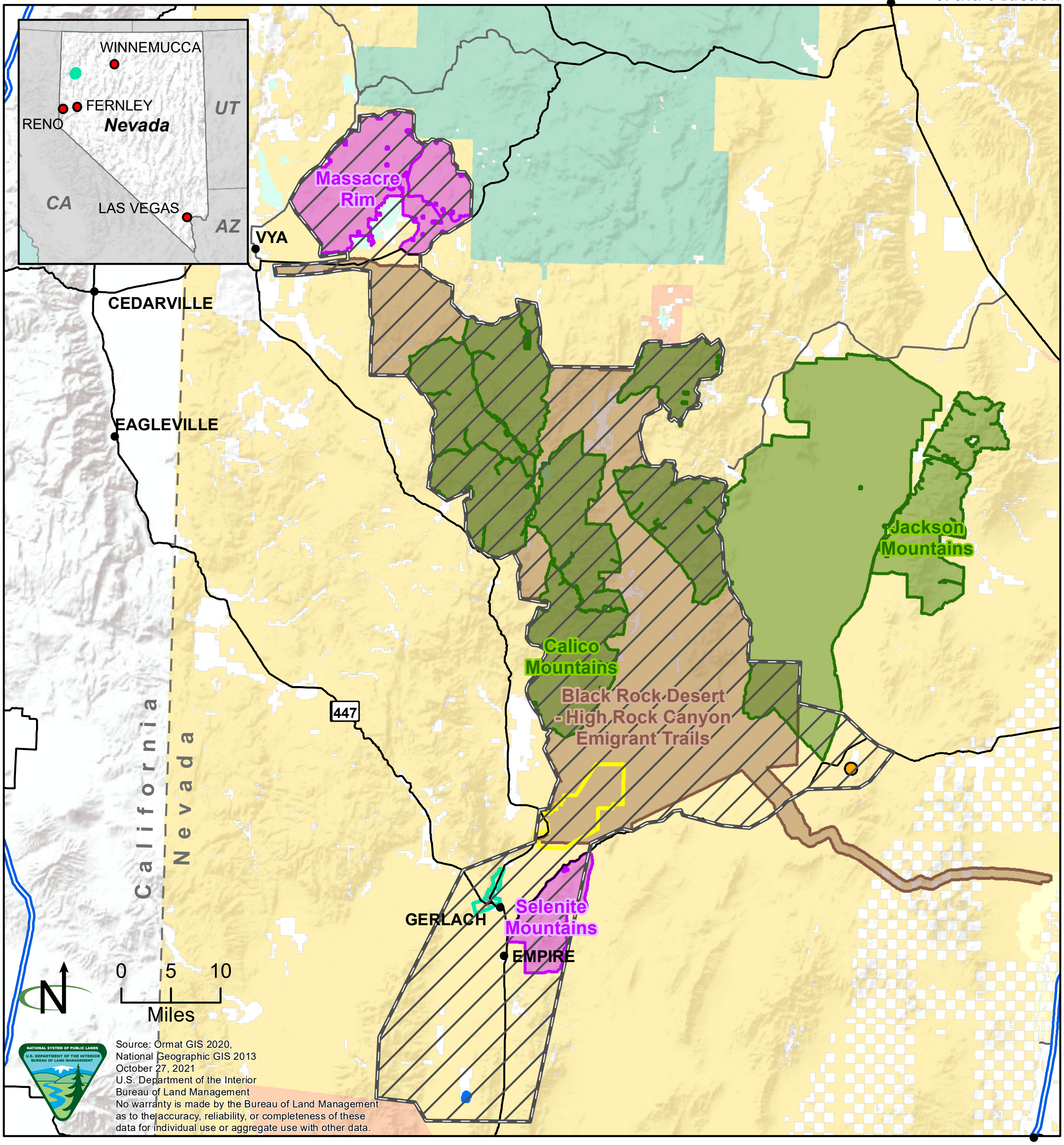

Night Skies Study Area

- Night Skies study area
- Hycroft Mine
- San Emidio geothermal power plant
- Gerlach geothermal AOI
- Burning Man special recreation permit area
- Wilderness area
- National conservation area
- Wilderness study area

Surface Management Agency

- Bureau of Indian Affairs
- Bureau of Land Management
- Bureau of Reclamation
- Private
- Fish and Wildlife Service
- Water

- Highway
- Major road
- Local road

Planning for night skies is evolving and becoming more widely incorporated in planning documents and regulations. Flagstaff, Arizona, pioneered night sky land use planning when it adopted ordinances in the 1960s regulating ALAN. More recently, other jurisdictions have followed suit by implementing ordinances and planning policies to control light pollution. Key strategies used to avoid ALAN impacts are to install low illumination lighting, use shielding to prevent light trespass, and specify the types of lighting allowed.

Section 2. Existing Conditions

2.1 Baseline Night Sky Conditions

The broader region that includes the northwest corner of Nevada is one of the least populated areas in the United States. It has few ALAN sources and is known for its night sky. **Figure 2** depicts the absence of ALAN in northwestern Nevada as observed in 2020 from the Day/Night Band of the Visible Infrared Imaging Radiometer Suite instrument (VIIRS) on two satellites.

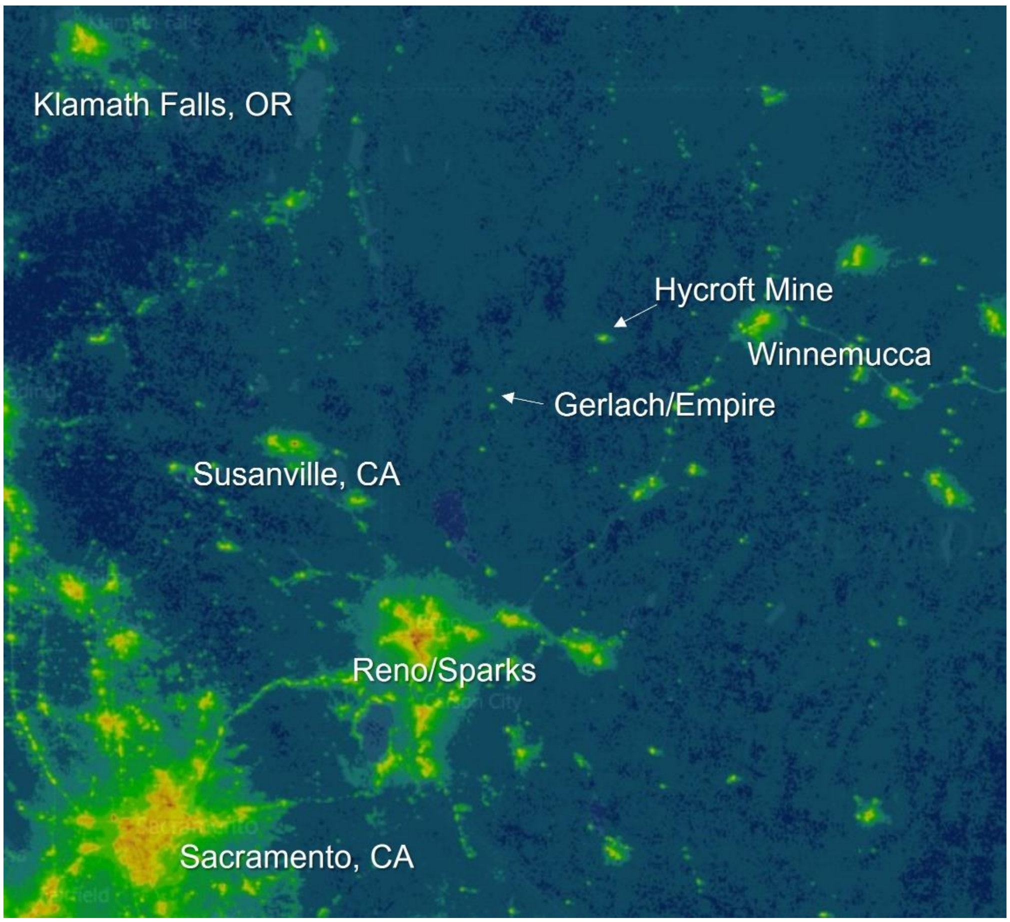

Figure 2. Radiance Map of Northern Nevada

Source: Earth Observation Group 2022

The proposed geothermal exploration project is approximately 75 miles north of the Reno-Sparks metropolitan area, which is the nearest major light source. Winnemucca, the only other significant source of year-round ALAN, is approximately 85 miles east of the AOI. Other notable sources of year-round ALAN in the study area are the community of Gerlach and the Hycroft Mine. The Burning Man event, which occurs on the Black Rock Desert playa in late-August and early September, is a major contributor of ALAN while the event is active. These notable sources of ALAN are discussed below and in **Appendix A**.

Figure 3, below, depicts the existing light sources in and near the study area as measured in average radiance (WRC 2021). Radiance is measured in energetic units of nano-watts per square centimeter per steradian[2] ($nWcm^{-2}sr^{-1}$). As shown in **Figure 3**, large portions of the study area have radiance values near zero. The Massacre Rim WSA in the northwestern corner of the study area is an International Dark Sky Sanctuary with effectively no ALAN.

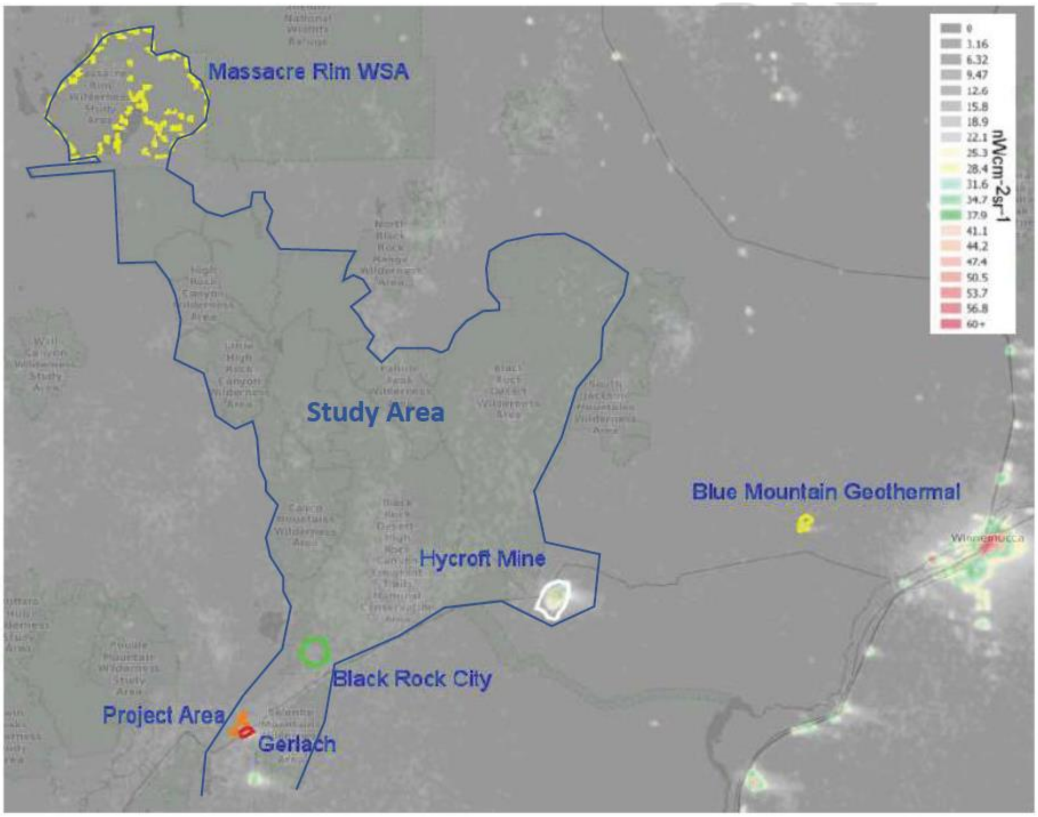

Figure 3. Radiance of Existing Light Sources in and near the Study Area

Section 4 of the technical report in **Appendix A** documents baseline night sky conditions in the study area. In the report, Western Research Company Inc. (WRC) assessed the baseline radiance levels in the study area during moonless, clear nights. The report relies on measurements and data collected using archived satellite data. The report also describes levels and the change in radiance for light sources in the study area.

In addition to the satellite analysis in **Appendix A**, staff from Environmental Management and Planning Solutions Inc. (EMPSi) and Wood Rodgers collected daytime and nighttime photographs from seven key observation points (KOPs) that were selected by the BLM (see **Figure 4**). The nighttime photographs document baseline ALAN and night sky conditions during new moon and bright moon settings. The photographic inventory of baseline night sky and ALAN conditions is **Appendix B**.

[2] A solid angle at the center of a sphere extending from a section on the surface of the sphere equal in area to the square of the radius of the sphere

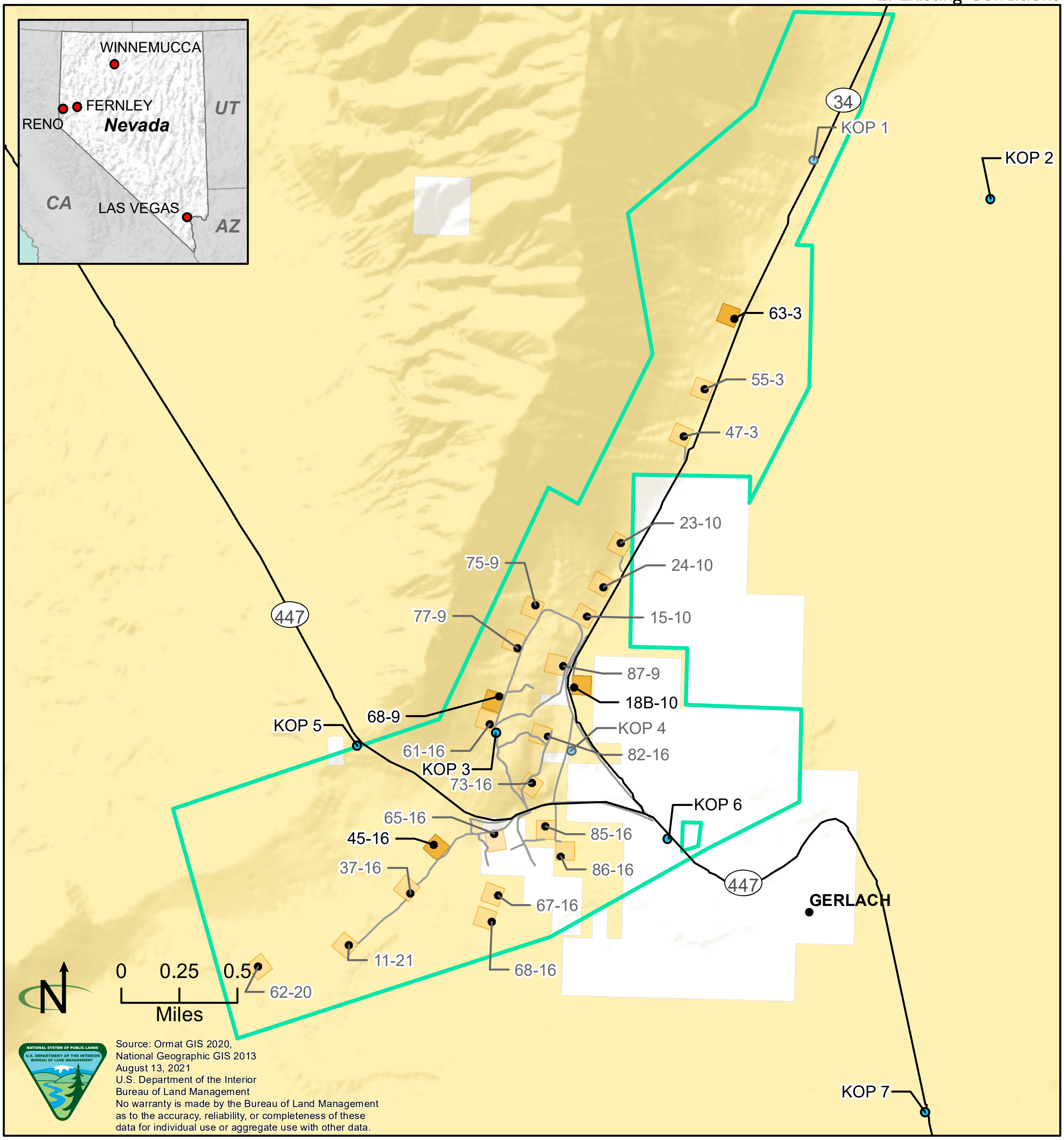

Night Skies KOPs

- KOP used in Night Skies simulations
- KOP
- Proposed well
- Proposed well pad used in Night Skies simulations
- Proposed well pad
- Gerlach geothermal AOI
- Existing road

Surface Management Agency

- Bureau of Land Management
- Private

2.1.1 Sky Brightness

Sky brightness, typically expressed in the form of luminosity of a celestial object (magnitude [mag]) relative to its distance (arcsec^2), is a commonly used method to quantify the relative darkness of the night sky. The higher the mag arcsec^2, the darker the sky and more readily visible the celestial objects are in the sky. As a reference point, during the new moon and with an air quality index near zero, the Massacre Rim WSA has a darkness value of 22.0 mag arcsec^2, which is near complete darkness (see Section 4.5 in **Appendix A**). In this area, the lack of ALAN and sky glow makes it possible to view distinct features of the Milky Way and other celestial objects that are otherwise occluded by sky glow and localized ALAN. The sky must be approximately 20.2 mag arcsec^2 or darker for the Milky Way to be seen (Williams 2015). Typical sky brightness for the central portion of a large city can be 15 mag arcsec^2, which allows viewers to see only the brightest objects in the night sky.

Sky brightness throughout the rest of the study area is slightly lower than it is in the Massacre Rim WSA. During a new moon and outside of the Burning Man event, the sky brightness at Gerlach is 21.69 mag arcsec^2. During the Burning Man event, it is 21.36 (see Section 4.5 in **Appendix A**). These values for Gerlach are representative of the sky brightness in the AOI.

2.1.2 Factors Influencing Night Sky Viewing

Ideal night sky viewing conditions are during the new moon phase when there are no clouds, wind, or other obstructions on the surface or in the atmosphere. The moon cycle greatly influences night sky viewing opportunities. The moon is typically at 50 percent or more illumination for 16 to 17 days each cycle. During the few days of the waxing and waning gibbous closest to the full moon, sky brightness can diminish markedly compared with a new moon night. The two sets of photos in **Appendix B**, taken at each of the seven KOPs on a bright moon night and a new moon night, respectively, demonstrate the difference in sky brightness between the two phases.

Weather is also a contributing factor. Clouds are the most notable visual obstruction for night sky viewing. Northwestern Nevada has on average approximately 230 days of partly cloudy or clear skies per year (NOAA 2021a). Windblown dust can also obstruct night skies. Especially in the summer months when soil moisture is low, winds often increase airborne particulate matter. Dust storms are common on the Black Rock Desert playa.

Wildfire smoke can also obstruct night skies, particularly during the summer and fall months. In 2021, wildfire smoke from the Dixie Fire and other wildfires in Northern California produced continuous heavy smoke throughout the study area. The smoke map in **Figure 5** depicts the smoke transport over the study area from the Dixie Fire to the east. From late-July through early October, the air quality index in Gerlach frequently exceeded 300 parts per million for particulate matter less than 2.5 microns in diameter ($PM_{2.5}$). On August 6, 2021, the consulting team visited the KOPs in an attempt to gather new moon photographs. **Figure 6** from KOP 1 depicts the visual obstruction created by the wildfire smoke. In the image, the object in the sky is the sun.

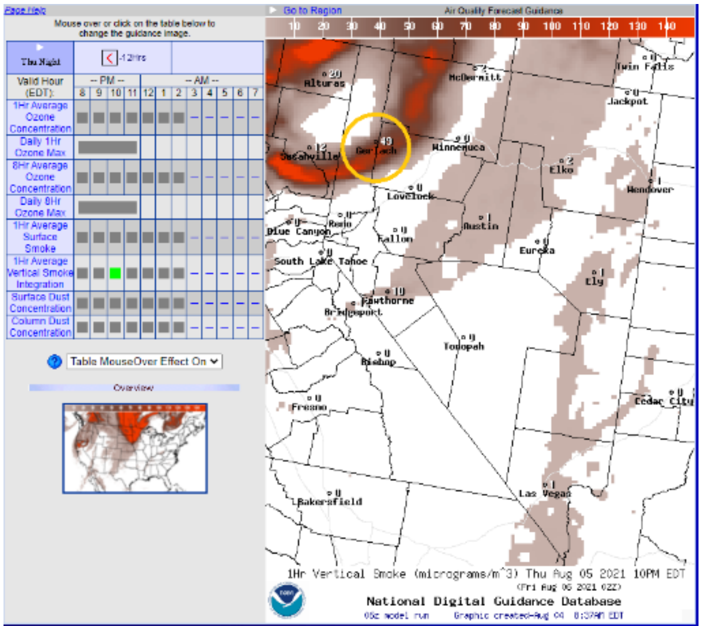

Figure 5. Smoke Transport from Wildfires (NOAA 2021b)

Figure 6. Smoke as Seen from KOP 1

2.1.3 Existing Sources of ALAN in the Study Area

In **Appendix A**, WRC uses a customized version of NASA's Skyglow Estimation Toolbox software to measure and describe relative sky brightness. The software generates images showing nighttime luminance (radiance). The zenith angle radiance index (ZARI) is another way to describe observed radiance using satellite imagery. A ZARI score is an effective means to quantify a particular location's level of nighttime luminance. For example, a community such as Sedona, Arizona, that has extensive night sky regulations and is an International Dark Sky Community, has a ZARI score of 51. Additional details on the ZARI are in **Appendix A**.

Gerlach and Empire

The AOI is less than 1 mile from the community of Gerlach and approximately 5 miles north of the community of Empire. Gerlach and Empire have a combined year-round population of approximately 200 residents, which contributes to relatively low ALAN outputs. WRC measured the sum radiance of Gerlach and Empire. The sum radiance for Gerlach was 14 $nWcm^{-2}sr^{-1}$; the sum radiance for Empire was 74 $nWcm^{-2}sr^{-1}$. WRC calculated the ZARI score for Gerlach and Empire. Gerlach's ZARI score was 36.4, and Empire's ZARI score was 74.7 (see Table 4.2 in **Appendix A**). Both communities experienced increasing radiance between 2018 and 2021 (see Figures 4.4 and 4.5 in **Appendix A**); the reason for the increase in Gerlach is not known. In Empire, the increase is likely explained by the increasing population and activity associated with reopening the gypsum mine under new ownership (Wiley 2021).

Hycroft Mine

The Hycroft Mine, located approximately 20 miles northeast of the AOI and 55 miles west of Winnemucca, is a gold and silver mine with an approved disturbance footprint of up to approximately 28,000 acres (BLM 2019). Operations include ore extraction, processing, dewatering, and backfilling. Observed radiance in March 2021 from the mine was 616 $nWcm^{-2}sr^{-1}$; the associated ZARI score was 50.5 (see Table 4.2 in **Appendix A**). Observations also depict an increase in radiance levels of approximately 1.7 percent since 2018, which is likely associated with the mine expansion that the BLM authorized in 2019 (see Figure 4.9 in **Appendix A**).

San Emidio Geothermal Power Plant

The San Emidio geothermal plant is located in the San Emidio Desert approximately 20 miles southwest of the AOI. The San Emidio geothermal power plant has been in operation since 1988. The BLM recently authorized two new geothermal power plants adjacent to the existing facility (BLM 2021). Observed radiance in March 2021 from the geothermal power plant was 27 $nWcm^{-2}sr^{-1}$; the associated ZARI score was 46.5 (see Table 4.2 in **Appendix A**). Observations depict a decrease in radiance levels of approximately 2 percent since 2018 (see Figure 4.7 in **Appendix A**). The reason for this decrease is that in 2018, Ormat replaced conventional lighting with motion-sensor lighting at four production well sites.[3]

WRC also analyzed radiance levels for the Blue Mountain and Don A. Campbell geothermal facilities, which are slightly beyond the study area. Observed radiance values and trends, and ZARI scores for these facilities resemble those of the San Emidio power plant (see Table 4.2 and Figure 4.8 in **Appendix A**).

Burning Man Event

The BLM issues a special recreation permit for the Burning Man event, which occurs annually in the Black Rock Desert from late-August to early September. In 2019, the BLM issued a record of decision to allow up to 80,000 people within a 14,320-acre closure area for the event. The duration of the permitted event is 74 days; however, the peak event population occurs during the 2 weeks before Labor Day (BLM 2019). The event is known for eclectic art, including extensive nighttime light displays.

As part of the BLM's 2019 environmental impact statement for the Burning Man event, WRC prepared a night sky report (WRC 2018) documenting ALAN at the 2018 Burning Man event and projected ALAN changes for various event population alternatives. The Burning Man event did not take place in 2020 or 2021 due to the COVID-19 pandemic. Outside of the permitted event period, or during nonevent scenarios, radiance and ZARI scores for the closure area are near zero.

As part of the technical report prepared for the proposed geothermal exploration project (see **Appendix A**), WRC conducted another assessment of ALAN from the Burning Man event using satellite data. The study concluded the radiance of the 2018 event was 7,568 $nWcm^{-2}sr^{-1}$ and the ZARI score was 127.5 (see Table 4.2 in **Appendix A**).

2.2 ASTROTOURISM

Astrotourism is the practice of traveling to a destination that has very low light pollution for the purpose of seeing the stars and visiting observatories (Altschuler 2019). There are several cities and national parks that have organized events and festivals around stargazing in order to increase astrotourism. For example, Lassen Volcanic National Park, which is in California approximately 4 hours west of Gerlach, hosts ranger-led astronomy programs and annual dark sky festivals (NPS 2021).

---

[3] Kim Carter, Ormat, email to Morgan Trieger, EMPSi, on February 8, 2022, subject regarding Gerlach Geothermal Exploration Project — night sky baseline report question.

Many locations in Nevada advertise dark skies to promote astrotourism. For example, Gerlach is known as America's darkest town (Roeder 2017). The Massacre Rim WSA, approximately 60 miles north of Gerlach, is one of 15 locations worldwide to be certified as an International Dark Sky Sanctuary. The International Dark-Sky Association issues this certification to remote, dark sky locations (International Dark-Sky Association 2021). While there are no data available to quantify the number of people who visit the study area specifically to engage in astrotourism, according to the Nevada Division of Tourism, the percentage of visitors who traveled to northern Nevada for the primary purpose of outdoor recreation grew from 3.8 percent in 2015 to 8.0 percent in 2019 (Travel Trak America 2019). This growth in outdoor recreation demand highlights the importance of astrotourism and other nature-related tourism for local economies in northern Nevada.

2.3 DESIGNATED AREAS

The proposed AOI is located approximately 4 miles south of the Black Rock NCA's southern boundary (see **Figure 1**). Congress established the Black Rock NCA and 10 associated wilderness areas (totaling 1,172,680 acres) to conserve, protect, and enhance resources associated with the historic Oregon and California emigrant trails and surrounding areas. The designation recognized the area's nationally significant historic trails; an absence of development; unique Great Basin biota; and significant cultural, archaeological, paleontological, and geographical resources. The act identified wilderness and recreation as values and resources to be conserved, protected, and enhanced.

Grazing and large-scale, permitted events are resource values that are expected to continue, in accordance with the 2004 Resource Management Plan for the Black Rock NCA (BLM 2004). The 65,000-acre Calico Mountains Wilderness is the nearest wilderness area to the AOI. It is located approximately 20 miles north of Gerlach.

A portion of the Selenite Mountains WSA is located immediately east of Gerlach. This WSA is in the northern portion of the Selenite Range, where the Selenite Mountains rise from 4,200 feet in the north end near the Black Rock Desert to 7,100 feet at Selenite Peak. It is bound by Highway 447 on the west, Jungo Road on the north, and ranching routes on the east and south (Nevada Wilderness 2021).

The Massacre Rim WSA is located in the BLM Applegate Field Office's administrative boundary. Located approximately 100 miles north of the AOI, the WSA consists of two volcanic plateaus surrounded by large, open valleys. The area's lack of physical obstructions and the absence of ALAN sources within 100 miles are the primary reasons the WSA is an internationally recognized stargazing destination.

Changes in night sky conditions, including increases in radiance observable from designated areas, can diminish sky brightness. Because of the remoteness of the designated areas in the study area, any new sources of ALAN or changes in sky brightness would have the potential to affect night sky viewing opportunities. These changes would also influence the natural quality of wilderness character in designated wilderness areas or wilderness characteristics in WSAs.

2.4 WILDLIFE

ALAN may affect many types of wildlife, particularly nocturnal birds, bats, other mammals, amphibians, and insects. Representative nocturnal wildlife that inhabits the AOI is below in **Table 1**. Nocturnal insects include beetles (order Coleoptera), moths (order Lepidoptera), aphids (order Aphidina), and flies (order Diptera).

Table 1. Representative Nocturnal Wildlife in the Project Area[1]

Mammals
Western jumping mouse (*Zapus princeps*)
Pale kangaroo mouse (*Microdipodops pallidus*)
Fringed myotis (*Myotis thysanodes*)
Hoary bat (*Lasiurus cinereus*)
Long-legged myotis (*Myotis volans*)
Mule deer (*Odocoileus hemionus*)
Pronghorn (*Antilocapra americana*)
Coyote (*Canis latrans*)
Kit fox (*Vulpes macrotis*)
Birds
Great-horned owl (*Bubo virginianus*)
Western screech-owl (*Megascops kennicottii*)
Black-crowned night-heron (*Nycticorax nycticorax*)
Amphibians
Western toad (*Anaxyrus boreas*)
Northern leopard frog (*Lithobates pipiens*)

Source: Ormat Nevada 2021
[1] Includes species that may be both nocturnal and diurnal

Nocturnal wildlife has adaptations to help navigate or find prey in the dark. For instance, mammals have special adaptations in the physiology of their eyes, such as large pupils and retinas with a higher concentration of rods, which help with night vision (Rich and Longcore 2006). Bats are well known to use echolocation, whereby they sound a call and use the resounding echoes to locate and identify objects. Owls have asymmetrical ears to enhance hearing and soft feathers for silent flight (McGrath 2020). Finally, nocturnal insects have compound eyes to maximize light capture as well as keen photoreceptors to improve contrast (Warrant 2017). ALAN may disrupt these adaptations, as described further in **Section 3.3.3**.

ALAN also may affect migratory birds, especially birds that migrate at night. The project area is within the Pacific Flyway, the path along which migratory birds travel in spring and fall between Alaska and Patagonia; at least a billion birds migrate along this flyway annually (Audubon 2021a). The project area is near several important bird areas (IBAs) identified by the Audubon Society. These include the High Rock Resource Area and Bilk Creek-Montana Mountains IBAs to the north, and the Pyramid Lake and Lahontan Valley Wetlands IBAs to the south (Audubon 2021b). See Appendix C in the Gerlach Geothermal Exploration Project Biological Resources Baseline Report (Ormat Nevada 2021) for a list of migratory birds potentially occurring in the project area by habitat type.

Changes in night sky conditions may have cascading effects across the food web, including for both nocturnal and diurnal species. This is because the effects on some species may adversely or beneficially affect the species upon which they prey. For instance, increased ALAN may allow some predators to find prey more easily. Conversely, the potentially disorienting effects of ALAN may reduce the success of predators in catching prey.

The project area has an extremely low level of ALAN, evidenced by satellite data showing low radiance levels (WRC 2021). Some of the existing ALAN likely originates from the nearby town of Gerlach. As a result, ALAN likely does not currently affect wildlife in the project area.

2.5 ENVIRONMENTAL JUSTICE

Changes in night sky conditions could have disproportionate effects on economies and people that rely on visitation from those seeking night sky viewing opportunities. The community of Gerlach is recognized in popular culture as America's darkest town (Roeder 2017), which presumably attracts visitors to the community for night sky viewing.

New sources of ALAN also have the potential to disproportionately affect populations living near the ALAN source. Studies demonstrate that prolonged exposure to ALAN can disrupt human brain wave patterns, which can alter hormone production and cell regulation. These changes can lead to negative health effects, such as insomnia, depression, cardiovascular disease, and cancer (Chepesiuk 2009).

Executive Order 12898 requires federal agencies to identify and address health and environmental effects that are disproportionately high and adverse on low-income populations and minority populations, including Native American tribes. **Table 2** shows the percentages of racial and ethnic minority populations and populations below the poverty line in Washoe and Pershing Counties. For both counties, the percentages of minority populations and low-income populations are below the state-wide average for Nevada. The data from the town of Gerlach were not reliable and had a very low sample size.

Table 2. Environmental Justice Consideration for Washoe and Pershing Counties (2015–2019)

Geographic Area	Total Population	Racial or Ethnic Minority Population[1] as Percentage of Total Population	Population Below Poverty as Percentage of Total Population
Washoe County	456,936	22.4	11.3
Pershing County	6,615	19.8	12.0
State of Nevada	2,972,382	34.4	13.1

Source: US Census Bureau 2019

[1] Minority population is calculated based on the total population minus those identifying as white or non-Hispanic descent.

This page intentionally left blank.

Section 3. Proposed Night Sky Conditions

3.1 Proposed Project Overview

According to the exploration operations plan, Ormat would drill exploration wells using a large rotary drilling rig. The rig would be up to 170 feet tall (see **Figure 7** and **Appendix D**). The estimated drilling time for each well would be 45 days; however, difficulties encountered during the drilling process could extend the drilling period to a total of 90 days. Ormat proposes to operate the drilling rig 24 hours per day. During nighttime drilling, 120-watt fluorescent lighting on the drill rig and 250-watt lighting on the rig floor would illuminate the structure and provide worker safety. Additional ground-based auxiliary lighting is also proposed.

During nighttime operations, Ormat is proposing three portable trailers with pole-mounted light-emitting diode (LED) lights. There would be a total of twelve 320-watt fixtures oriented toward the drill rig and angled at approximately 45 degrees downward. Ormat proposes the total lumens per fixture to be 38,500 for a total light output of 462,000 lumens from the ground-based lights. The drill rig and ground-based lighting specifications provided by Ormat are in **Appendix D**.

Ormat would only drill one well at a time. Accordingly, it is assumed for the purposes of this report that there would never be more than one drill rig and associated lighting in the AOI at one time.

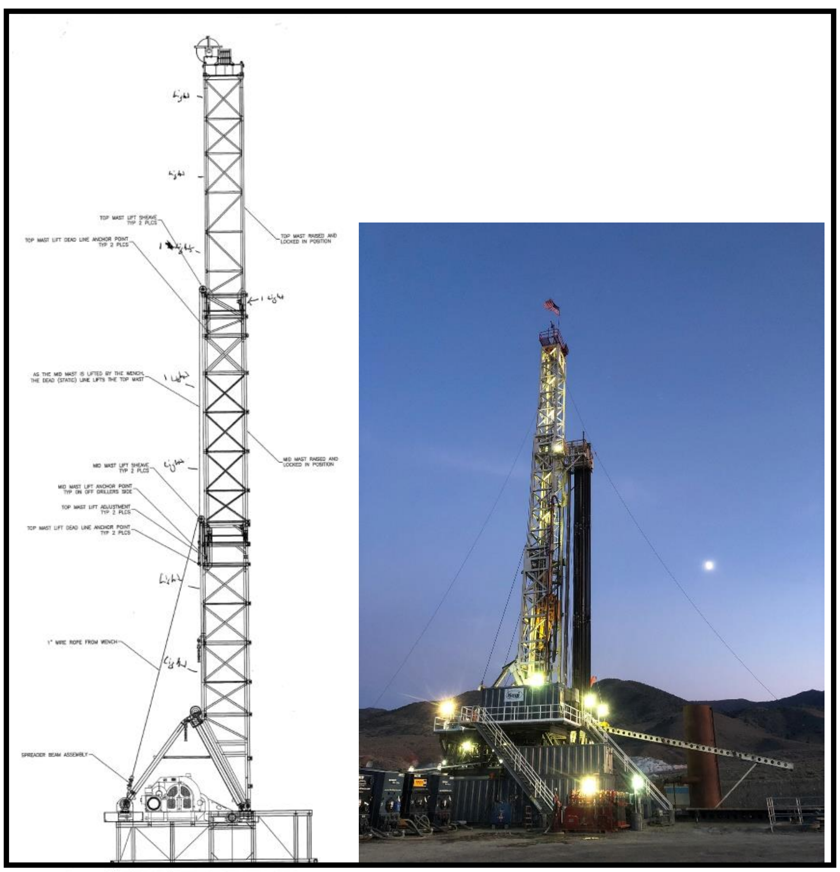

Figure 7. Schematic and Example Image of Proposed Drill Rig

3.2 SIMULATED LIGHT CONDITIONS

To understand the potential contributions of ALAN from the proposed project and the associated changes to baseline sky brightness, the consulting team of EMPSi, Wood Rodgers, and WRC, on behalf of the BLM and Ormat, conducted the following types of simulations:

- Radiance simulations using VIIRS images
- Sky brightness models
- Ground-based photographic simulations

The consulting team prepared the simulations based on the lighting specifications provided by Ormat for the proposed drilling activity (see **Appendix D**) and the scope of the project, as described in **Section 3.1**. Simulations provide a reference for understanding the potential ALAN and changes in sky brightness under predetermined site and atmospheric conditions. Simulations depict the proposed project in a new moon phase with near zero atmospheric obstructions such as smoke or clouds.

3.2.1 Radiance Simulations

WRC modeled three scenarios of nighttime ground radiance associated with the proposed project. These scenarios are:

- Expected lighting from associated drilling activities and proposed lighting with radiance values using empirically determined standard curves with values of 8.116 nWcm-2sr^{-1}
- A worse-case scenario with 1.5 times the expected lighting with a radiance value of 10.647 nWcm-2sr^{-1}
- A hypothetical scenario using mobile light plants with LED lights instead of fluorescent lighting for a radiance value of 5.485 nWcm^{-2}sr^{-1}

The simulated images for pad 63-3 are shown in Figure 4.14 in **Appendix A**. The expected radiance during active drilling is shown in Figure 4.14B in **Appendix A**; this can be compared with the ground radiance with no active drilling in Figure 4.14A in **Appendix A**. The simulations conclude the radiance of an active drill rig with the specified lighting in Appendix D to be 8.116 nWcm-2sr^{-1}. As a comparison, Gerlach's radiance is 10.4 nWcm-2sr^{-1} and Empire is 55 nWcm-2sr^{-1}. The radiance from the drill pad is concentrated over a smaller area than the lighting in Gerlach or Empire, which is more dispersed.

Figure 4.14C in **Appendix A** depicts proposed ALAN at 1.5 times the specifications in Appendix D. This scenario would result in radiance up to 10.647 nWcm-2sr^{-1} for an operational drill rig. This would be equivalent to the total radiance for Gerlach.

Figure 4.14D in **Appendix D** depicts the simulated result of using the LED-configured mobile light plants, which would result in a radiance level of 5.485 nWcm-2sr^{-1}. This scenario would reduce the radiance by nearly 40 percent compared with the specified lighting in **Appendix D** and would result in a radiance of approximately 50 percent that of Gerlach.

3.2.2 Sky Brightness Models

A change in sky brightness is a concern for astronomers and visitors participating in casual stargazing, particularly in an area as dark as the study area. Using a customized version of the Skyglow Estimate

Toolbox software from the National Aeronautics and Space Administration, WRC prepared sky glow models for proposed lighting at well pads 18B-10, 45-16, and 63-3 as viewed from KOPs 2 and 7. WRC ran the model using the proposed lighting scenario, worse-case scenario, and LED alternative. Model results are summarized in Section 4.5 and presented in Tables 4.4 through 4.9 in **Appendix A**.

In summary, the model results indicate that sky glow changes for drill rig lighting, as viewed from the selected KOPs, would be less than a 0.23 magnitude. The level of change would be less for viewers at the KOPs looking away from the drill rigs.

3.2.3 Ground-Based Photographic Simulations

On September 9, 2021, the consulting team collected baseline photographs for the photographic simulations of the proposed geothermal exploration project. Baseline photographs are in **Appendix B**. As directed by the BLM, Wood Rodgers prepared photographic simulations for KOPs 2, 3, 5, 6, and 7. For each KOP, there are four images; each image depicts an operational drill rig at one of four proposed well pads. The BLM selected the following proposed well pads for the simulations: 18B-10, 45-16, 63-3, and 68-9 (see Figure C-1 in **Appendix C**). The purpose of the images is to simulate the anticipated ALAN from the proposed project, which would include a single operational drill rig at one of the proposed well pads. Wood Rodgers prepared the simulations using a three-dimensional model and inputs based on the proposed drill rig and ancillary lighting specifications provided by Ormat (see **Appendix D**).

The photographic simulations, which are in **Appendix C**, demonstrate that depending on the well pad location being actively drilled, the illuminated drill rig would be visible from the KOPs. From KOP 2, a drill rig at well 63-3 would be the most visible of the simulated well locations. Drill rigs at the other locations would either not be visible or would be nearly indistinguishable from the other ALAN from Gerlach.

For a viewer at KOP 3 looking northeast, a drill rig at well pad 18B-10 would be the most visible. A drill rig at well 63-3 would be visible in the distance. Drill rigs at well pads 45-16 and 68-9 would not be visible; however, ALAN from the nearby well pad 68-9 would introduce glare in the viewer's foreground.

A viewer looking east from KOP 5 would only be able to see lights from the drill rig at 45-10. The other well pad locations used in the simulation would not be visible. Similarly, a drill rig at well pad 63-3 would be the only simulated well pad activity visible from KOP 6. ALAN at well pad 63-3 would be faint because KOP 6 is over 2 miles from the well pad.

From KOP 7 looking north, drill rigs at well pads 18B-10, 45-16, and 68-9 would be visible but would be difficult to distinguish from the ALAN of Gerlach. A drill rig at well pad 63-3 would be visible in the distance and would stand apart from the Gerlach lights.

3.3 POTENTIAL NIGHT SKY IMPACTS

The proposed geothermal exploration project would include active drilling over an approximately 45-day period. Drill rigs would use metal halide lamps that produce 1,766,000 lumens. The drill rigs would result in localized, short-term impacts on astrotourism. Of the four well pads anticipated to be drilled within the study area, pad 63-3 is the farthest drilling location from the town of Gerlach and is where the effects from introduced sources of light would be most observable from the perspective of persons engaged in astrotourism. Drilling on pad 63-3 is expected to produce a radiance of about 8.116 nWcm-2sr^{-1}. In comparison, the total radiance for the town of Gerlach is about 10.4 nWcm-2sr^{-1}, and it is about 55 nWcm-2sr^{-1} for the town of Empire. Although the predicted radiance from the drill pad would be concentrated over a much smaller area compared with the lighting present in the towns, which is more dispersed, light spillover would be present and noticeable to observers in the vicinity of the drill sites for the 45-day duration.

3.3.1 Astrotourism

The prosed drill activity would introduce a new, temporary, localized source of ALAN to the study area. As depicted in the photographic simulations (**Appendix C**), drill rig lighting at the simulated well pad locations would be visible mostly in the distance. In most cases, ALAN from the drill rigs would be largely indistinguishable from the existing lights in Gerlach, or it would be far enough in the distance to not interfere with night sky viewing.

Those observing the night sky directly adjacent to a drill rig during operation, such as a person at KOP 3 during active drilling of well 68-9, would experience glare from the ground-based and rig-mounted lights. The level of glare would be highest for a viewer looking directly at the drill rig lighting. However, as shown in the KOP 3 simulation for well 68-9, shifting the viewing perspective away from the drill rig lights would nearly eliminate the glare. The intensity of the glare would decrease with distance from the light source.

As a result, effects on astrotourism would be measurable and adverse for those attempting to view the night sky from directly adjacent to a drill rig during the 45- to 90-day period of operation. However, these impacts could be mitigated through distance from the drill rig and by taking a viewing perspective looking away from the drill rig.

Evidence indicates that potential astrotourism impacts from sky glow resulting from the proposed project would be negligible. Under a worst-case scenario, which assumes 1.5 times the amount of expected lighting would be produced, the radiance of the drill rig would increase to 10.647 nWcm-2sr^{-1}. This radiance level would be equivalent to the observed radiance of Gerlach (see **Appendix A**). The modeled changes in sky glow described in **Section 3.2.2** would be observable to those engaged in astrotourism; however, it would be highly unlikely that the changes would be of a magnitude to discourage astrotourism in the region or displace visitors engaged in the activity.

3.3.2 Designated Areas

During the 45- to 90-day period of active drilling, the ALAN, radiance, and sky glow described in **Section 3.2** would be noticeable to observers located along the western ridge of the Selenite Mountains in the Selenite Mountains WSA. However, because the WSA is located approximately 5 miles from the AOI and the wilderness characteristics are influenced by the existing ALAN from Gerlach and Empire, it is unlikely that the modeled changes in ALAN, radiance, and sky brightness would change the existing wilderness character.

Similarly, given the distance from the AOI to the edge of the Calico Mountains Wilderness and the presence of existing ALAN and sky glow from Gerlach and Empire, changes to wilderness character would likely be imperceptible.

3.3.3 Wildlife

ALAN has been shown or inferred to have a number of effects on mammals. These include:

- Disruption of foraging patterns, including reduced activity and movements, thereby reducing food consumed (Brown et al. 1988; Rich and Longcore 2006)
- Increased predation risk due to increased visibility (Rich and Longcore 2006; Shier et al. 2020)
- Disruption of biological clocks, leading to potential changes in activity times, melatonin production, and reproductive success (Rich and Longcore 2006; Robert et al. 2015)
- Disruption of dispersal movements through artificially lighted landscapes (Rich and Longcore 2006; Bliss-Ketchum et al. 2016)

Amphibians, including frogs and toads, may be susceptible to effects from ALAN and may be particularly attracted to light in the blue end of the spectrum. These effects include increased susceptibility to predator or vehicle collisions, changes to reproductive behavior or hormonal activity, reduced larval development, and disrupted movement patterns (Rich and Longcore 2006; Perry et al. 2008). For instance, while frogs and toads have been observed to congregate at lights to forage on insects attracted to such lighting, this may make them more susceptible to vehicle collisions on nearby roads (Rich and Longcore 2006; Perry et al. 2008). ALAN may also lead amphibians to require more time to adjust to nearby dark areas, potentially changing their ability to select a mate, defend a territory, or detect and avoid predators (Rich and Longcore 2006).

ALAN may attract nocturnal insects, including insect pollinators, in the immediate vicinity. This may interfere with insect development, movement, foraging, and reproductive success (Owens et al. 2020; Firebaugh and Haynes 2019). Insects attracted to the lighting may then attract insect-eating birds or bats, leading to increased mortality of insects and successful predation for birds and bats (Owens et al. 2020). In fact, food intake by some bat species has been shown to be higher at lights than in other habitats (Minnaar et al. 2015). This has been attributed to lights attracting insects, which then provide a concentrated source of prey for bats (Rich and Longcore 2006). However, artificial light may affect bats' abilities to navigate, since it may obscure the afterglow from sunset, which is used for orientation after roost emergence in some species (Mathews et al. 2015). Artificial light may also affect bats' circadian rhythms, particularly during hibernation, which may reduce overwinter survival (Stone et al. 2015).

ALAN may disorient migrating birds or attract birds away from suitable stopover habitat. This causes an unanticipated energy expenditure due to delays and altered migration routes, use of areas with reduced food abundance, mortality from collisions with glass during the daytime, and delayed arrival at breeding or wintering grounds (Rich and Longcore 2006; McLaren et al. 2018).

In the study area, the likelihood for the impacts described above to occur is relatively low compared with areas with higher ALAN. Simulations of the proposed drilling activity, as described in **Section 3.2** and depicted in **Appendixes A** and **C**, demonstrate that new ALAN would be highly localized. The impacts described above would be confined to those areas immediately adjacent to the drill rig and would last only for the duration of the drilling activity, which is proposed for 45–90 days per well.

3.3.4 Environmental Justice

As described in **Section 2.5**, for both Washoe and Pershing Counties, the percentages of minority populations and low-income populations are below the state-wide averages for Nevada. Evidence from simulated night sky conditions (**Section 3.2**) indicated that adverse impacts from proposed nighttime lighting during the 45- to 90-day drilling period would occur indiscriminately and nearly imperceptibly on area communities. It is unlikely that any measurable adverse effects would be experienced disproportionately by low-income and minority populations in Gerlach or the surrounding areas.

3.4 BEST MANAGEMENT PRACTICES

Implementing best management practices into lighting and facility design and operation can minimize or avoid light trespass, which results in localized glare and radiance increases, and contributes to reduced sky darkness. Several environmental protection measures identified in the exploration operations plan would minimize the potential night sky impacts discussed in **Section 3.3**. In addition to the applicant-proposed environmental protection measures, the following best management practices, adapted from the National Park Service and International Dark-Sky Association, and those in Section 5.3.4 in **Appendix A**, are presented for consideration as opportunities to minimize ALAN from the proposed project.:

- Use shielding to contain lighting within the project footprint.
- Apply a shielded light fixture with smaller wattage lights. For example, if LED-configured mobile light plants were used to reduce impacts from lighting, the predicted radiance produced at the drill site would be 5.485 nWcm-2sr^{-1}. This is about half the current radiance from Gerlach.
- Select lamps with warmer colors. Amber-colored lights emit longer wavelengths, which give more protection to the eyes and minimize sky glow.
- Use full cut-off light fixtures that can be adjusted to point directly downward.

Section 4. References

Altschuler, Wendy. 2019. "Is astrotourism the next big thing? Incredible nightime outdoor adventures for stargazers." *Forbes*. Internet website: https://www.forbes.com/sites/wendyaltschuler/2019/08/31/is-astrotourism-the-next-big-thing-incredible-nighttime-outdoor-adventures-for-stargazers/?sh=2ca5af4151d3.

Audubon. 2021a. Pacific Flyway. Internet website: https://www.audubon.org/content/pacific-flyway.

_____. 2021b. Nevada Important Bird Areas. Internet website: https://www.audubon.org/important-bird-areas/state/nevada.

Bliss-Ketchum, L. L., C. E. de Rivera, B. C. Turner, and D. M. Weisbaum. 2016. "The effect of artificial light on wildlife use of a passage structure." *Biological Conservation* 199: 25–28.

Brown, J. S., B. P. Kotler, R. J. Smith, and W. O. Wirtz II. 1988. "The effects of owl predation on the foraging behavior of heteromyid rodents." *Oecologia* 76: 408–415.

Bureau of Land Management (BLM). 2004. Proposed Resource Management Plan and Final Environmental Impact Statement for the Black Rock Desert-High Rock Canyon Emigrant Trails National Conservation Area and Associated Wilderness, and Other Contiguous Lands in Nevada. Winnemucca, Nevada.

_____. 2019. Hycroft Mine Phase II Expansion Project Final Environmental Impact Statement. Winnemucca, Nevada.

_____. 2021. North Valley Geothermal Development Project at the San Emidio Geothermal Field Final Environmental Assessment. Winnemucca, Nevada.

Challeat, S., K. Barre, A. Laforge, D. Lapostolle, M. Franchomme, C. Sirami, I. Le Viol, J. Milian, and C. Kerbiriou. 2021. Grasping darkness: the dark ecological network as a social-ecological framework to limit the impacts of light pollution of biodiversity. Ecology and Society 26(1): 15.

Chepesiuk, R. 2009. "Missing the Dark: Health Effects of Light Pollution." *Environmental Health Perspectives* 117(1): A20–A27.

Earth Observation Group. 2022. Radiance Light Trends. Internet website: https://lighttrends.lightpollutionmap.info/

Falchi, F., P. Cinzano, D. Duriscoe, C. Kyba, C. Elvidge, K. Baugh, B. Portnov, et al. 2016. "The new world atlas of artificial night sky brightness." *Science Advances* 2(6). Internet website: https://advances.sciencemag.org/content/2/6/e1600377.

Firebaugh, A., and K. J. Haynes. 2019. "Light pollution may create demographic traps for nocturnal insects." *Basic and Applied Ecology* 34: 118–125.

Hamacher, D.W., K. De Napoli, and B. Mott. 2020. :Whitening the Sky: light pollution as a form of cultural genocide.: *Journal of Dark Sky Studies* 1.

International Dark-Sky Association. 2021. International Dark Sky Sanctuaries. Internet website: https://www.darksky.org/our-work/conservation/idsp/sanctuaries/.

Kyba, C. C. M., T. Kuester, A.S. de Miguel, K. Baugh, A. Jechow, F. Holker, J. Bennie, C. D. Elvidge, K. J. Gaston, L. Guanter. 2017. "Artificially lit surface of Earth at night increasing in radiance and extent." *Science Advances* 3(11).

Mathews, F., N. Roche, T. Aughney, N. Jones, J. Day, J. Baker, and S. Langton. 2015. "Barriers and benefits: Implications of artificial night-lighting for the distribution of common bats in Britain and Ireland." *Philosophical Transactions of the Royal Society B* 370: 20140124.

McGrath, C. 2020. "Highlight: Adaptations that rule the night." *Genome Biology and Evolution* 12(10): 1909–1910.

McLaren, J. D., J. J. Buler, T. Schreckengost, J. A. Smolinsky, M. Boone, E. Emiel van Loon, D. K, Dawson, et al. 2018. "Artificial light at night confounds broad-scale habitat use by migrating birds." *Ecology Letters* 21: 356–364.

Minnaar, C., J. G. Boyles, I. A. Minnaar, C. L. Sole, and A. E. McKechnie. 2015. "Stacking the odds: Light pollution may shift the balance in an ancient predator-prey arms race." *Journal of Applied Ecology* 52: 522–531.

Narisada, K. and D. Schreuder. 2004. Light Pollution Handbook. Volume 322 of Astrophysics and Space Science Library.

Nevada Wilderness. 2021. Selenite Mountains Wilderness Study Area. Internet website: https://www.nevadawilderness.org/selenite_mountains_wilderness_study_area.

National Oceanic and Atmospheric Administration (NOAA). 2021a. Cloudiness: Mean Number of Days (Clear, Partly Cloudy, Cloudy). Internet website: https://www.ncei.noaa.gov/pub/data/ccd-data/clpcdy18.dat

_____. 2021b. National Digital Guidance Database 1hr Vertical Smoke Map for August 4, 2021. Internet website: https://airquality.weather.gov/sectors/nevadaLoop.php#tabs.

NPS (US Department of the Interior, National Park Service). Night Skies as a Natural Resource. Internet website: https://www.nps.gov/subjects/nightskies/natural.htm.

_____. 2021. Stargazing – Lassen Volcanic National Park. Internet website: https://www.nps.gov/lavo/planyourvisit/stargazing.htm.

Ormat Nevada. 2021. Biological Resources Baseline Report. Gerlach Geothermal Exploration Project. Ormat Nevada, Inc. Reno, Nevada.

Owens, A. C. S., P. Cochard, J. Durrant, B. Farnworth, E. K. Perkin, and B. Seymoure. 2020. "Light pollution is a driver of insect declines." *Biological Conservation* 241: 108259.

Perry, G., B. W. Buchanan, R. N. Fisher, M. Salmon, and S. E. Wise. 2008. "Effects of artificial night lighting on amphibians and reptiles in urban environments." *Herpetological Conservation* 3: 239–256.

Rich, C., and T. Longcore, eds. 2006. *Ecological Consequences of Artificial Night Lighting*. Island Press, Washington, DC.

Robert, K. A., J. A. Lesku, J. Partecke, and B. Chambers. 2015. "Artificial light at night desynchronizes strictly seasonal reproduction in a wild mammal." Proceedings of the Royal Society B 282: 20151745.

Roeder, Oliver. 2017. The Darkest Town in America. FiveThirtyEight. Internet website: https://fivethirtyeight.com/features/darkest-town-in-america/.

Shier, D. M., A. K. Bird, and T. B. Wang. 2020. "Effects of artificial light at night on the foraging behavior of an endangered nocturnal mammal." *Environmental Pollution* 263: 114566.

Stone, E. L., S. Harris, and G. Jones. 2015. "Impacts of artificial lighting on bats: A review of challenges and solutions." *Mammalian Biology* 80: 213–219.

Travel Trak America. 2019. Nevada Territory Visitor Facts: Cowboy Country, 2015–2019. Reported by Nevada Industry Partners. Internet website: https://travelnevada.biz/wp-content/uploads/Cowboy-Country-Territory-CY15-19.pdf.

US Census Bureau (US Department of Commerce, Census Bureau). 2019. 2015–2019 American Community Survey 5-year estimates. Reported by Headwaters Economics' Economic Profile System. Internet website: https://headwaterseconomics.org/tools/populations-at-risk/.

Warrant, E. J. 2017. "The remarkable visual capacities of nocturnal insects: Vision at the limits with small eyes and tiny brains." *Philosophical Transactions of the Royal Society B* 372: 20160063.

Wiley, M. 2021. "The true story of Empire, Nevada, the tiny desert town from 'Nomadland' that shut down in 2011, forcing all of its residents out." *Insider.* Internet website: https://www.insider.com/nomadland-true-story-of-empire-nevada-abandoned-ghost-town-mining-2021-4.

Williams, M. 2015. What can't we see the center of the Milky Way? Internet website: https://phys.org/news/2015-07-center-milky.html.

WRC (Western Research Company Inc.). 2018. Black Rock City, Nevada Artificial Light at Night Assessment. Tucson, Arizona.

_____. 2021. Satellite Measurement of Artificial Light at Night. Geothermal Exploration Project near Gerlach, Nevada. Tucson, Arizona.

This page intentionally left blank.

Appendix A

Satellite Measurement of Artificial Light at Night

This page intentionally left blank.

Western Research Company, Inc. Technical Report 1021-01

SATELLITE MEASUREMENT OF ARTIFICIAL LIGHT AT NIGHT

GEOTHERMAL EXPLORATION PROJECT NEAR GERLACH, NV

PREPARED BY

BRIAN L. CRAINE

ERIC R. CRAINE

OCTOBER 27, 2021

Western Research Company INCORPORATED

WESTERN RESEARCH COMPANY, INC
3275 W. INA RD. SUITE 221
TUCSON, AZ 85741

TABLE OF CONTENTS

FIGURES

TABLES

ABBREVIATIONS

θ_Z	Zenith angle
ALAN	Artificial light at night
BUG	Classification system to evaluate light output from outdoor lights (acronym for Backlight, Uplight and Glare)
CI	Cloud Index
CLASS	Comprehensive Large Array-data Stewardship System is an electronic library of NOAA environmental data
DNB	Day/Night band is the night time imagery obtained by satellite
EMPSi	Environmental Management and Planning Solutions, Inc.
EOG	Earth Observations Group at NOAA National Centers for Environmental Information
ESRI	Environmental Systems Research Institute which regulates the shapefile format (a popular geospatial vector data format for geographic information system software)
FOV	Field of view
HDF5	File format used for storing the satellite data
IBA	Important Bird Area
KOP	Key obervation point
km	kilometer
mcd	Milli-candela
MW	Mega-Watts
NASA	National Aeronautics and Space Administration
NCEI	National Centers for Environmental Information
netCDF-4	File format used for storing some satellite data files
NOAA	National Oceanic Atmospheric Administration
NPP	Suomi National Polar-orbiting Partnership satellite with VIIRS sensor
$nWcm^{-2}sr^{-1}$	Measure of radiance energy, nano-Watts per square centimeter per steradian
pySuomiutils	A proprietary collection of python routines for analyzing DNB satellite data
SED	Spectral energy distribution
SG:BG	Ratio of modelled skyglow at a location to the skyglow background defined as the skyglow measured at the Massacre Rim Wilderness Study Area.
SET	Skyglow Estimation Toolkit software developed by NASA
SNR	Signal to noise ratio
UH	Uplight High, component of BUG classification (light from 0-80° zenith angle)
VIIRS	Visible Infrared Imaging Radiometer Suite carried by Suomi-NPP and NOAA-20 satellites
WSA	The Massacre Rim Wilderness Study Area
ZA	Zenith angle
ZARI	Zenith angle radiance index

1. INTRODUCTION

This is the Final Report by Western Research Company, Inc. (WRC) of Tucson, AZ, submitted pursuant to the Contract titled "Satellite Measurements of Light at Night: Geothermal Exploration Project Near Gerlach, NV" (executed 2021 August 20) in support of a request from the United States Bureau of Land Management. The proposed Gerlach Geothermal Exploration Project (Project) located at Gerlach, Nevada would include the drilling and testing of geothermal wells and access road construction. During periods of active drilling, work may proceed around the clock and the associated nocturnal activity will involve introduction of artificial light at night (ALAN) in the region of interest. This report deals with certain environmental impacts of that activity.

The purpose of this report is four-fold: 1) to analyze satellite data of ALAN in the region of interest in order to establish a baseline against which future measurements may be compared, 2) to estimate the nighttime appearance of proposed drilling operations in the Gerlach, NV area and to generate associated simulated satellite images, 3) to produce models of sky brightness from observation points in or near Gerlach, NV resulting from the nocturnal drilling operations, and 4) to discuss various protocols that could avoid or minimize the effects of ALAN attributable to the drilling operations.

This report describes the methodology of data collection, the results of the data collection, and a discussion of the use of the data. This report also contains graphical and tabular representations of the measurements, and appendices with data. We note that the Contract specifies WRC perform the analysis using measurements obtained from state-of-the-art archived satellite data (the Suomi NPP and NOAA-20 satellites) and did not involve on-site data collection by WRC teams.

2. BACKGROUND

The Bureau of Land Management (BLM) has sought an assessment of the baseline artificial light at night (ALAN) levels in the general area of Gerlach, Nevada (including comparison with local features including the proposed Project area, Gerlach, Black Rock City, Hycroft Mine, and the Blue Mountain Geothermal Plant) utilizing the satellite-based Visible Infrared Imaging Radiometer Suite (VIIRS) nighttime quantitative measurement capabilities. This assessment was prompted by a project application for geothermal drilling and testing by Ormat Nevada (Ormat).

The goal of this report is to measure parameters characterizing artificial light at night (ALAN) emitted from specific targets near the Project area to establish the trend and baseline night light environment and to model the impact of ALAN on sky brightness. There are three types of target areas: 1) existing communities, 2) industrial facilities, and 3) the Project area. Measurements were made of each of these targets as follows:

1. The trends and baseline levels were measured using monthly radiance averages obtained from moonless, clear nights.

2. The zenith angle targets were measured for integrated intensity observed from several different zenith angles in order to calculate a metric related to efficiency of energy use, potential mitigation strategies, and evaluation of above horizon light that may adversely affect the environment. ZA function was measured for a single epoch, March 2021 (except for Black Rock City, August 2018).

3. Model projections were prepared using customized software developed by NASA which transforms VIIRS DNB measurements into approximations of sky brightness as a ratio of the brightness to that of the natural background.

All measurements were made using archived Suomi-NPP and NOAA-20 satellite data. The data were pre-processed using WRC proprietary software, and the specified measurements were tabulated. Analyses are represented as appropriate graphical or statistical presentations. Note that the VIIRS nighttime spectral response is about 500-900 nm and the analyses are restricted to that wavelength range.

3. METHODS

3.1 SATELLITE DATA

Quantitative measurements of nighttime ground radiance were obtained from the Suomi NPP and NOAA-20 satellites which each carry a Visible Infrared Imaging Radiometer Suite (VIIRS) imaging package. The Suomi NPP and NOAA-20 satellites [29] image the Project area on a nightly basis, providing a useful resource for monitoring upward radiating light levels. To measure the artificial light at night component it is preferable to obtain imaging in the absence of moonlight and the absence of interfering cloud-cover.

3.1.1 Nightly Satellite Imaging

The first criterion of absent moonlight can be achieved by using satellite measurements obtained when the lunar zenith angle is greater than or equal to 110° (i.e., the moon is at least 20° below the horizon).

The second criterion of cloud screening is based on the spectral analysis of the VIIRS sensor data using cloud identification algorithms developed by NASA [9]. The NASA analysis characterizes the cloud status over each pixel in the satellite image using a four-point confidence scale (0-3) regarding cloud-free status. A score of 0 indicates a 100% confidence of a cloud-free pixel. A score of 1 is 50-99% confidence, a score 2 is 1-49% confident and a score of 3 is 100% confident of cloud-cover. The pySuomiutils™ software (Western Research Company, Inc., Tucson, AZ) calculates values (C1 through C4) which are the sum of the number of pixels in an area with the corresponding cloud score (0 through 3). The software uses these values to calculate a cloud index (CI) for each identified area in the image:

$$CI=1-(C\_1/(C\_1+C\_2+C\_3+C\_4))$$

The CI index varies from 0 to 1, with 0 being highest confidence of cloudless pixels and 1 being the highest confidence of cloud interference. For this report we have used only images that have a CI ≤ 0.1 over an area of interest.

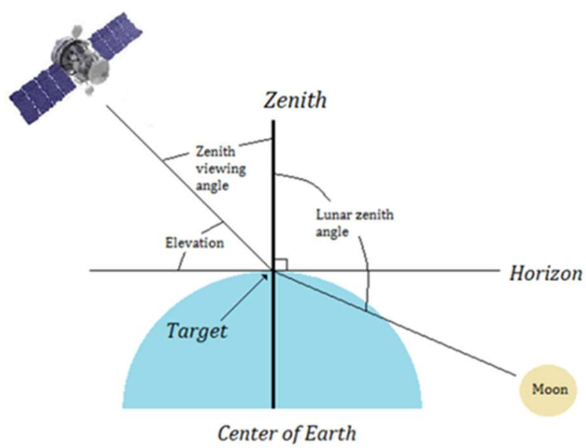

Figure 3. 1. Illustration of zenith angle and elevation definition.

Raw satellite HDF5 or NetCDF-4 data files (including radiance files, geo-position files, and the VIIRS Cloud Mask Intermediate product) for moonless nights are downloaded from the CLASS system [28]. The nightly files are processed using the pySuomiutils™ software package. pySuomiutils™ opens the HDF5/ NetCDF-4 data file and ESRI shape files from which it can extract sum radiance, average radiance, satellite zenith angle, satellite azimuth angle, lunar zenith angle, and calculate the cloud index for geo-locations specified by the shape file. This preliminary analysis allows for the determination of the above listed suitability criteria. The nighttime observations fulfilling the criteria are listed in Appendix D.

The accepted data files (radiance and corresponding geo-position files) were segmented to a rectangular region encompassing Gerlach and surrounding area (coordinates: Upper Left (123°25'1.4"W, 47°52'30.9"N); Lower Left (123°25'1.4"W, 46°23'32.9"N); Upper Right (121°25'30.4"W, 47°52'30.9"N); Lower Right (121°25'30.4"W, 46°23'32.9"N). The data were converted to GeoTIFF format images with pixel size of 461x393 meters to match the NOAA monthly composite format for further analysis. The original radiance values are floating point numbers with units of $Wcm^{-2}sr^{-1}$ but are converted to $nWcm^{-2}sr^{-1}$ for convenience.

3.1.2 Monthly Composite Satellite Data

The Earth Observations Group (EOG) at NOAA/NCEI is producing a Version 1 suite of average radiance composite images using nighttime data from the VIIRS Day/Night Band (DNB). Prior to averaging, the DNB data are filtered to exclude data impacted by stray light, lightning, lunar illumination, and cloud-cover. Cloud-cover is determined using the VIIRS Cloud Mask product (VCM). In addition, data near the edges of the swath are not included in the composites. Temporal averaging is done on a monthly and annual basis [26].

The products are produced in 15 arc-second geographic grids and are made available in GeoTIFF format as a set of 6 tiles. Each tile is actually a set of images containing average radiance values and numbers of available observations.

In the monthly composites there are many areas of the globe where it is impossible to get good quality data coverage for that month. This can be due to cloud-cover, especially in the tropical regions, or due to solar illumination, as happens toward the poles in their respective summer months. Therefore, it is imperative that users of these data utilize the cloud-free observations file and not assume a value of zero in the average radiance image means that no lights were observed.

The Version 1 monthly series of composites is run globally using two different configurations. The first excludes any data impacted by stray light. The second includes these data if the radiance values have undergone the stray-light correction procedure [26]. These two configurations are denoted in the filenames as "vcm" and "vcmsl" respectively. The "vcmsl" version, that includes the stray-light corrected data, will have more data coverage toward the poles, but will be of reduced quality.

The files are obtained as compressed tarballs, each containing a set of GeoTIFFs. Files with extensions "avg_rade9" contain floating point radiance values with units in $nWcm^{-2}sr^{-1}$. Note that the original DNB radiance values have been multiplied by $1x10^{9}$. This was done to alleviate issues some software packages have with the very small numbers in the original units. Files with extension "cf_cvg" are integer counts of the number of cloud-free coverage, or observations that went into constructing the average radiance image. Files with extension “cvg” are integer counts of the number of coverages or total observations available (regardless of cloud-cover).

The data files to be used were segmented to a rectangular region encompassing Gerlach and surrounding area (coordinates: Upper Left (123°25'1.4"W, 47°52'30.9"N); Lower Left (123°25'1.4"W, 46°23'32.9"N); Upper Right (121°25'30.4"W, 47°52'30.9"N); Lower Right (121°25'30.4"W, 46°23'32.9"N). The amount of light radiating from sites of interest was measured by integrating the energy readings within the corresponding shape file.

The composite images provide a useful overall view of the magnitudes of ALAN but are not suitable for the analysis of zenith angle dependency of the radiance since the zenith angle information is not preserved in the composites as it is in the nightly images.

3.2 MODELLING SKY BRIGHTNESS

The sky brightness is modelled using the Skyglow Estimation Toolbox (SET) software developed by NASA [27] and customized by Western Research Company (Tucson, AZ) to produce relative sky brightness maps. These maps are typically sky brightness luminance relative to the natural background light levels (SG:BG). The SET software uses real world measurements in the form of quantitative nighttime VIIRS DNB images. Light propagation algorithms are applied to determine the amount of light that would be observed by a viewer at a chosen site from all the sources within a 200 km radius. The ratio of the light intensity to that of the natural background is then displayed as a hemispheric Hammer projection [10] with a logarithmic pseudo-color mapping of the ratio for visualization. The determined ratio, SG:BG, can be converted to a commonly used magnitude (mag $arcsec^{-2}$) using the function defined in Figure 3.2.

The Massacre Rim Wilderness Study Area (WSA) is not only one of the darkest places in Nevada but also the contiguous United States and was designated as an International Dark-Sky Sanctuary in 2019 [24]. The WSA has essentially zero artificial illumination with a nighttime luminance reported at about 0.171 mcd/m^2 or a darkness value of 22.0 mag arcsec^{-2}[6]. This location (119° 29' 2.4"W, 41° 41' 13.2"N) is relatively close (about 115 km) to the current study area and therefore was chosen as an empirical measure of natural skyglow background to which other sites of interest can be compared. This comparison can be done within each image to compensate for inevitable changes in imaging conditions.

To predict the contribution of nighttime drilling to the sky brightness we use empirically determined expected VIIRS response to lighting associated with the drilling. The VIIRS response to known mobile lighting scenarios was used to develop a standard curve relating the mobile light lumen ratings to the satellite measure of nWcm^{-2}sr^{-1}. This allows the incorporation of anticipated lighting impacts into the sky brightness modelling described above. The resulting standard curve is shown in Figure 3.3. Two curves were produced for lighting measured from 1) actual working drilling rigs, and 2) from shielded mobile light plants all pointed below a 90° zenith angle (~135° zenith angle). Note that the actual field drilling rigs typically have some lighting pointing above the 90° zenith angle to illuminate some of the drilling tower and rather meager shielding.

The satellite measurements show a reasonably linear response to the number of employed lumens. The actual drill rig data, however, show a larger radiance than the strictly directed and better shielded mobile lighting plants. The proposed lighting arrangements at the Ormat drill pads include both rig lighting and multiple mobile light plants. The estimation of the satellite observed radiance is therefore calculated by using the lumen rating for the various types of lighting (see Appendix E) and the corresponding standard curve shown in Figure 3.3. These considerations lead to an estimation of about 1,776,000 lumens of light employed at a pad during drilling. When broken down by lighting type the expected satellite observed radiance would be 8.12 nWcm^{-2}sr^{-1}.

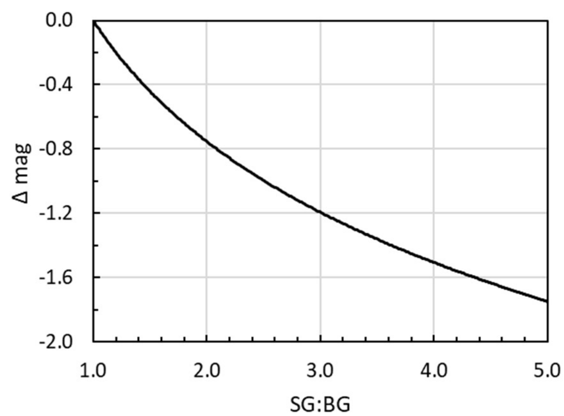

Figure 3.2. Relation of sky brightness ratio to magnitude.

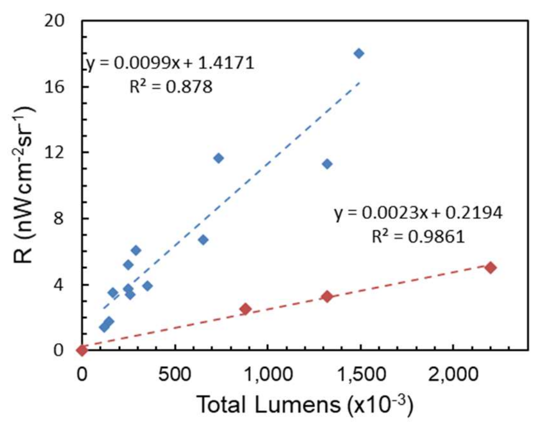

Figure 3.3. Empirical calibration of radiance observed by VIIRS radiometer. VIIRS measurements as a function of industrial mobile lighting luminance rating (nWcm^{-2}sr^{-1}) [3]. The blue diamonds are obtained from drill rig lighting. The red diamonds are from roadside portable light plants.

3.3 CALCULATION OF ZENITH ANGLE RADIANCE INDEX (ZARI)

ZARI is intended to provide a summary measure of the amount of misdirected light (light that corresponds to the UH light in the BUG classification [21]) observed by satellite imaging of a defined fixed geographic region (e.g., a town, an airport, resort area, etc.). The index is determined by measuring the radiance observed over a range of satellite zenith angles, typically from 0-75° on cloudless nights with the lunar zenith angle greater than 110^{0}.

Radiance as a function of the zenith angle is determined by a second-degree polynomial regression fit to the measured values:

$$R = a\theta_z^2 + b\theta_z + c$$

$$R_0 = c$$

Where R is radiance, θ_z is the zenith angle, c is a constant, and R_0 is the radiance at 0 zenith angle.

The rationale behind the ZARI is to determine the amount of upwardly directed light normalized to the theoretical level if all the light were scattered light from appropriately downward directed sources (see Figure 3.4). Scattered light has a maximum intensity at a zenith angle of 0. The level of scattered light is proportional to $\cos(\theta_z)$ and is 0 at a zenith angle of 90°.

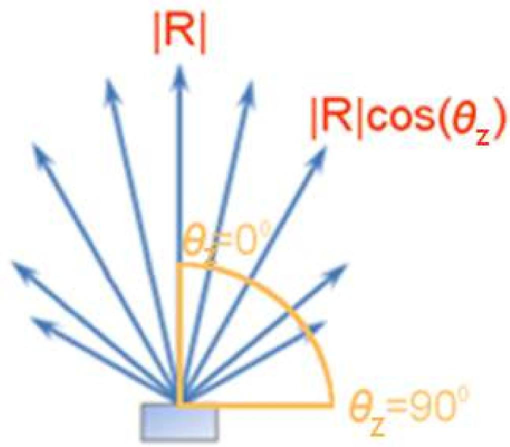

Figure 3. 4. Scattered light vectors.

The ZARI can be thought of as the upward directed light in excess of the scattered component from shielded, downward-directed light and expressed as the ratio of the total light minus the scattered light divided by the scattered component:

$$ZARI = \frac{\int_0^{80}(a\theta_z^2 + b\theta_z + R_0)d\theta - \int_0^{80}(R_0 \cos\theta_z)d\theta}{\int_0^{80}(R_0 \cos\theta_z)d\theta}$$

As a point of reference, the ZARI for Sedona, Arizona, which is a recognized model Dark-sky Community [32] that has adopted a strict lighting code, has a score of 51 (see Figure 3.5A). For comparison see a similar representation for Tucson, AZ with a score of 101 in Figure 3.5B. These scores are used as reference points for the ALAN analysis in the following section.

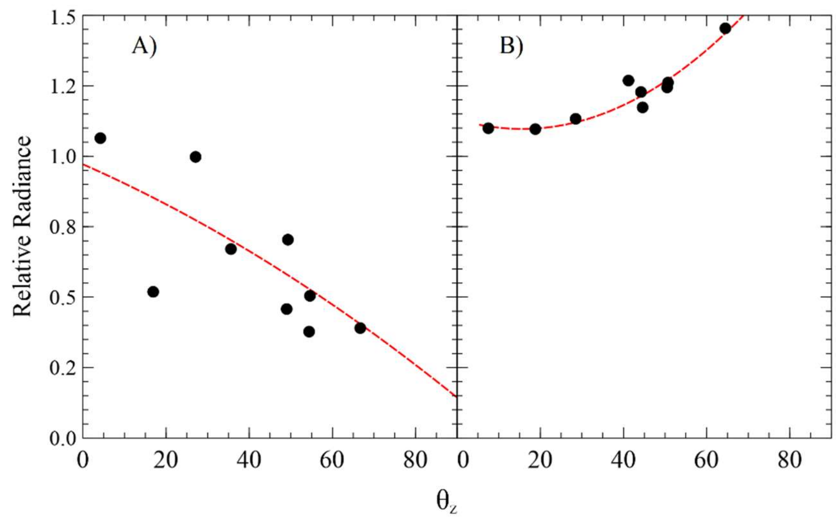

Figure 3. 5. Example zenith angle curves. A) Zenith angle curve for certified Dark Sky Community [11]. The zenith angle curve for Sedona, Arizona yields a ZARI score of 51. Note the downward slope at higher zenith angles. B) Zenith angle curve for Tucson, AZ with substantial misdirected light evidenced by the upward slope. The resulting ZARI score for Tucson is 101. θ_Z, is zenith angle.

3.4 STATISTICAL ANALYSIS

Statistical and graphical analyses were performed primarily using Microsoft Excel. Testing for the difference between sample means was done using a two-sample t-test (null hypothesis that the means are equal). The probability (P) that the null hypothesis is true was calculated. A typically applied 95% confidence level was used to define statistical significance (i.e., $P \leq 0.05$ indicates the null hypothesis is false). Calculations were completed using the Solver function in Microsoft Excel.

ALAN growth rates for areas of interest were calculated using integrated radiance values obtained at one-month intervals from January 2018 to March 2021. The growth rate, k, is given by the equation (where R_t is radiance at time t, R_{t_0} is radiance at time 0, and t is time):

$$R_t = R_{t_0} e^{kt}$$

This equation can be written as:

$$ln(R_t) = kt + \ln\,(R_{t_0})$$

The value for *k* and probability that *k* is not 0 is then determined by least squares estimation using Excel's *linest* function.

4. MEASUREMENTS

4.1 Regional ALAN Overview

The broad region including most of northern Nevada, southeastern Oregon, and southwestern Idaho is undeveloped with few light sources providing a coveted natural environment with benefits to wildlife and opportunities for astro-tourism. According to the International Dark-Sky Association, Massacre Rim (about 115 km from the Project area) is one of the darkest places in the contiguous United States, with just a few ranches and homes in its vicinity. Massacre Rim was certified in 2019 as the seventh International Dark Sky Sanctuary in the world [24].

The lack of artificial light is shown in the overview map (Figure 4.1), which shows an overlay of the average nightly radiance from the year 2020 represented in a pseudo-color scale. The vast majority of the area has very low radiance levels (generally gray). Much of the very light gray regions (e.g., around Black Rock City) are reflections of natural lighting from the high albedo desert terrain. The higher levels of radiance are seen to be associated with population (e.g., Gerlach, Winnemucca) and industrial operations (Hycroft Mine and Blue Mountain Geothermal plant).

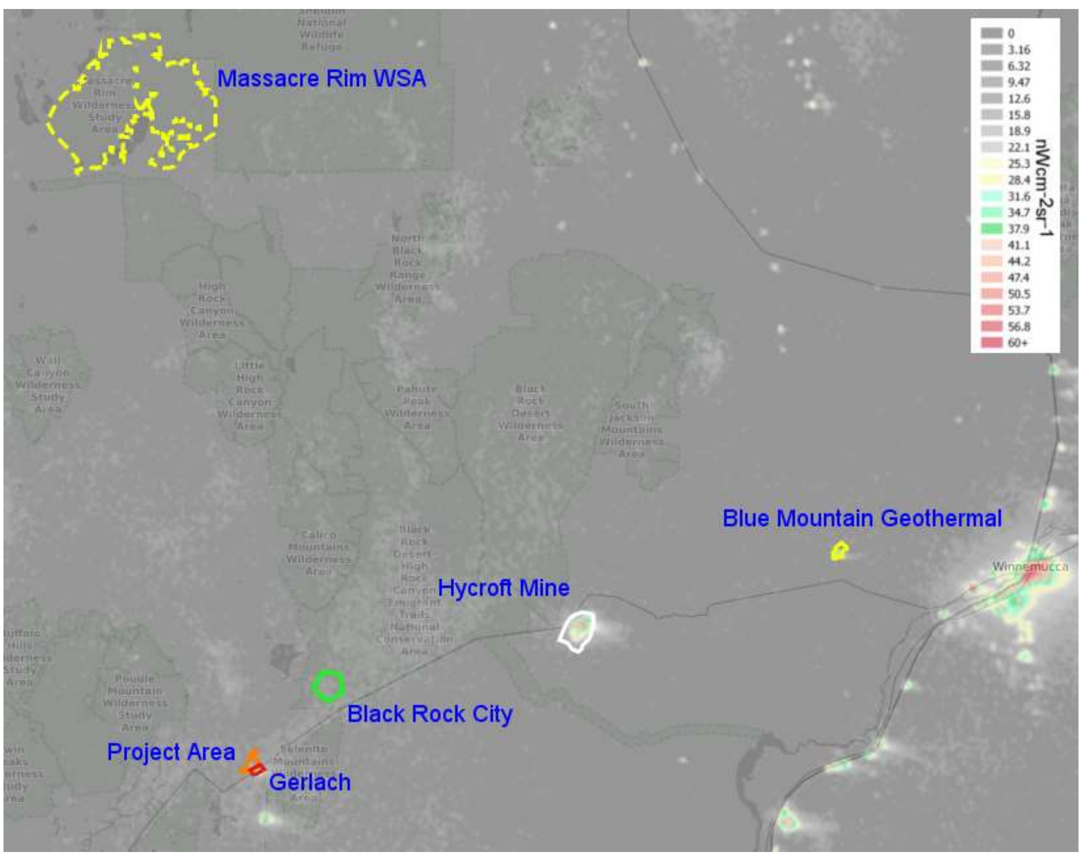

Figure 4. 1 Night lights observed from orbit. The radiance is shown in pseudo-color and partially transparent to show underlying geography. This image is an average radiance for March 2021.

The ALAN in the area of the proposed Project can be seen better in the magnified view shown in Figure 4.2. It is notable that the proposed Project area currently has an extremely low level of ALAN, some of which is most likely originating in Gerlach itself. Also indicated on Figure 4.2 are the two key observation points (KOP) that will be utilized in the predictive modelling of drilling impact on sky brightness (see *Section 4.4 Modelling of Projected Test Drill Site ALAN*).

Figure 4.3 includes a similar map but for average radiance observed in the year 2019. This map is included to illustrate the unusual situation at Black Rock City. Black Rock City is rather unique city which reconstitutes itself annually during the month of August to host the Burning Man festival. This event results in a statistically significant increase in the ALAN in the region. This increase in ALAN can be seen comparing the Black Rock City radiance from the 2021 map for March when there are no festival activities (Figure 4.2) with that seen in August of 2019 when the festival was held. In fact, when Black Rock City is hosting the festival, it becomes one of the brightest locations in Nevada. Although the festival is only a 10-day event the elevated radiance in the area is experienced for about 5 weeks due to pre- and post-festival activities.

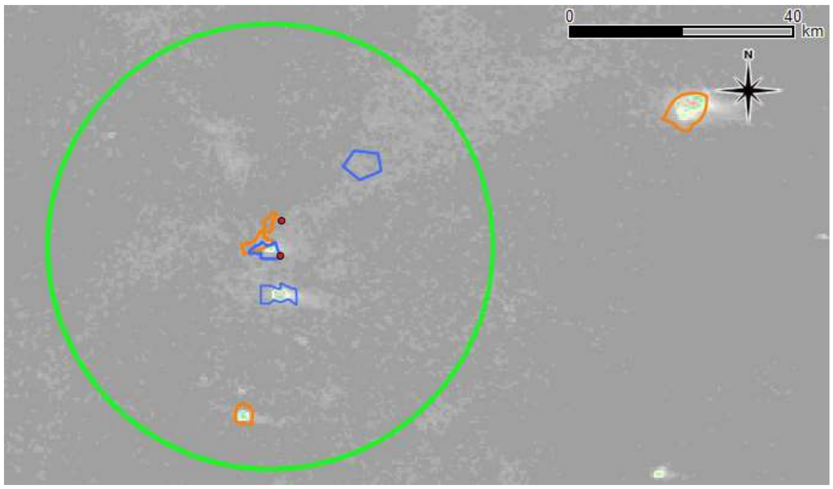

Figure 4. 2. Detail of the Gerlach region in March 2021. This image obtained when Black Rock City was not active. Note the high albedo of the Black Rock Desert playa seen as diffuse light gray. The red dots are KOP. The blue is census designated places or Black Rock City Boundary. The orange are industrial activity areas. The green circle is a 40km radius around Gerlach.

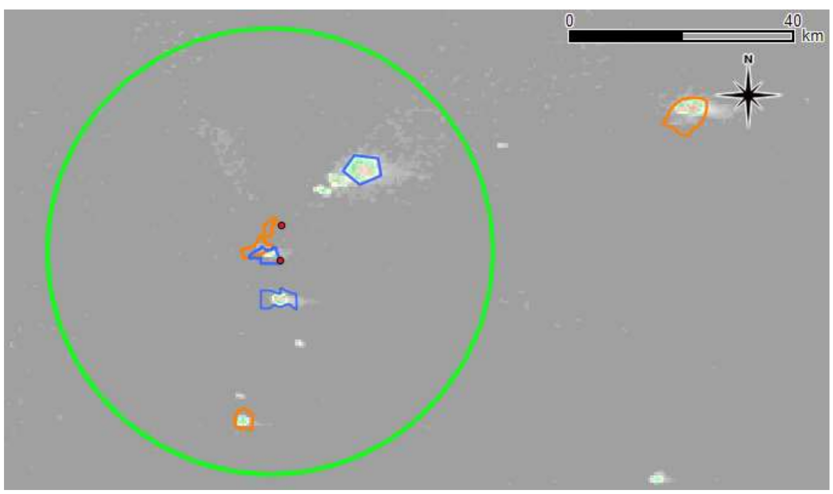

Figure 4. 3. Detail map of the Gerlach region August 2019. Note the large increase in radiance at the Black Rock City location. The red dots are KOP. The blue is census designated places or Black Rock City boundary. The orange are industrial activity areas. The green circle is a 40km radius around Gerlach.

4.2 Local ALAN Baseline and Trends (2018-2021)

Recognition of baseline levels and trends in night lighting in the Project region is an important component for planning for future mitigation and accommodation. It was therefore of interest to quantitatively measure levels and changes in radiance in the recent past (2018-2021) for activities near the Project area.

The location of the proposed geothermal exploration does not include any significant artificial lighting except for a very low level of spillover from adjacent Gerlach. The radiance levels at the proposed Project site are near background with some expected fluctuations, but the mean level has been constant since January 2018 with no statistically significant trends (Pearson's r = -0.003, $P_{(UNCORRELATED)}$= 0.702) observed (see Figure 4.4). It should be noted that the Project area is about 2.7-times the size of Gerlach resulting in the sum of the near background levels depicted in Figure 4.4 appearing to be a greater fraction of the Gerlach radiance than it really is.

Gerlach does provide measurable ALAN above background levels. The radiance levels from Gerlach are also shown in Figure 4.4 and exhibit some fluctuations from month to month. However, there is a statistically significant positive trend in radiance since Jan 2018 (r = 0.47, $P_{(UNCORRELATED)}$ = 0.002). This trend represents a monthly growth rate of about 0.98% ($P_{(NO\ GROWTH)}$ = 0.002, see Table 4.1). The cause of this growth has not been determined but is typically due to an increasing population or commercial activity. Depending upon the causes the trend could continue, plateau or reverse. The Gerlach baseline is, therefore, already a dynamic feature of the community that may require future reassessment for planning issues.

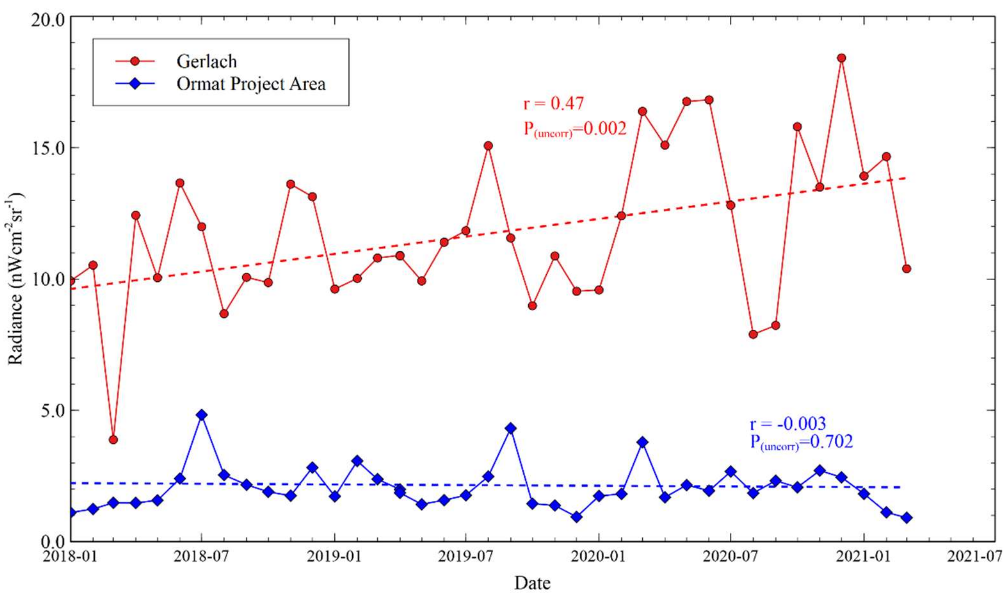

Figure 4. 4. Monthly radiance sums measured at Gerlach and Project Area. Gerlach (red circles) and the Project area (blue diamonds) from Jan 2013 through Mar 2021. The dotted lines are a linear regression fit.

The closest community to Gerlach is Empire, NV which is about 9 km to the south of Gerlach. Empire with a larger population than Gerlach (estimated 2021 populations of 104 versus 34 [5, 8, 14]) exhibits a greater average radiance by a factor of about 5 (see Figure 4.5). The general pattern of the nighttime lighting is very similar with fluctuations from month to month and a positive trend in radiance since January 2018 (r = 0.44, $P_{(UNCORRELATED)}$ = 0.0056). This trend represents a monthly growth rate of about 1.54% ($P_{(NO\ GROWTH)}$ = 0.006, see Table 4.1). Like Gerlach, the nighttime lights of Empire are a dynamic feature of the region that may require future reassessment.

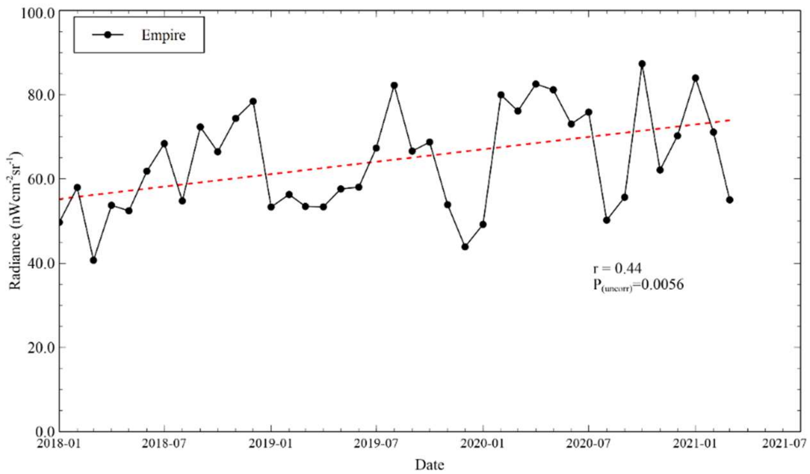

Figure 4. 5. Monthly radiance sums measured at Empire, NV.

Black Rock City is a boundary established through a special recreation permit with the BLM within which the annual Burning Man event occurs that has a large impact upon the ALAN levels experienced in the region. However, Black Rock City is unusual in that it is constructed and destructed annually during the months of August and September. The current timeframe of 2018-2021 further skews the data for Black Rock City since the Covid-19 pandemic has interrupted the construction of Black Rock City for the year 2020. The radiance associated with Black Rock City is shown in Figure 4.6 and reflects this situation. It can be seen that during most of the year Black Rock City is at a baseline level with minimal ALAN. However, in months 8 and 9 of both 2018 and 2019 there is a large increase in the radiance. The 2018 data underestimates the radiance levels because of weather conditions that interfered with the compilation of the satellite data. As expected, there was no increase in radiance in the year 2020 (cancellation of the Burning Man festival due to Covid pandemic). Due to the periodic nature of Black Rock City and the Covid interruption a sensible trend analysis for this period is not possible. However, the magnitude of the levels of ALAN normally produced at Black Rock City should not be ignored when considering the impacts of ALAN in this region.

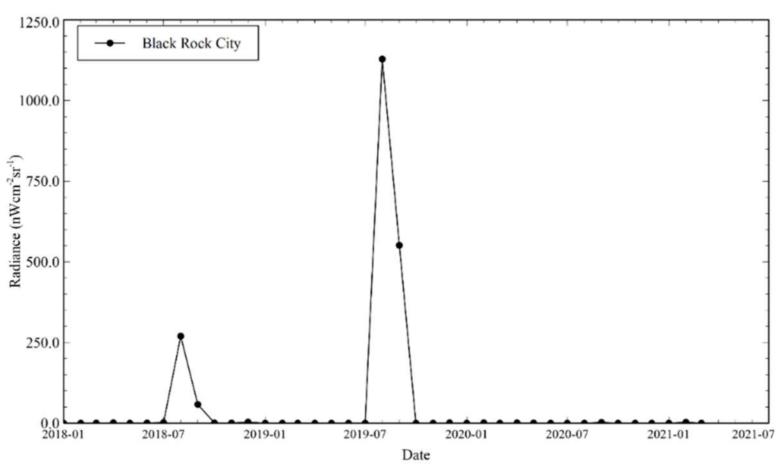

Figure 4. 6. Monthly radiance measurements over the Black Rock City community. Each point is typically the average of 12-14 moonless and cloudless nights.

It may also be noted that although the official Burning Man event was cancelled for 2021 an impromptu unofficial gathering did occur. Although a smaller event, the resulting ALAN was a major feature in the region. The event was coincident with major wildland fires in California which produced heavy smoke precluding the quantitative assessment of ALAN produced by the gathering. However, the smoke cleared during the night of September 3, 2021 allowing for a clear satellite view confirming the magnitude of ALAN produced (see Figure 4.7).

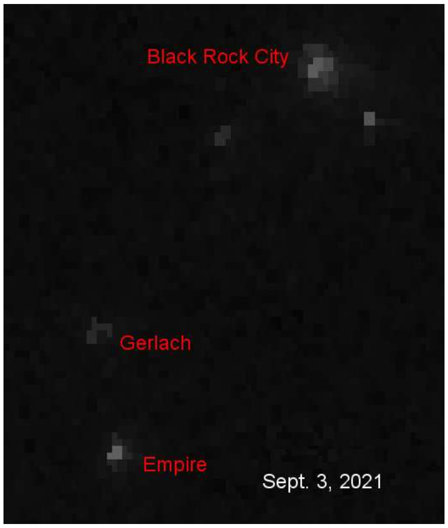

Figure 4. 7. Satellite view of the Project area on September 3, 2021.
The increased night lighting in the playa and the Black Rock City location is evident.

Another source of ALAN within a 40-km radius of the Project site is the San Emidio geothermal plant. The overall trend since 2018 has been a decreasing associated radiance (r = -0.42, $P_{(UNCORRELATED)} = 0.0089$, see Figure 4.8) consistent with the level of activity at the San Emidio site. One of the two geothermal power plants at that location was recently decommissioned. This trend represents a negative growth rate of -1.95% ($P_{(NO\ GROWTH)} = 0.009$) per month (see Table 4.1). The San Emidio geothermal plant is currently at a similar level to that of the community of Gerlach.

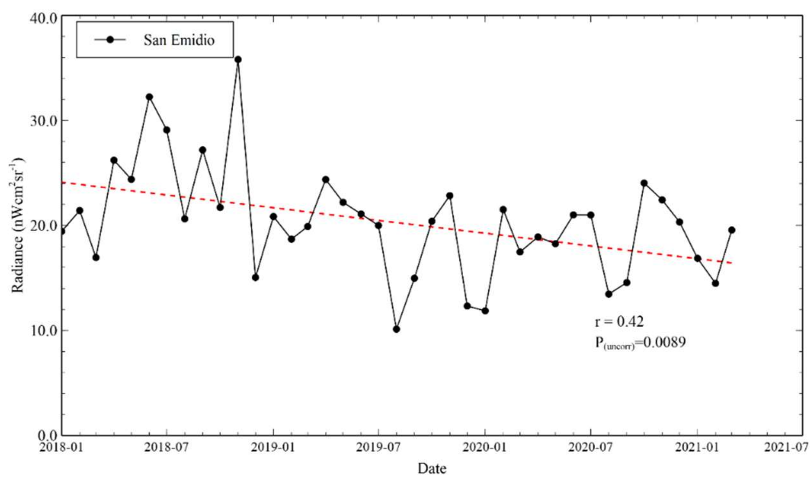

Figure 4. 8. Monthly radiance measurements at San Emidio geothermal plant.

Northern Nevada has a number of example geothermal energy plants. The radiance associated with two additional plants (Blue Mountain Geothermal and Don A. Campbell Plant) was measured for comparison. The Blue Mountain Geothermal Plant (118°08'34.31"W, 40°59'39.43"W, see Figure 4.1) is relatively close being about 110km to the east of Gerlach. The Blue Mountain Geothermal Plant was commissioned in

October 2009 and the plant has a total installed capacity of 49.5MW [2]. A second comparative facility is the Don A. Campbell geothermal plant (38°50'10"N 118°19'27"W) about 195 km to the south with a total capacity of 39MW. The plant came online in 2013 and increased capacity in 2015 [30].

The total radiance associated with the Blue Mountain geothermal plant had an overall highly statistically significant decreasing trend in brightness ($r = -0.64$, $P_{(UNCORRELATED)} = 1.2x10^{-6}$) over the measured period (2018-2021). This represents a negative growth rate of -2.64% ($P_{(NO\ GROWTH)} = 1.2x10^{-6}$) per month (see Figure 4.9). For comparison, the Don A. Campbell geothermal plant also had a statistically significant decreasing trend in brightness ($r = -0.29$, $P_{(UNCORRELATED)} = 0.049$) over the same period. This trend represents a negative growth rate of -0.96% ($P_{(NO\ GROWTH)} = 0.049$) per month (see Table 4.1). An unusual spike in radiance was observed during Feb-2019. This could have been the result of an onsite construction project and was transient.

The reason for the decreasing facility brightness was not investigated but could be due to 1) natural maturation of the facilities to a stable configuration, 2) macro-economic factors impacting the energy production, or 3) directed efforts to improve dark-sky friendly policies reflecting heightened public awareness (e.g., Nevada Senate Bill SB52, 81st Legislature [4]).

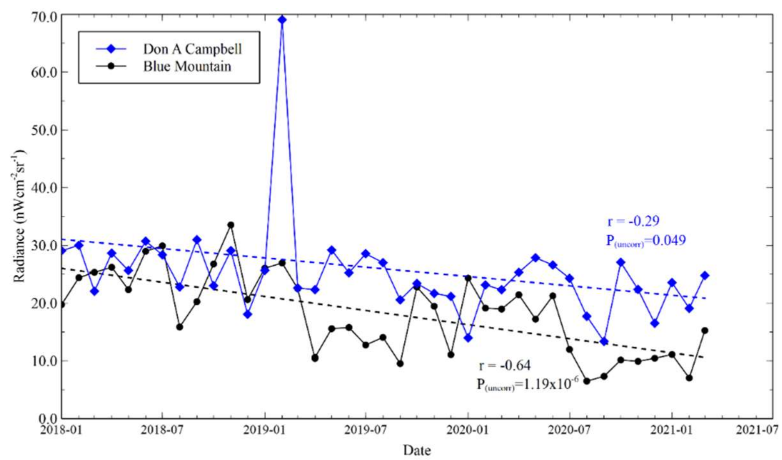

Figure 4. 9. Monthly radiance over the Blue Mountain or Don A. Campbell Geothermal Plant. The black symbols are for the Blue Mountain plant. The blue symbols are for the Don A. Campbell plant. The dashed lines are a linear regression line (r is Pearson's correlation coefficient and P the probability that the radiance is not correlated with time).

The region is rich in natural resources and activities include mining and geothermal energy production. Examples of the impact of these activities on ALAN are, therefore, of interest. Mining at Hycroft initially began in 1983 and production started at the Brimstone oxide open pit mine in 1987[20]. Hycroft Mining (formerly Allied Nevada Gold) is undertaking an expansion of its Hycroft gold mine (118°41'31.65"W, 40°52'04.7"W, see Figure 4.1). A Feasibility study for the two-phase expansion project was completed in 2014 and phase one construction began in December 2018. Mining operations at the site began in April 2019, while production was achieved in August the same year [20]. The trends in ALAN were consequently measured for the Hycroft Mine and shown in Figure 4.10. The radiance associated with the mine is greater than Gerlach but significantly less than that at Black Rock City (during Burning Man festival). The ALAN trend has exhibited a statistically significant increase over the measurement period ($r = 0.71$, $P_{(UNCORRELATED)} = 3.5x10^{-8}$). This is a growth rate of about 1.73% ($P_{(NO\ GROWTH)} = 3.5x10^{-8}$) per month (see Table 4.1). This growth is certainly consistent with the expansion activities occurring at the site and may be expected to continue until expansion has completed.

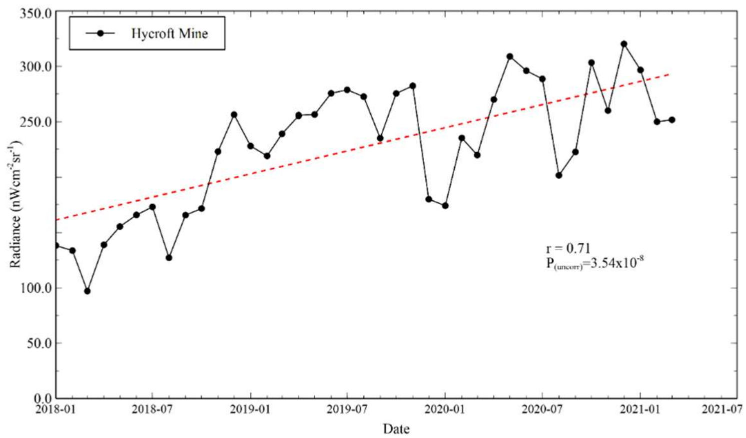

Figure 4. 10. Monthly radiance measurements over the Hycroft Mine. The dashed red line is a linear regression line (r is Pearson's correlation and $P_{(UNCORRELATED)}$ the probability that the radiance is not correlated with time).

A summary of the baseline ALAN at the locations of interest is presented in Table 4.1. The relative levels of ALAN radiance for the different sites range from a near background level of 1.1 $nWcm^{-2}sr^{-1}$ at the Project area to 138.1 $nWcm^{-2}sr^{-1}$ at the Hycroft Mine. The radiance levels are dynamic with changes over the period 2018-2021 occurring at all locations except the Project area. Most notably the Hycroft Mine has been increasing in radiance while the geothermal plants have decreased in radiance.

Table 4. 1. Summary of growth of nighttime radiance from 2018 to 2021.

Location	Radiance (2021) ($nWcm^{-2}sr^{-1}$)	Change ($nWcm^{-2}sr^{-1}$)	Growth Rate[1] (%)	P[2]
Project Area	1.1	0.19	-0.29	0.856
Gerlach	9.9	0.50	0.98	0.002
Empire	55.2	18.68	1.54	0.006
San Emidio	24.1	-7.68	-1.95	0.009
Don A. Campbell	29.1	-4.30	-0.97	0.049
Blue Mountain	19.7	-4.40	-2.46	$1.2x10^{-6}$
Hycroft Mine	138.1	113.60	1.73	$3.5x10^{-8}$

[1]Percent growth per month.
[2]Probability growth is zero.

4.3 Characterization of ALAN Zenith Angle Dependency

ALAN that is misdirected in an upward direction is almost always an undesirable occurrence. This type of pollution is a waste of energy and has the greatest environmental impacts [1, 22, 23]. The misdirected light can be monitored by measuring the radiance while the satellite is observing from a range of angles allowing for the assessment of zenith angle dependency of ALAN (see *Section 3.3 Calculation of Zenith Angle Radiance Index*). This analysis provides an important metric for judging whether night lighting has been implemented in a dark-sky friendly manner and can be quite informative in determining strategies and best management practices to minimize light output. It was therefore of interest to assess the zenith angle dependency of nighttime radiance from the local communities and industrial facilities.

Gerlach, NV is a small community with low radiance levels and has a very favorable zenith angle curve that continually decreases with increasing angle (see Figure 4.11A). Calculating the ZARI from the zenith angle curve, see Figure 4.11A, results in a value of 36.4 (see Table 4.2). This ZARI value is even better than the model dark-sky city of Sedona, AZ that is a certified dark-sky community by the International Dark-sky association [32]. In contrast, a similar analysis of the night lighting in August 2018 at Black Rock City, NV, resulted in a ZARI of 127.5 (see Figure 4.11C) indicative of a large component of misdirected lighting of the type most harmful to the environment [1, 22, 23]. Empire, NV has a zenith angle curve that is between the extreme values seen for Gerlach and Black Rock City (see Figure 4.11B). The relatively flat curve for Empire corresponds to a ZARI value of 74.7 which is a moderate value but the highest of the permanent centers of significant nighttime light in the immediate region. This would imply an opportunity to discover lighting fixtures in Empire that could be improved with respect to stray light.

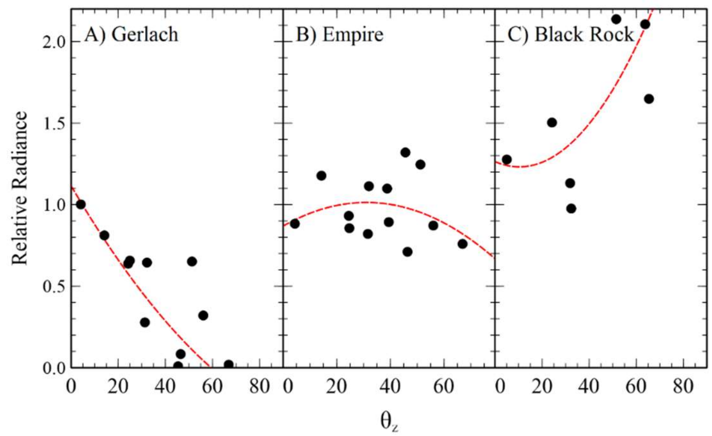

Figure 4. 11. ALAN zenith angle dependency of Gerlach, NV, Empire NV, and Black Rock City, NV. A) Gerlach, B) Empire and C) Black Rock City (August 2018). The relative radiance (normalized to projected zenith value) as a function of zenith angle (θ_Z) in degrees. The red dash is a second-degree polynomial least squares fit.

The night lighting from the San Emidio, Blue Mountain and Don A. Campbell geothermal plants was also analyzed (see Figure 4.12). The ZARI values were all less than the Sedona benchmark with the San Emidio plant being 46.5, Blue Mountain plant being 39.7 and the Don A. Campbell plant being 41.7 (see Table 4.2). These data would suggest implementation of successful shielding and direction of nighttime lighting fixtures in an environmentally favorable manner.

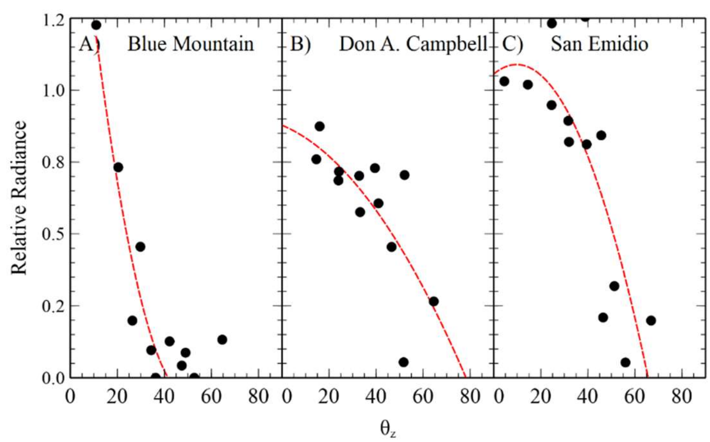

Figure 4. 12. Comparison of geothermal plant zenith angle dependency of ALAN. A) Blue Mountain geothermal plant, B) Don A. Campbell geothermal plant, and C) San Emidio geothermal plant. The relative radiance (normalized to projected zenith value) as a function of zenith angle (θ_Z) in degrees.

To complete the survey, the zenith angle curve for the Hycroft Mine was determined (see Figure 4.13) and had a very good ZARI score of 50.5. This is a very commendable score since most older open-pit mines have significant amounts of misdirected lighting. It is also important that the Hycroft Mine has such a favorable ZARI score since it is one the brighter locations in the greater region. Having a score of 50.5 suggests a successful mitigation of environmental night lighting by the mine.

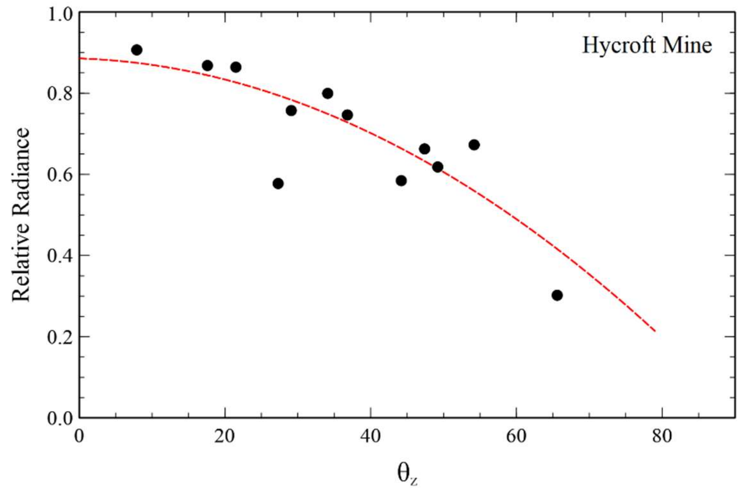

Figure 4. 13. Zenith angle dependency of ALAN at the Hycroft Mine facility. The relative radiance (normalized to projected zenith value) as a function of zenith angle (θ_Z) in degrees.

Table 4. 2. Summary of the ZARI values calculated from zenith angle curves such as Figures 4.9-4.11. Radiance ($nWcm^{-2}sr^{-1}$) at the zenith (θ_z=0°) indicates the general brightness of the location.

Location	**Radiance (θ_z=0°)**	**ZARI[2]**
IDA approved community[1]	2,430	50.9
Gerlach	48	36.4
Black Rock City[3]	7,568	127.5
Empire	115	74.7
San Emidio geothermal	27	46.5
Blue Mountain geothermal	18	39.7
Don A. Campbell geothermal	64	41.7
Hycroft Mine	616	50.5

[1]Sedona, AZ [32].
[2]ZARI scores measured for March 2021 except for Black Rock City (August 2018)
[3]Determined during the Burning Man festival.

4.4. Simulating Nighttime Satellite Images of Active Drill Pads

The VIIRS nighttime satellite images provide a unique method to assess the presence of ALAN quantitatively and visually. The quantitative nature of the images also provides an opportunity to construct reasonable simulations of the impact of the proposed test drilling upon the environment. Such simulations may be instructive on their own and serve as the basis for the modelling of sky brightness (which is presented in *section 4.5 Modelling of Projected Test Drill Site ALAN*).

The average nighttime lighting environment near Gerlach, NV and the Project area during March 2021 is shown in Figure 4.14. Figure 4.14A and 4.14B are the same image but presented with different grey level scaling. This illustrates the effect of saturation when displaying the satellite images (which have 16-bit resolution) in a typical printed form that only utilizes 8-bits of resolution. Gerlach is clearly seen in Figure

4.14A but Empire is saturated. The scaling in Figure 4.14B corrects the saturation observed at Empire but renders Gerlach more difficult to visually appreciate. Similarly, since the simulated pads have their radiance concentrated in a small number of pixels the images must be scaled to prevent saturation at those sites.

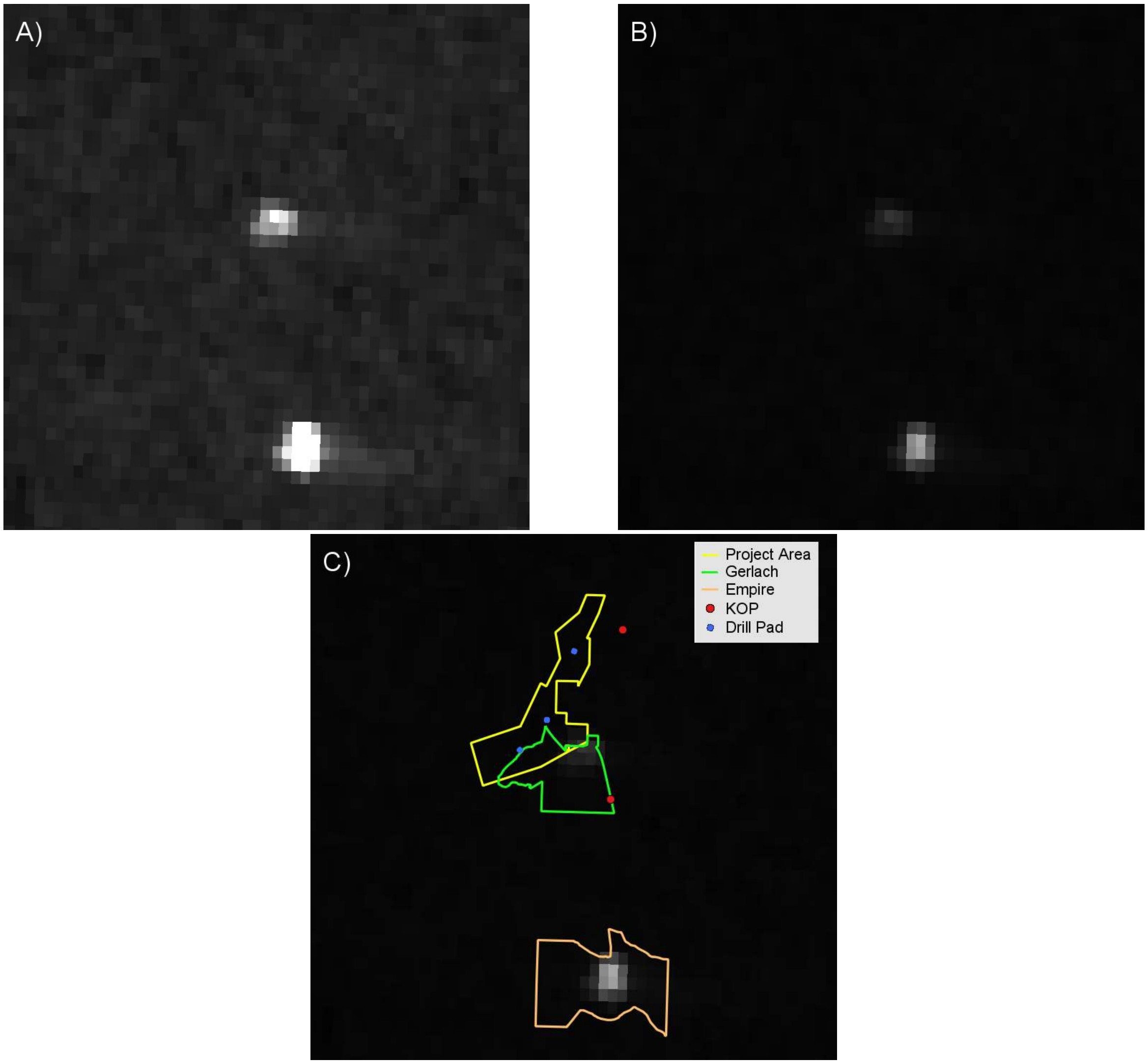

Figure 4. 14. VIIRS satellite image of immediate area around Gerlach, NV. A) Image with grey level scaled from 0 to 2 nWcm⁻²sr⁻¹. B) Image with grey level scaled from 0 to 10 nWcm⁻²sr⁻¹, and C) same as B but with landmarks annotated.

The VIIRS images of simulated test drilling were prepared for three different drilling pads (pad 63-3, 45-16 and 18B-10) and for three scenarios including 1) the expected lighting associated with drilling, 2) a worst-case scenario with 1.5 times the expected lighting and 3) lighting levels attained by use of LED based mobile light plants. The first scenario, referred to as the <u>expected</u> test drill lighting or <u>expected radiance</u>, is based upon lumens ratings of the proposed lighting (1,766,000 lumens) converted to radiance levels using empirically determined standard curves (8.116 $nWcm^{-2}sr^{-1}$, see Appendix E). The second scenario (1.5x expected) provides for a 50% under estimation error in lumen inventory which was judged to be greater than would be encountered used a radiance level of 10.647 $nWcm^{-2}sr^{-1}$ (worst case scenario). The third scenario substituted LED lamps for the metal halide lamps in the mobile light plants which reduced the total test drill lumens to 602,000 lumens. This configuration would result in a radiance level of about 5.485 $nWcm^{-2}sr^{-1}$.

The simulated images for pad 63-3 are shown in Figure 4.15. The expected radiance during active drilling is shown in Figure 4.15B and can be compared to no active drilling in Figure 4.15A. The total radiance for Gerlach is about 10.4 $nWcm^{-2}sr^{-1}$ while the active drill pad is predicted to produce about 8.116 $nWcm^{-2}sr^{-1}$. The radiance from the drill pad is concentrated over a much smaller area than the lighting in Gerlach which is more dispersed. The total radiance for Empire, NV is about 55 $nWcm^{-2}sr^{-1}$ for comparison. The worst-case simulation is shown in Figure 4.15C and would bring the radiance of the drill pad up to 10.647 $nWcm^{-2}sr^{-1}$ which would be equivalent to the total radiance for Gerlach and about 20% of that from Empire, NV. Finally, Figure 4.15D depicts the simulated result of using the LED configured mobile light plants which result in radiance levels of 5.485 $nWcm^{-2}sr^{-1}$. This level of lighting would be about half that currently from Gerlach.

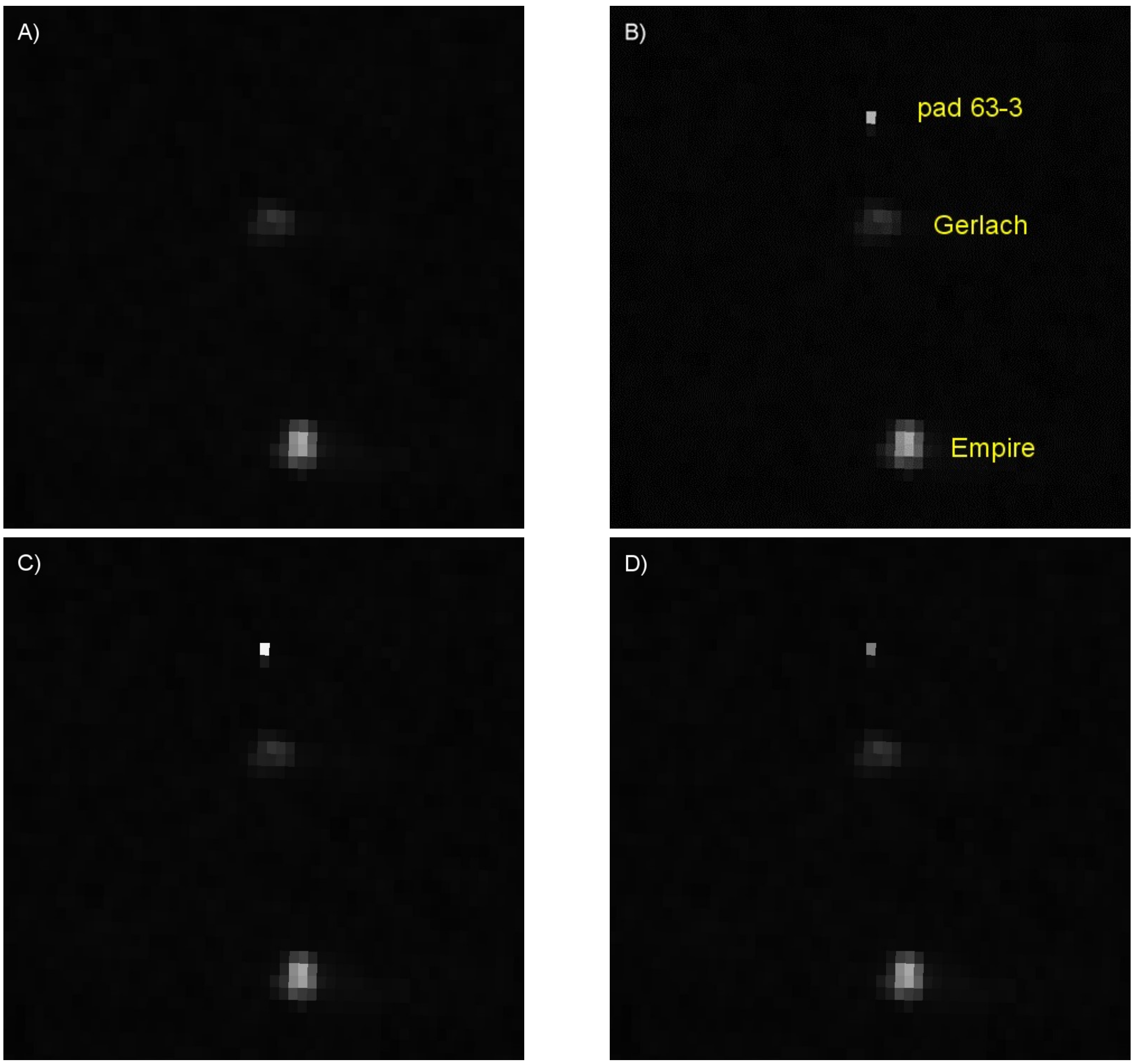

Figure 4. 15. Pad 63.3 nighttime test drill simulated VIIRS images. A) actual site in absence of drill lights (Gerlach in the center and Empire at the bottom of the images), B) expected level of lighting during active drilling, C) 1.5 times the expected level of lighting during drilling, and D) level of lighting during drilling with LED substituted lamps in mobile light plants.

The results from the other two pads (45-16 and 18B-10) are quantitatively the same as those for pad 63-3. The location of the light source changes and the visual appearance changes. This is particularly true for pad 45-16 which was located at the intersection of 4 image pixels. This spreads the signal among the four pixels and reduces the visual intensity although not the sum radiance. These remaining simulations, since similar to pad 63-3, can be reviewed in Appendix B.

4.5 Modelling of Projected Test Drill Site ALAN

The VIIRS satellite radiometer provides a sensitive and quantitative measure of the amount of light radiating into space. This light may be direct or scattered and while it is a major contributor to the observed sky brightness it is different from the sky brightness. The VIIRS measurements provide a good measure of the levels of artificial light radiated or reflected up at the earth's surface. This information can be used as key input to be able to model on a large scale the expected sky brightness due to the strong relationship between the surface artificial light and the sky brightness [6, 7]. This report will model the sky brightness as observed from three viewing locations 1) in Gerlach NV (119°21'19.0"W, 40°39'06.0"N), 2) KOP7 about 2km to the south-east of Gerlach (119°20'24.2"W, 40°38'15.8"N), and 3) KOP2 about 5km north-east of Gerlach (119°21'12.1"W, 40°41'41.3"N, see Figure 4.1) as described in *Section 3.2 Modelling Sky brightness Near Gerlach*. In addition, the impact of adding radiant sources simulating test drill rigs at three different proposed drill pad locations will be presented.

Modelling Baseline Sky Brightness Around Gerlach

Massacre Rim WSA is one of two International Dark-sky Parks located in Nevada. It is essentially free from ALAN and during moonless nights measures a sky brightness of magnitude 22 mag arcsec^{-2} [6]. Since it is only about 115 km from the Project area it is possible to measure radiance at Massacre Rim and the study area in the same image and express sky brightness as a ratio at selected viewpoints to that at the WSA. This provides an internal standard for the measurements which should help reduce sources of error.

Although the dark-sky designation was assigned to the Massacre Rim WSA the entire region down to Gerlach represents some of the darkest skies in the lower 48 states. Since the area is so dark the modelled sky brightness ratio is presented using an expanded logarithmic pseudo-color scale from 1.0 to 2.0, so that small differences from the natural background (i.e., Massacre Rim's 22 mag arcsec^{-2}) will be apparent. From a viewpoint in Gerlach the modelled sky brightness varies between 1.12x to 1.84x that of the natural background depending upon the zenith angle and azimuth that one views (see Figure 4.16, top panel). The average sky brightness is about 1.33x the natural background which corresponds to change in magnitude of -0.31 or a magnitude of 21.69 mag arcsec^{-2}.

During the Burning Man event the region's lighting inventory is very significantly impacted. Therefore, the sky brightness from Gerlach was also modelled using satellite data obtained during the Burning Man event of August 2019. The impact on Gerlach, which is about 15 km from Black Rock City, was measurable and statistically significant (see Figure 4.16, bottom panel). The ratio of sky brightness ranged from 1.27x to 7.11x the natural background depending upon the zenith angle and azimuth that one views. The average ratio was 1.81x the natural background resulting in an average sky brightness of 21.36 mag arcsec^{-2}.

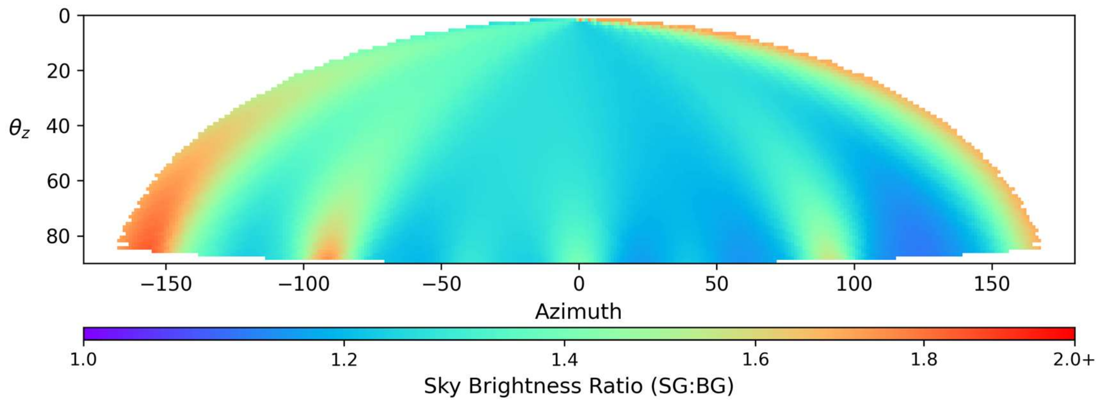

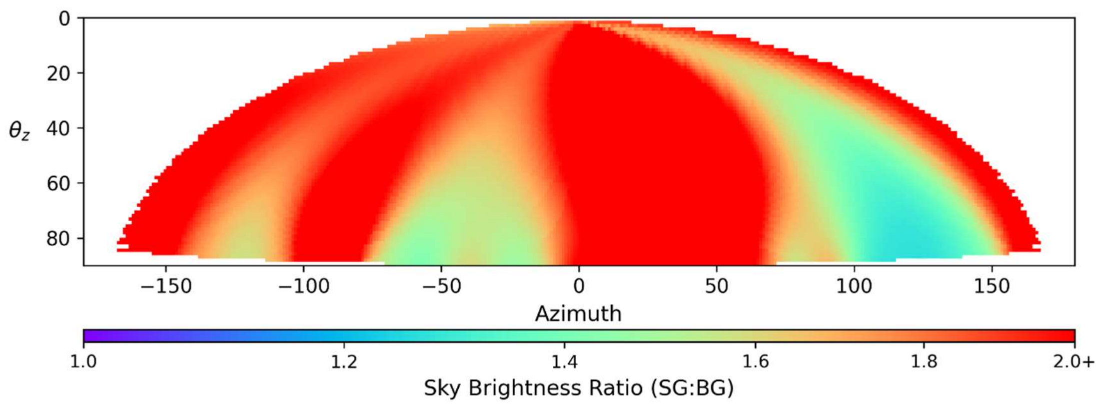

Figure 4. 16. Modelling baseline sky brightness from a view location in Gerlach, NV. Top panel is the model when Black Rock City is not active. Bottom panel is model when Black Rock City is active.

Seven key observation points (KOP) a short distance from Gerlach, NV were developed by the BLM and EMPSi to help evaluate the potential visual impacts of the proposed project. It was of interest to evaluate the sky brightness at two of these points (KOP7 and KOP2) which were at a short distance from the direct influence of ALAN in Gerlach. For example, these KOP's represent conveniently close areas for astro-tourism activities.

KOP7 is located at the south-east boundary of undeveloped Gerlach, NV along Route 447 (see Appendix Figure A2). This is about 2 km from the center of Gerlach. The result of modelling sky brightness from KOP7 is shown in Figure 4.17. The top panel shows the model for an average sky during March 2021 and could be compared to that view from within Gerlach (Figure 4.16, top panel). The most notable difference is the generally dispersed brightness at all azimuths seen within Gerlach is already greatly diminished. The sky brightness ranged from 1.06x to 2.45x the natural background. The average sky brightness is about 1.23x the natural background which corresponds to change in magnitude of -0.22 or a magnitude of 21.77 mag arcsec^{-2} (see Table 4.3). Again, the most significant impact on sky brightness occurs when Black Rock City is active with the average sky brightness increasing to 21.29 mag arcsec^{-2}, as can be seen in the bottom panel of Figure 4.17.

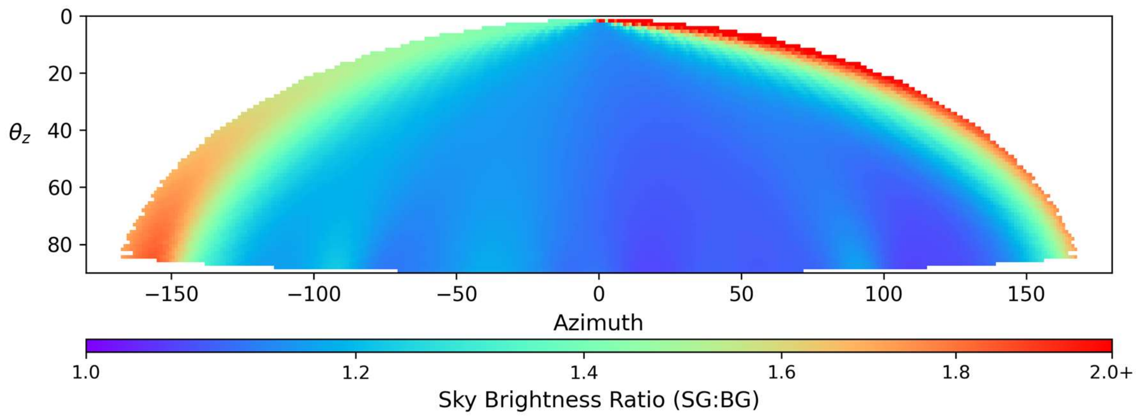

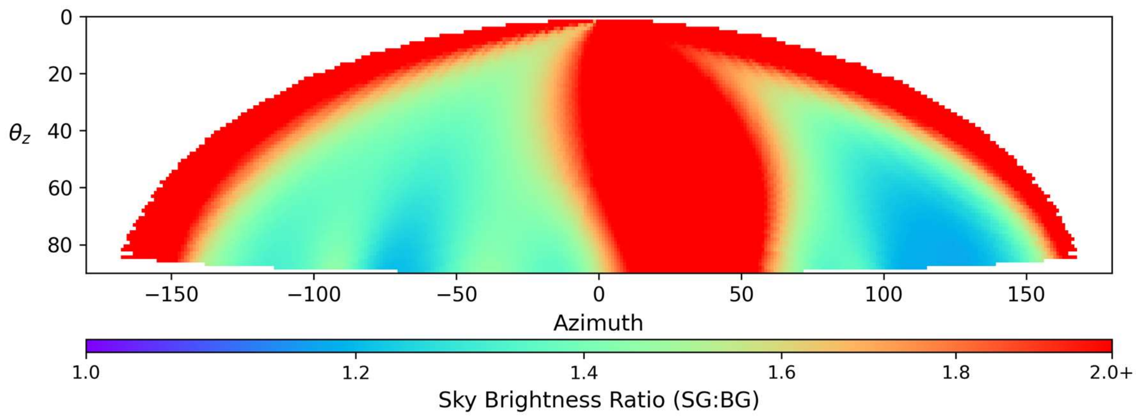

Figure 4. 17. Modelling baseline sky brightness from KOP7. Top panel is the model when Black Rock City is not active. Bottom panel is model when Black Rock City is active.

KOP2 is about 5 km to the north and east of Gerlach on the Black Rock desert playa (see Figure 4.14C, top panel). The same modelling methods were applied, and the results showed an expected slightly darker view. The ratio of sky brightness ranged from 1.02x to 1.92x the natural background (see Figure 4.18). The influence of Gerlach can be seen as the orange plume around the -155° to -169° azimuth. The average ratio was 1.18x the natural background resulting in an average sky brightness of 21.82 mag arcsec^{-2}. This would be a very good dark-sky viewing area despite the close proximity to Gerlach.

The impact of an active Black Rock City would be expected to be even greater at this location which is closer to Black Rock City than the Gerlach site. This can be seen to be the case in Figure 4.18 bottom panel, which shows the model determined from satellite data from August 2019 (during an active Black Rock City). Black Rock City has a bearing of about 50° from KOP2 as can be seen as a large red plume. It can also be observed that the light plume attributed to Gerlach also increases during this period probably reflecting a concurrent increase in activity with the Burning Man festival. The ratio of sky brightness ranged from 1.09x to 8.67x the natural background. The average ratio was 1.93x the natural background resulting in an average sky brightness of 21.29 mag arcsec^{-2} (see Table 4.3). This would be a noticeable degradation in sky quality during this transient event.

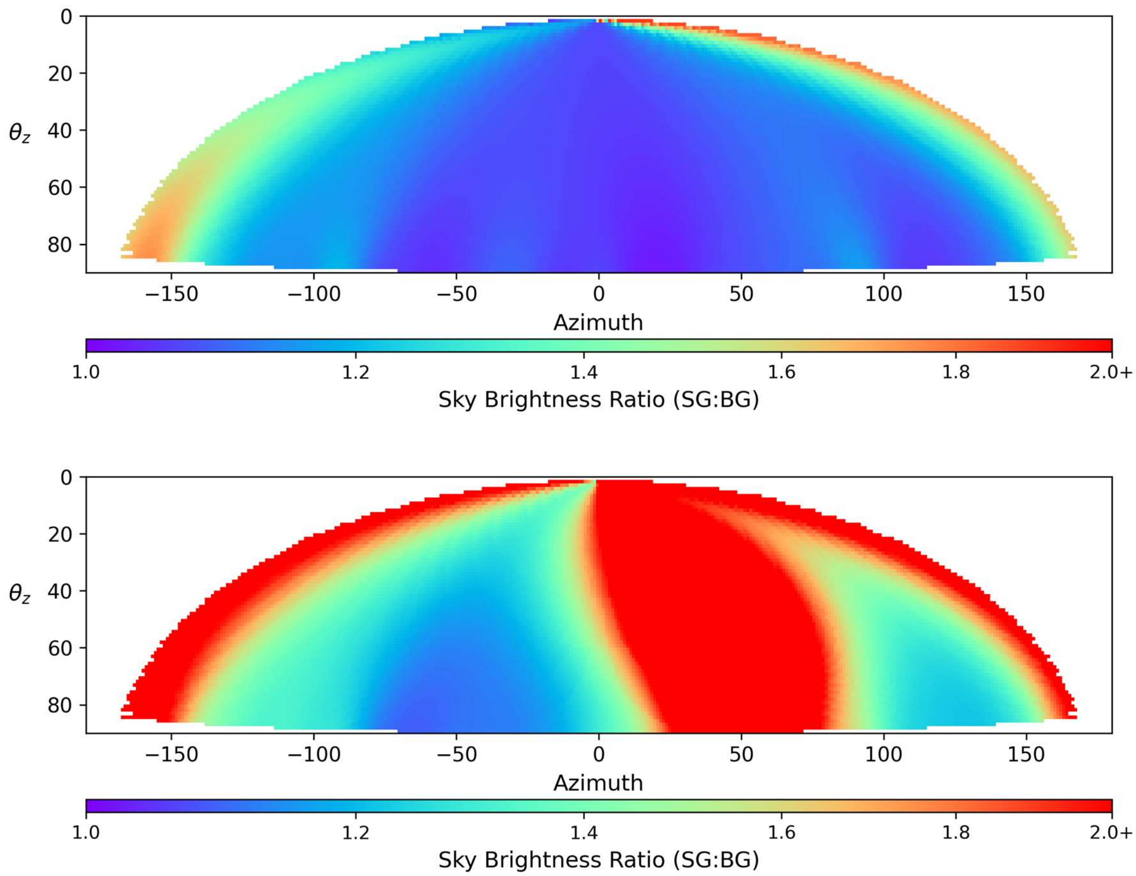

Figure 4. 18. Modelling baseline sky brightness from KOP2. Top panel is the model when Black Rock City is not active. Bottom panel is model when Black Rock City is active.

Table 4. 3. Summary of modelled baseline sky brightness.

	Sky Brightness Ratio						
Model	**minimum**	**maximum**	**mean**	**sd[1]**	**Δ mag**	**mag[2]**	**P[3]**
Viewer Location: Inside Gerlach							
March 2021	1.12	1.84	1.33	0.14	-0.31	21.69	
August 2019	1.27	7.11	1.81	0.75	-0.64	21.36	<0.0001
Viewer Location: KOP7 ~2km SE of Gerlach							
March 2021	1.06	2.45	1.234	0.1994	-0.228	21.772	
August 2019	1.17	6.47	1.920	0.7689	-0.708	21.292	<0.0001
Viewer Location: KOP2 ~5 km NE of Gerlach							
March 2021	1.02	1.92	1.178	0.1633	-0.178	21.822	
August 2019	1.09	8.67	1.930	1.0203	-0.714	21.286	<0.0001

[1]sd, standard deviation

[2]mag, average modelled night sky brightness in mag arcsec^{-2}

[3]Probability the means are the same as the March 2021 mean by *t*-test

Modelling Predicted Sky Brightness Associated with Drilling

This modelling method can be used to predict the impact of test drilling for the geothermal project on sky brightness. This can be accomplished by simulating the expected satellite radiance images associated with drilling prior to modelling with the SET software. Based upon previous empirical measures of test drill rigs and mobile light plants the lumens allotted per test drill pad site were translated to radiance measures in the satellite nighttime image of the Project area (see *Section 3.2 Modelling Sky Brightness near Gerlach* and Appendix E and C). Models were prepared for 3 different drill pads (pad 63-3, 45-16 and 18B-10) and viewed from both key observation points (KOP7 and KOP2). In addition to the expected pad site models were also prepared for a worst-case scenario with 1.5 times the proposed luminance and an alternative lowered luminance that could be achieved by the use of mobile lighting plants utilizing LED bulbs (see Appendix E).

Impact of Drilling at Pad 63-3

The resulting model for test drilling pad 63-3 as viewed from KOP7 is compared to no test drill sites in Figure 4.19 (models for all situations can be seen in Appendix C). The light blue plume at about -38° to -42° is from Gerlach itself with the viewpoint to the east of Gerlach. The brighter plume at about -150° to -180° is primarily from Reno. The impact of the expected drill rig lighting upon the average sky brightness from viewpoint KOP7 (~5.6 km from the drill pad) was not statistically significant with no measurable change in the average brightness (from 22.772 to 22.769 mag arcsec^{-2} with drilling, $P_{(SAME)}$ = 0.236, see Table 4.4). Indeed, bumping the rig luminance to 1.5x expected levels still did not result in a statistically significant change in the average sky brightness in the absence of drilling (from 21.772 to 21.768 mag arcsec^{-2}, $P_{(SAME)}$ = 0.099).

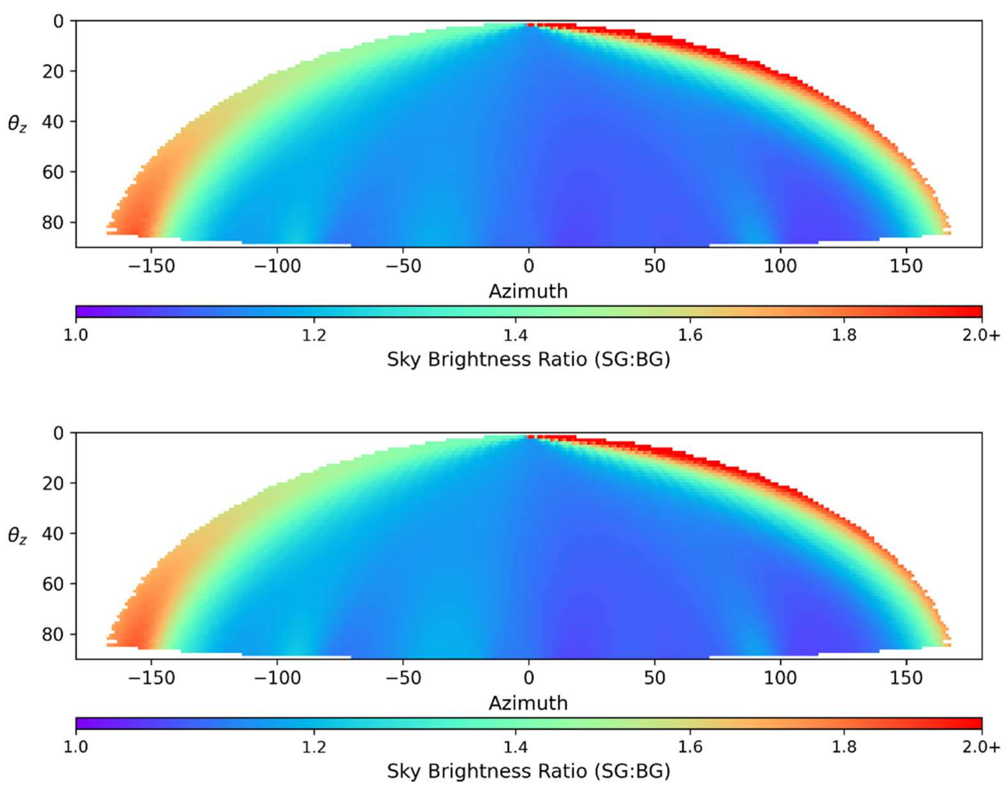

Figure 4. 19. Modelling impact of test drilling at pad 63-3 upon sky brightness for a viewer at KOP7. Top panel is sky brightness from March 2021 with no drilling. Bottom panel shows sky brightness with expected test drilling employing 1,766,000 lumens of lighting. Bearing to drill pad from KOP7 is ~ -15°.

The viewer location will have some impact upon the measured sky brightness. KOP2 is about 5 km to the northeast of Gerlach, NV and only ~2 km from pad 63-3. The model for test drilling pad 63-3 as viewed from KOP2 is compared to no test drill sites in Figure 4.20. The bright plume at about -150° to -180° is primarily from Reno and Gerlach combined. The impact of the expected drill rig lighting upon the average sky brightness from viewpoint KOP2 (~2 km from the drill pad) was statistically significantly different in average brightness compared to no drilling (21.799 mag arcsec^{-2} compared to 21.822 mag arcsec^{-2} with no drilling, $P_{(SAME)}$ <0.0001, see Table 4.4). A rig luminance of 1.5x expected levels also had a statistically significant change in the average sky brightness compared no drilling (21.790 mag arcsec^{-2} compared to 21.822 mag arcsec^{-2} with no drilling, $P_{(SAME)}$ <0.0001). Both compare favorably to the modelled value of 21.822 mag arcsec^{-2} in the absence of drilling with a worst-case brightening of only 0.032 mag arcsec^{-2} (see Table 4.4).

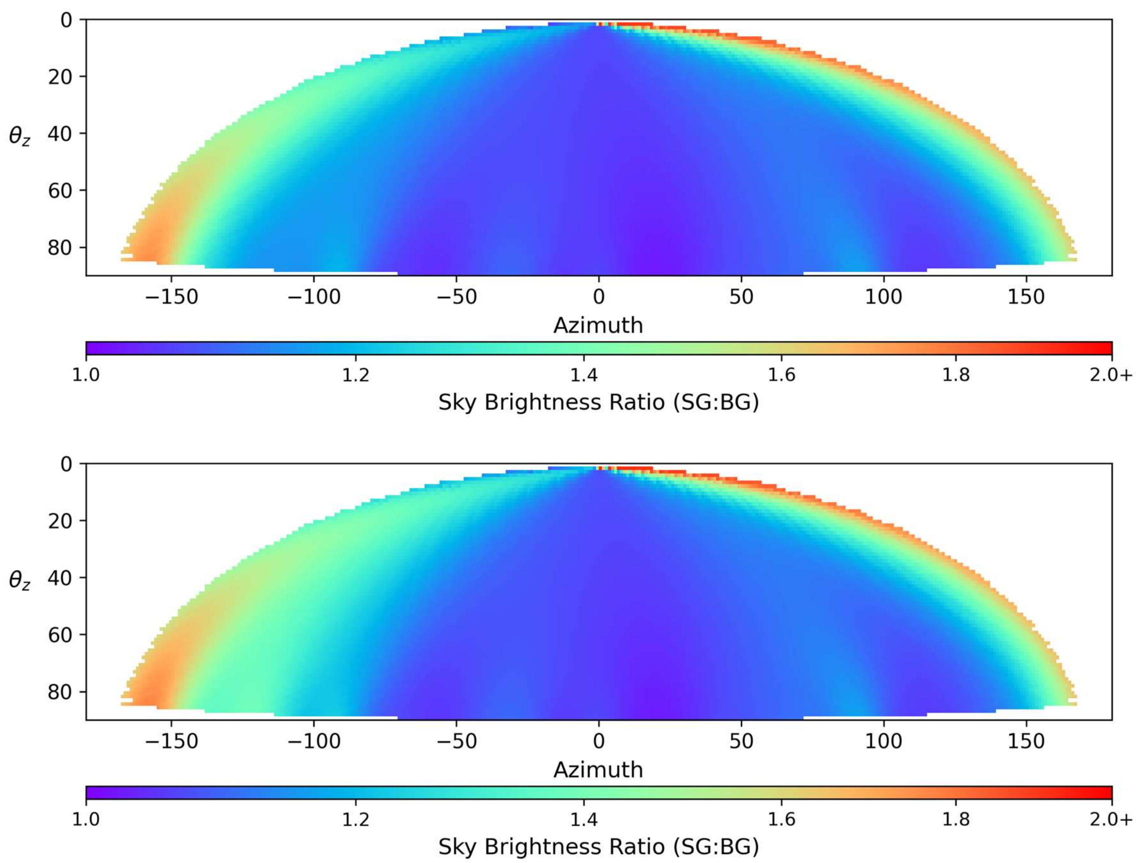

Figure 4. 20. Modelling impact of test drilling at pad 63-3 upon sky brightness for a viewer at KOP2. Top panel is sky brightness from March 2021 with no drilling. Bottom panel shows sky brightness with expected test drilling employing 1,766,000 lumens of lighting. Bearing to drill pad from KOP2 is ~ -115°.

Table 4. 4. Summary of predicted sky brightness modelling for pad 63-3.

Model	Sky Brightness Ratio minimum	maximum	mean	sd[1]	Δ mag	mag[2]	P[3]
Viewer Location: KOP7 ~2km SE of Gerlach							
March 2021	1.06	2.45	1.2344	0.1994	-0.228	21.772	
Expected rig lumens	1.06	2.45	1.2370	0.1983	-0.231	21.769	0.236
1.5x Expected	1.06	2.45	1.2380	0.1980	-0.232	21.768	0.099
LED lighting	1.06	2.45	1.2360	0.1987	-0.230	21.770	0.471
Viewer Location: KOP2 ~5 km NE of Gerlach							
March 2021	1.02	1.92	1.1776	0.1633	-0.178	21.822	
Expected rig lumens	1.03	1.93	1.2036	0.1755	-0.201	21.799	<0.0001
1.5x Expected	1.03	1.93	1.2135	0.1823	-0.210	21.790	<0.0001
LED lighting	1.02	1.93	1.1953	0.1705	-0.194	21.806	<0.0001

[1]sd, standard deviation
[2]mag, average modelled night sky brightness in mag arcsec^{-2}
[3]Probability the means are the same as the March 2021 mean by *t*-test

Observing the changes in the total average sky brightness may "dilute" the impact of the proposed Project compared to looking just in the direction of the drill pad. This possibility prompted an analysis of the impact test drill sites have when viewing directly toward the active drill pad compared to looking away from the drill pad. From the KOP7 viewpoint (see Appendix A) the test pad 63-3 drill sites would be at a bearing of -14° to -17°. This view angle would provide the maximum expected effect of the test drilling. The measured impact for a drill pad with the expected luminance rating was a small but statistically significant change of -0.012 magnitude (from 21.846 to 21.834 mag arcsec^{-2}, P = 0.0046) (see Table 4.5). For comparison, looking away from the pad 63-3 at a view angle of 50 to 53°, resulted in no measurable change to the sky brightness due to drilling activity (see Table 4.5).

The same analysis was applied to the view from KOP2 to the northeast of Gerlach. From this site the Project area has a bearing between -111 to -119°. For the expected drill rig luminance rating, the model predicts a statistically significant change of magnitude from 21.846 to 21.834 mag arcsec^{-2}($P_{(SAME)}$ = 0.0046, see Table 4.5). Looking away from the Project area (i.e., heading 61-69°) resulted in a no statistically significant change of in magnitude ($P_{(SAME)}$ = 1.000). KOP2 is closer to pad 63-3 than KOP7 which may explain the greater impact (nearly a change ~0.1 compared to ~0.01 mag arcsec^{-2}) for observers at KOP2. An observer at KOP2 looking away from the actual drill pad (i.e., 61-69°) would see no statistically significant change in sky brightness with active drilling compared to no drilling (21.831 to 21.828 mag arcsec^{-2}, $P_{(SAME)}$ = 0.6507).

Table 4. 5. Comparison of looking toward drill pad 63-3 with looking away.

Model	View angle (°)	Sky Brightness Ratio mean	error	mag[2]	[1]$P_{(SAME)}$
Viewer Location: KOP7					
March 2021 no drill	-17 to -14	1.1520	0.049	21.846	-
Expected lumens	-17 to -14	1.1650	0.045	21.834	0.0046
March 2021 no drill	50 to 53	1.1840	0.206	21.817	
Expected lumens	50 to 53	1.1840	0.205	21.817	1.0
Viewer Location: KOP2					
March 2021 no drill	-119 to -111	1.3140	0.125	21.704	
Expected lumens	-119 to -111	1.4360	0.061	21.607	<0.0001
March 2021 no drill	61 to 69	1.1680	0.140	21.831	-
Expected lumens	61 to 69	1.1720	0.142	21.828	0.6507

[1]Probability the means are the same as the March 2021 mean by *t*-test
[2]mag, average modelled night sky brightness in mag arcsec^{-2}

Impact of Drilling at Pad 45-16

The resulting model for test drilling pad 45-16 as viewed from KOP7 is compared to no test drill sites in Figure 4.21. The light blue plume at about -38° to -42° is from Gerlach itself with the viewpoint to the east of Gerlach. The brighter plume at about -150° to -180° is primarily from Reno. The impact of the expected drill rig lighting upon the average sky brightness from viewpoint KOP7 (~5.6 km from the drill pad) from 21.772 to 21.768 mag arcsec^{-2} was not statistically significant ($P_{(SAME)}$ = 0.100, see Table 4.6). Raising the rig luminance to 1.5x expected levels resulted in a small brightening from 21.772 to 21.767 mag arcsec^{-2} which was statistically significant ($P_{(SAME)}$ = 0.0257) compared to no rig lighting.

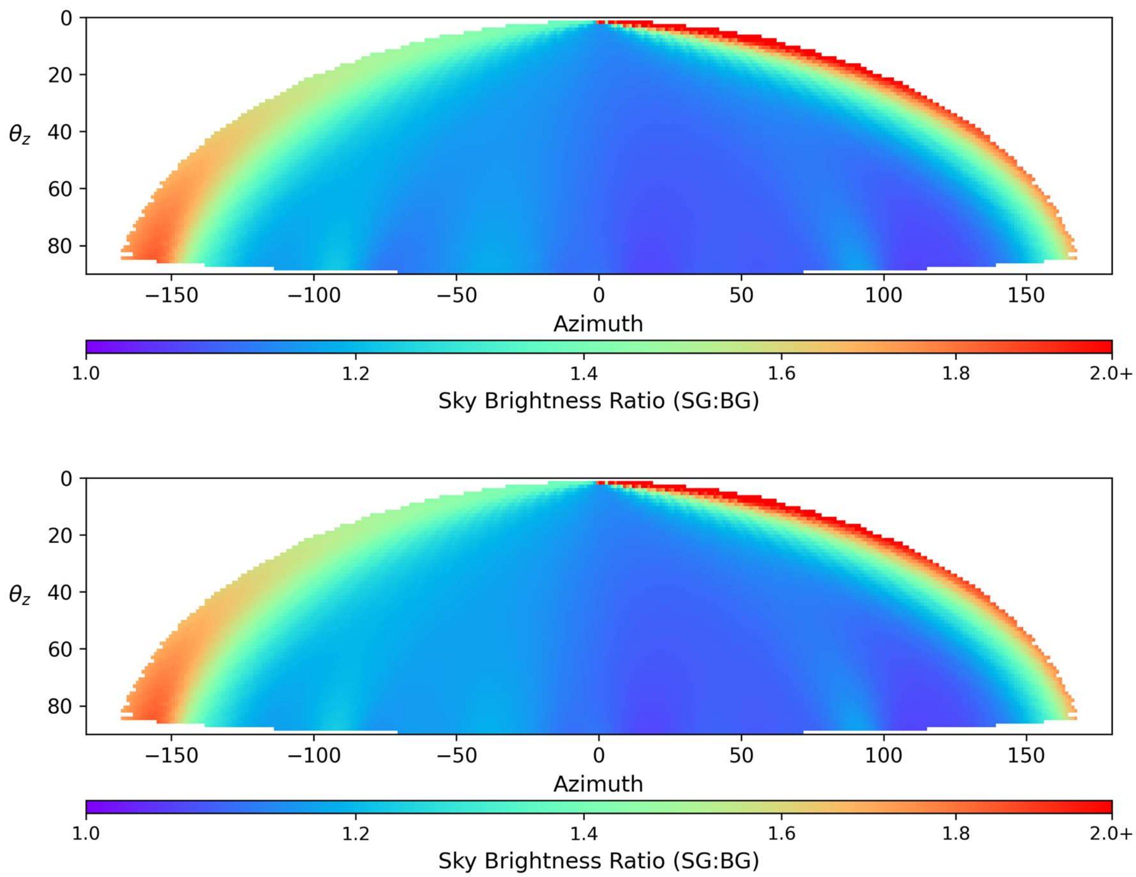

Figure 4. 21. Modelling impact of test drilling at pad 45-16 upon sky brightness for a viewer at KOP7. Top panel is sky brightness from March 2021 with no drilling. Bottom panel shows sky brightness with expected test drilling employing 1,766,000 lumens of lighting. Bearing to drill pad from KOP7 is ~ -63°.

The viewer location KOP2 is about 5 km to the northeast of Gerlach, NV and about ~5.9 km from pad 45-16. The model for test drilling pad 45-16 as viewed from KOP2 is compared to no test drill sites in Figure 4.22. The bright plume at about -158° to -180° is primarily from Reno, Gerlach, Empire and San Emidio combined. The impact of the expected drill rig lighting upon the average sky brightness from viewpoint KOP2 was not statistically significantly different in average brightness compared to no drilling (21.820 for the former compared to 21.822 mag arcsec^{-2} for the latter, $P_{(SAME)}$ = 0.1420, see Table 4.6). A rig luminance of 1.5x expected levels had a statistically significant change in the average sky brightness compared to the absence of drilling (21.819 compared to 21.821, $P_{(SAME)}$ = 0.0477).

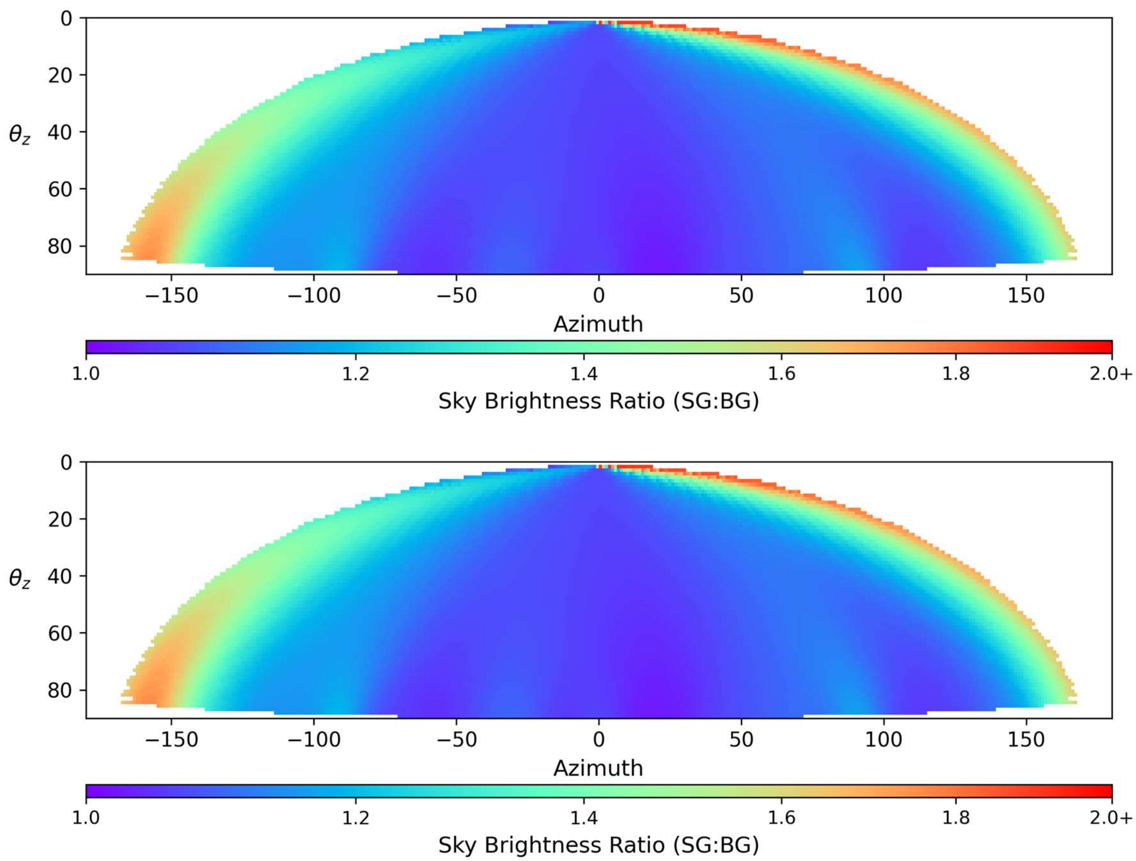

Figure 4. 22. Modelling impact of test drilling at pad 45-16 upon sky brightness for a viewer at KOP2. Top panel is sky brightness from March 2021 with no drilling. Bottom panel shows sky brightness with expected test drilling employing 1,766,000 lumens of lighting. Bearing to drill pad from KOP2 is ~ -141°.

Table 4. 6. Summary of predicted sky brightness modelling for pad 45-16.

	Sky Brightness Ratio						
Model	**minimum**	**maximum**	**mean**	**sd[1]**	**Δ mag**	**mag[2]**	**P[3]**
			Viewer Location: KOP7 ~2km SE of Gerlach				
March 2021 no rig	1.06	2.45	1.2344	0.1994	-0.228	21.772	
Expected rig lumens	1.06	2.45	1.2380	0.1983	-0.231	21.768	0.1000
1.5x Expected	1.06	2.45	1.2393	0.1980	-0.232	21.767	0.0257
LED lighting	1.06	2.45	1.2367	0.1987	-0.230	21.769	0.2985
			Viewer Location: KOP2 ~5 km NE of Gerlach				
March 2021 no rig	1.02	1.92	1.1776	0.1633	-0.1775	21.822	
Expected rig lumens	1.02	1.92	1.1803	0.1661	-0.1800	21.820	0.1420
1.5x Expected	1.02	1.92	1.1812	0.1671	-0.1808	21.819	0.0477
LED lighting	1.02	1.92	1.1793	0.1650	-0.1791	21.821	0.3520

[1]sd, standard deviation

[2]mag, average modelled night sky brightness in mag arcsec^{-2}

[3]Probability the means are the same as the March 2021 mean by *t*-test

From the KOP7 viewpoint (see Appendix A) the test pad 45-16 drill sites would be at a bearing of -61° to -65°. This view angle would provide the maximum expected effect of the test drilling. The measured impact for a drill pad with the expected luminance rating was a small brightening that was not statistically significant (from 21.795 to 21.781 mag arcsec^{-2}, $P_{(SAME)}$ = 0.0645) (see Table 4.7). For comparison, looking away from the pad 45-16 at a view angle of 115 to 119°, resulted in no measurable change to the sky brightness due to drilling activity ($P_{(SAME)}$ = 1.000, see Table 4.7).

The same analysis was applied to the view from KOP2 to the northeast of Gerlach. From this site the Project area has a bearing between -139 to -142°. For the expected drill rig luminance rating, the model predicts a statistically significant brightening from 21.480 to 21.469 mag arcsec^{-2} ($P_{(SAME)}$ = 0.0131, see Table 4.7). Looking away from the Project area (i.e., heading 38-41°) resulted in a non-statistically significant change of magnitude (from 21.869 to 21.868 mag arcsec^{-2}, $P_{(SAME)}$ = 0.9435).

Table 4. 7. Comparison of looking toward drill pad 45-16 with looking away.

Model	View angle (°)	Sky Brightness Ratio mean	error	mag[2]	[1]$P_{(SAME)}$
		Viewer Location: KOP7			
March 2021 no drill	-61 to -65	1.2080	0.103	21.795	-
Expected lumens	-61 to -65	1.2240	0.093	21.781	0.0645
March 2021 no drill	115 to 119	1.2440	0.221	21.763	
Expected lumens	115 to 119	1.2440	0.221	21.763	1.0000
		Viewer Location: KOP2			
March 2021 no drill	-139 to -142	1.6150	0.042	21.480	
Expected lumens	-139 to -142	1.6310	0.039	21.469	0.0131
March 2021 no drill	38 to 41	1.1280	0.143	21.869	-
Expected lumens	38 to 41	1.1290	0.143	21.868	0.9435

[1]Probability the means are the same as the March 2021 mean by *t*-test
[2] mag, average modelled night sky brightness in mag arcsec^{-2}

Impact of Drilling at Pad 18B-10

The resulting model for test drilling pad 18B-10 as viewed from KOP7 is compared to no test drill sites in Figure 4.23. Visually the two models appear equivalent. The light blue plume at about -38° to -42° is from Gerlach itself with the viewpoint to the east of Gerlach. The brighter plume at about -150° to -180° is primarily from Reno. The impact of the expected drill rig lighting upon the average sky brightness from viewpoint KOP7 (~3.8 km from the drill pad) was a brightening of 0.003 mag arcsec^{-2} which was not statistically significant ($P_{(SAME)}$ = 0.0940, see Table 4.8). Raising the rig luminance to 1.5x expected levels resulted in a small brightening of 0.004 mag arcsec^{-2} which was statistically significant ($P_{(SAME)}$ = 0.0255) compared to no rig lighting.

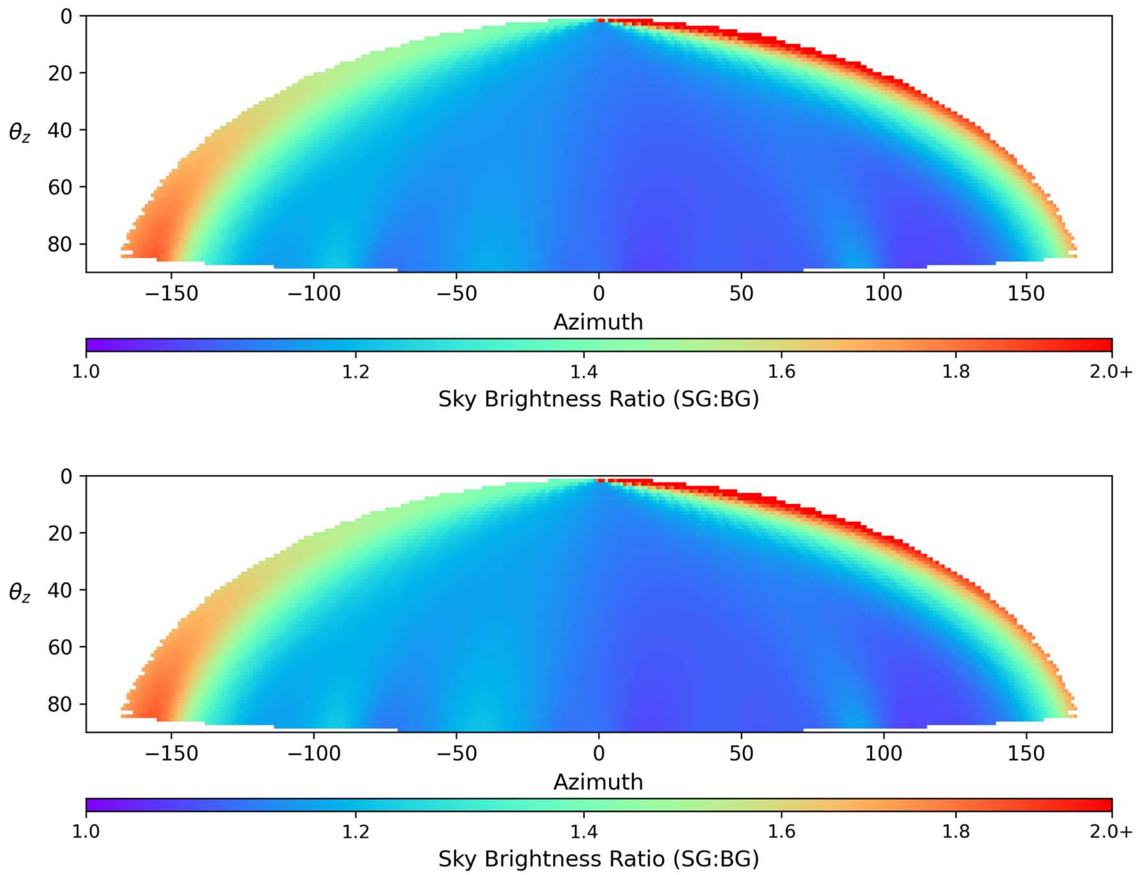

Figure 4. 23. Modelling impact of test drilling at pad 18B-10 upon sky brightness for a viewer at KOP7. Top panel is sky brightness from March 2021 with no drilling. Bottom panel shows sky brightness with expected test drilling employing 1,766,000 lumens of lighting. Bearing to drill pad from KOP7 is ~ -40°.

The viewer location KOP2 is about 5 km to the northeast of Gerlach, NV and about ~4.4 km from pad 18B-10. The model for test drilling pad 18B-10 as viewed from KOP2 is compared to no test drill sites in Figure 4.23. The bright plume at about -158° to -180° is primarily from Reno, Gerlach, Empire and San Emidio combined. The impact of the expected drill rig lighting upon the average sky brightness from viewpoint KOP2 was a statistically significant brightening compared to no drilling (21.819 for the former compared to 21.822 mag arcsec^{-2} for the latter, $P_{(SAME)}$ = 0.0371, see Table 4.8). A rig luminance of 1.5x expected levels had a statistically significant change in the average sky brightness compared to the absence of drilling (21.818 compared to 21.822, $P_{(SAME)}$ = 0.0057).

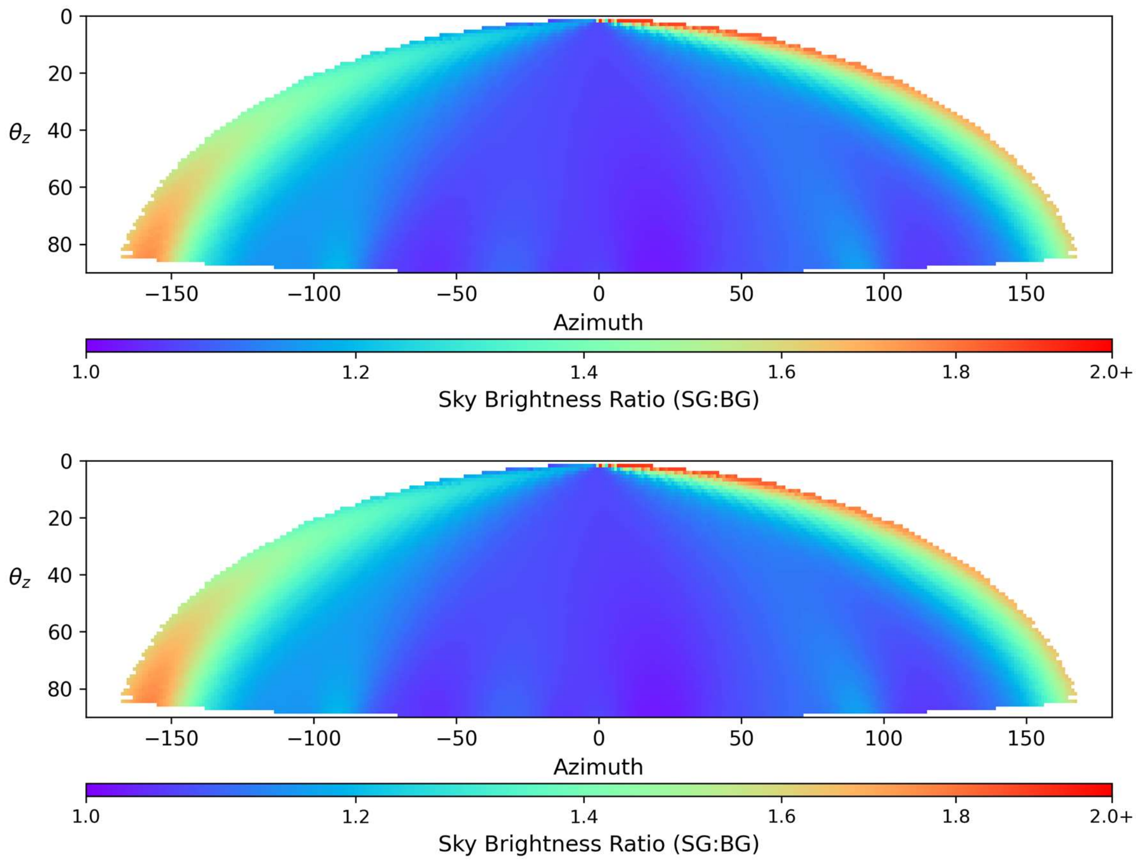

Figure 4. 24. Modelling impact of test drilling at pad 18B-10 upon sky brightness for a viewer at KOP2. Top panel is sky brightness from March 2021 with no drilling. Bottom panel shows sky brightness with expected test drilling employing 1,766,000 lumens of lighting. Bearing to drill pad from KOP2 is ~ -142°.

Table 4. 8. Summary of predicted sky brightness modelling for pad 18B-10.

Model	Sky Brightness Ratio				Δ mag	mag[2]	P[3]
	minimum	**maximum**	**mean**	**sd[1]**			
Viewer Location: KOP7 ~2km SE of Gerlach							
March 2021 no rig	1.06	2.45	1.2344	0.1994	-0.229	21.772	
Expected rig lumens	1.06	2.45	1.2381	0.1982	-0.232	21.768	0.0940
1.5x Expected	1.06	2.45	1.2393	0.1978	-0.233	21.767	0.0255
LED lighting	1.06	2.45	1.2368	0.1986	-0.231	21.769	0.2755
Viewer Location: KOP2 ~5 km NE of Gerlach							
March 2021 no rig	1.02	1.92	1.1776	0.1633	-0.178	21.822	
Expected rig lumens	1.02	1.92	1.1814	0.1675	-0.181	21.819	0.0371
1.5x Expected	1.02	1.93	1.1826	0.1689	-0.182	21.818	0.0057
LED lighting	1.02	1.92	1.1801	0.1660	-0.180	21.820	0.1730

[1]sd, standard deviation
[2]mag, average modelled night sky brightness in mag arcsec^{-2}
[3]Probability the means are the same as the March 2021 mean by *t*-test

From the KOP7 viewpoint (see Appendix A) the test pad 18B-10 drill sites would be at a bearing of -38° to -42°. This view angle would provide the maximum expected effect of the test drilling. The measured impact for a drill pad with the expected luminance rating was a small brightening that was statistically significant (from 21.811 to 21.796 mag arcsec^{-2}, $P_{(SAME)}$ = 0.0028) (see Table 4.9). For comparison, looking away from the pad 18B-10 at a view angle of 138 to 142°, resulted in no measurable change to the sky brightness due to drilling activity ($P_{(SAME)}$ = 1.000, see Table 4.9).

The same analysis was applied to the view from KOP2 to the northeast of Gerlach. From this site the Project area has a bearing between -140 to -143°. For the expected drill rig luminance rating, the model predicts a statistically significant brightening from 21.469 to 21.454 mag arcsec^{-2} ($P_{(SAME)}$ = 0.0003, see Table 4.9. Looking away from the Project area (i.e., heading 38-41°) resulted in a non-statistically significant change of magnitude (from 21.869 to 21.868 mag arcsec^{-2}, $P_{(SAME)}$ = 0.9435).

Table 4. 9. Comparison of looking toward drill pad 18B-10 with looking away.

Model	View angle (°)	Sky Brightness Ratio mean	error	mag[2]	[1]$P_{(SAME)}$
Viewer Location: KOP7					
March 2021 no drill	-38 to -42	1.190	0.069	21.811	-
Expected lumens	-38 to -42	1.207	0.065	21.796	0.0028
March 2021 no drill	138 to 142	1.380	0.185	21.650	
Expected lumens	138 to 142	1.380	0.185	21.650	1.0000
Viewer Location: KOP2					
March 2021 no drill	-140 to -143	1.631	0.037	21.469	
Expected lumens	-140 to -143	1.653	0.037	21.454	0.0003
March 2021 no drill	37 to 40	1.128	0.148	21.869	-
Expected lumens	37 to 40	1.129	0.149	21.868	0.9454

[1]Probability the means are the same as the March 2021 mean by *t*-test
[2]mag, average modelled night sky brightness in mag arcsec^{-2}

5. CONCLUDING COMMENTS

The purpose of this report has been to extract and analyze nighttime satellite data in the vicinity of Gerlach, NV where a geothermal exploration project is proposed. The ALAN in the Project area has been evaluated using nighttime radiance data obtained from satellite based VIIRS radiometers.

5.1 Current Status of ALAN in Northern Nevada

A main objective of this report is to measure the current state of ALAN distribution in northern Nevada in the region around the Project area. Quantitative measures of ALAN provided by regular (nightly) imaging by the sophisticated VIIRS radiometer instrument carried by the Suomi-NPP and NOAA-20 satellites was used as the basis for this analysis. It should be kept in mind that these radiance measures are the amount of light directed upward and are not a direct measure of "sky brightness".

The study area has relatively few centers of human activity which has resulted in northern Nevada being one of the darkest areas in the lower 48 states. The two communities Gerlach and Empire, NV have small populations (~200 people between them) which has resulted in a low contribution of ALAN to the region. While the sum radiances are small (about 14 $nWcm^{-2}sr^{-1}$ for Gerlach and about 74 $nWcm^{-2}sr^{-1}$ for Empire), it is notable that the ALAN is dynamic but displaying an increasing trend over the last 2 years. Growth trends in ALAN are usually associated with population growth, improving economies, and/or increased industrial activity. Although the ALAN in these communities is currently growing at a rate of 10-15% per year, it should be noted that the existing lighting is commendably environmentally sensitive, as measured by the excellent zenith angle curves that both communities exhibit.

The third major center of human activity is Black Rock City associated with the Burning Man event. This is an unusual community that typically forms itself once a year and provides measurable levels of ALAN for only about 6 weeks spanning the construction, 10 days of festival, and a period of dismantling. It should also be noted that even in the absence of the official Burning Man event the occurrence of an unofficial event may take place as happened in August and September of 2021. During these events it is the greatest source of ALAN in the immediate region with sum radiances of up to about 1000 $nWcm^{-2}sr^{-1}$. In addition, the lighting is not environmentally friendly, as measured by the up-turned zenith angle curves.

The Hycroft Mine is a major center of ALAN in the region. The current average sum radiance for the mine is about 290 $nWcm^{-2}sr^{-1}$, nearly three times that of Gerlach and Empire combined. The mine has also shown a clearly increasing trend in ALAN over the last two years (about 17% per year). This increase has paralleled the expansion of mining activities. Mines and quarries often have poor upward lighting profiles, in part due to the high albedo of the exposed terrain. It is, therefore, encouraging and to the mine's credit that their associated ALAN has a good zenith angle curve. The Hycroft Mine has an essentially equivalent ZARI score to the IDA Dark Sky certified community of Sedona, AZ.

Finally, geothermal plants (a very pertinent activity) are producers of ALAN in the region. The closest facilities include Blue Mountain and San Emidio geothermal plants. These plants have similarly low outputs of radiance with current average levels of about 11-16 $nWcm^{-2}sr^{-1}$ (similar to Gerlach). It is particularly notable that these facilities have shown decreasing trends in ALAN over the last two years of about -20% per year. In addition, both facilities are characterized by ALAN with very good zenith angle curves suggesting near optimal environmental performance. The favorable trends in lighting over the last two years may be a result of plant maturation and completion of construction projects.

The overall status of the region regarding ALAN would have to be characterized as currently quite good but dynamic. The installed lighting in both communities and industrial centers is environmentally conscious as evidenced by good to excellent zenith angle dependency measures. However, all major centers of ALAN in the region are experiencing change with the overall trend being growth over the last two years of about 10% per year except for the geothermal industry which has experienced a decrease in ALAN with facility maturation. In terms of absolute size of ALAN, the growth has been dominated by recent expansion in mining activity.

5.2 Projected Impact of Test Drilling Project

The expected impact of the test drilling at a single drill pad upon ALAN can be simulated from the lumen ratings of the proposed lighting strategy for the active drill pad. It should be noted that the Project proposes drilling at only one pad at a time. The lumen rating is converted into the expected radiance calculated from the provided lumens inventory (1,776,000 lumens, see Appendix E) by using a standard curve relating known lumen ratings for similar known rigs and mobile lighting plants and measured radiance. This conversion model indicates that the expected radiance associated with test drilling at a single drill pad would be about 8 $nWcm^{-2}sr^{-1}$ or about 80% as bright as Gerlach, NV. The simulations of drill pad radiance can be further employed to model actual sky brightness.

Modelling sky brightness using the NASA developed SET software [27] suggests that the general region is quite dark being only about 0.2 mag $arcsec^{-2}$ brighter than the Massacre Rim WSA (~0.3 mag $arcsec^{-2}$ when inside of Gerlach). The modelling also confirms that the greatest impact on sky brightness in the region occurs around the time of the Burning Man festival at Black Rock City. Further, the modelling suggests that the test drilling would have a small impact on average sky brightness (from statistically no change to a small but statistically significant change of -0.02 mag $arcsec^{-2}$ depending on viewer location). The impact varies somewhat depending on the location of the observer (distance from drill pad and intervening light sources). The impact also depends upon whether the observer is looking in the exact direction of the drill pad or away from the pad. The modelling indicates that looking away from the pad results in no statistically significant difference in sky brightness with or without drilling. Differences in sky brightness are only measurable when viewing in the direction of the active drill pad and those differences ranged in brightening from 0.011 to 0.097 mag $arcsec^{-2}$. Differences in this range are generally not discernible to the human eye. *[It should be kept in mind that the modelling encompasses zenith angles 0 to 85° and does not consider a direct line of sight to the illuminating light source. Obviously, direct observation of a light source would be noticeable.]*

5.3 ALAN Best Practices for Exploration Project

Examination of satellite images indicates some of the darkest night skies in the continental U.S. lie within a 160 km radius of the proposed drill sites at Gerlach, NV. Night skies that experience significantly reduced levels of ALAN are highly prized by many people for environmental and esthetic reasons; they are also known to be beneficial in some instances for the well-being of nocturnal indigenous or migratory wildlife [31]. It is desirable to plan, implement, and monitor significant new installations of ALAN so as to minimize their most deleterious effects in this regard.

In the case of the Ormat exploratory drilling project near Gerlach, NV there are three activities and elements that were identified by BLM as at potential risk from associated ALAN: 1) astro-tourism, 2) wildlife, and 3) areas with wilderness characteristics. We will briefly address issues associated with each of the three, and then indicate best practices for minimizing ALAN.

5.3.1 Astro-tourism

There are apparently no major professional optical astronomy observatories currently operating within a 160 km radius of Gerlach, NV. The principal astronomical impact of the proposed project will thus fall on the amateur astronomical community. Amateur astronomy is an activity that embraces many different interests and a wide diversity of applications and commitments. To understand impacts and mitigations it is necessary to have some notion of the scope of these activities.

Amateur astronomy can run the gamut from casual unaided visual examination of the sky (constellation study, meteor or comet observation, etc.) to photographic or spectroscopic imaging of discrete regions of the sky using highly sophisticated telescopes and camera equipment. Between these extremes are a range of usually visually aided observing programs that often fall into the realm of so-called "star parties". All these activities have legitimate values and are quite important to serious, or even amateur, devotees.

Astro-tourism, as it relates to nighttime astronomy, generally involves of a quest for dark skies. The virtue of such skies is their provision of higher contrast levels for celestial objects of a range of brightness compared with the adjacent sky background brightness. Simply put, dark skies allow one to see fainter stars and hence larger numbers of stars. If celestial objects are the "signal" one seeks, and the sky brightness is the associated "noise", then dark skies have the highly desirable effect of increasing the signal to noise ratio (SNR). Conversely, the introduction of ALAN will, to one degree or another, diminish the SNR.

The extent to which this is a problem, or even a noticeable effect, depends not only on the nature of the ALAN under discussion, but on the nature of the astronomical activity. Delving into this subject in any detail is well beyond the scope of this report, but we can discuss specific mitigations of the proposed drill project that can be helpful across the entire spectrum of astronomical activity.

Since this project focuses on the Gerlach, NV region it is worth understanding where astro-tourism is most likely to take place, or at least be impacted by local ALAN. A Google search reveals three amateur astronomy clubs in the state of Nevada: 1) Western Nevada Astronomical Society (Carson City, NV), 2) Las Vegas Astronomical Society (Las Vegas, NV), and 3) Astronomical Society of Nevada (Sparks, NV) [17]. There are quite likely others, but these seem to have the highest Web profiles.

A list of favored dark sky observing locations in the Nevada area used by members of these clubs is as follows [18]: 1) Black Rock Desert, 2) Cathedral Gorge, 3) Death Valley, 4) Galena Creek SP, 5) Grand Canyon-Parashant NM, 6) Great Basin NP, 7) Massacre Rim WSA, 8) Sand Mountain, and 9) Tonopah Star Park. The Black Rock Desert and Massacre Rim WSA are about 5km and about 115 km from the study area, respectively. The other areas are well beyond the geographic scope of study area.

One objective of this report is to determine baseline sky brightness of the region of interest. In the case of the planned exploratory drill site lighting there is another, more nuanced, affect that can potentially diminish the astronomical viewing opportunities afforded by the region. For purposes of completeness, it is important to note how this effect comes into play. Depending upon the viewing location and the direction of observation the drill rig lights may or may not be visible in the instantaneous field of view (FOV). If the lights are in the observer's FOV, and especially if they are nearby, then the lights may diminish the ability of the observer's eye to accommodate for optimal night vision (the pupils will close to some extent to accommodate the bright drill lights). This will have the effect of decreasing the limiting magnitude of the faintest observable stars even though the night sky will give the impression of being even darker than it really is. In this instance special emphasis on shielding direct light from the viewer's position, often meaning directing the light below 90 – 120° zenith angle would minimize impacts on night sky viewing.

5.3.2 Wildlife

This project is not a survey of wildlife or its distribution and behavior in the area of interest (~160 km radius of Gerlach, NV). Instead, it is an acknowledgement that ALAN is known to have several negative effects on a wide range of animal species including mammals, birds, reptiles, and insects [31]. For more information on wildlife in the Project area, please refer to the Biological Resources Baseline Report prepared for the proposed Gerlach Geothermal Exploration Project Environmental Assessment.

There are 488 species of birds that live, visit, and breed in the State of Nevada. Several hundred thousand of those birds migrate in Spring and Fall along the Pacific Flyway between Alaska and Patagonia and many can be seen throughout the state. Sites listed by the Audubon Society as Important Bird Areas (IBA) include the Bilk Creek-Montana Mountains IBA NE of Gerlach, the Pyramid Lake IBA and Lahontan Valley Wetlands IBA south of Gerlach, and the Black Rock Desert just north of Gerlach [15, 16].

The role of high-intensity lights in the disruption of bird migration, and the mortality of bird populations has been documented in many studies [cf. 34]. Principal mitigations of light effects on such wildlife include several protocols outlined in *Section 5.3.4 ALAN Best Management Practices* below.

5.3.3 Areas with Wilderness Characteristics

The Wilderness Act, which was signed into law by President Lyndon B. Johnson on September 3, 1964 states, **"…..wilderness, in contrast with those areas where man and his works dominate the landscape, is hereby recognized as an area where the earth and its community of life are untrammeled by man, where man himself is a visitor who does not remain....[L]and retaining its primeval character and influence, without permanent improvements or human habitation, which is protected and managed so as to preserve its natural conditions…"[35].** However, it should be noted that there are no designated Wilderness Areas in the vicinity of the Project area

A substantial part of the Nevada desert surrounding Gerlach is both sparsely populated and extremely dark at night. The adjacent Massacre Rim Wilderness Study Area, NW of Gerlach, is a part of only 2.7% of the landmass of the continental United States that is federally protected. The immense value of these lands is both subjective and unquantifiable.

With regard to ALAN the best realistic protections for areas with wilderness characteristics are to preserve the very dark zenith skies and to restrain the growth of high zenith angle sky brightness. Several protocols that help achieve these goals are outlined in *Section 5.3.4 ALAN Best Management Practices* below.

5.3.4 ALAN Best Management Practices

The installation of new, nighttime light sources, particularly in the case of environmentally sensitive areas, can benefit from implementation of a plan of best management practices geared toward minimizing the deleterious impacts of ALAN. The specific practices to be followed can be dependent upon many variables and must be organized with consideration to the scope of the project, the nature of the environment, and various pressures that are brought to bear with regard to eventual outcomes.

Such practices should be given careful consideration. ALAN impacts that may seem negligible to one party may be viewed with alarm by another. A perfect example accrues to astronomical interests in the night sky where one can argue that a hypothetical increase in sky background of 0.05 mag arcsec^{-2} is not visually observable, while some in the astronomical community look at the same data and become exercised over the cumulative effects of additional photons being added to the night sky.

Presented here is a list of proven strategies that can provide substantial and quantifiable reductions in ALAN environmental impacts. The strategies are listed generally in order of greatest to least benefit, though it is recognized that some may not be feasible or deemed necessary to implement as noted below. Some of these strategies (specifically items 3, 5, 8, and 9) have already been incorporated in some degree into the Project planning.

1. Field-verify the use of best lighting practices by an ALAN monitoring program. Benefits all of the above applications. Two strategies lend themselves well to this effort: 1) to construct the most comprehensive baseline of ALAN data possible, and 2) to repeat at least appropriate subsets of the baseline measurement protocols as time and events dictate. This protocol enables several analyses: 1) do the actual light installations meet expectations? 2) are there specific light sources that are

noticeably out of specification, and 3) are there unexpected ALAN characteristics of the site that need mitigation? This is arguably the single most important mitigation strategy to implement for the simple reason that in its absence one has no homogeneous quantitative data with which to measure performance.

2. Do not work the drill site during sundown hours. Benefits all of the above applications. This is the simplest mitigation of all but is understood in some instances to be not economically or operationally feasible.

3. Limit the number of concurrent drill sites being worked. Benefits all of the above applications. This is essentially a reasonable compromise of 2 above. The current plan is to operate at a single drill pad at a time rather than have several illuminated concurrently. This should be considered a significant mitigation already in place.

4. Reduce total lumens emitted by drill rig light fixtures. Benefits all of the above applications. This could be a significant mitigation but must be thoughtfully balanced against operational safety issues. The issue of excess ALAN is a relatively recent concept that may not have been given thoughtful consideration by most drill rig operators before, leaving some room for such mitigation while not impairing site safety [3]. A specific example would be an evaluation of the operational feasibility of substituting the reduced lumen LED configured mobile light plants for the proposed metal halide mobile light plants.

5. For the generator/mast-mounted portable lighting maximize downward pointing of the light source fixtures to illuminate only the relevant work area. Benefits all of the above applications; perhaps especially astronomy and wildlife applications. In these instances, above-the-horizon light is both wasted energy and a significant source of *bona fide* light pollution.

6. As much as possible, all of the rig lighting should have its above-horizon components fully shielded. Benefits all of the above applications. With some careful attention this is perhaps one of the simplest to implement and most effective of mitigations.

7. Implement the use of surfactants. Benefits all of the above applications; perhaps most astronomy. A significant contributor to nighttime sky glow can be reflection of light from ground surfaces. The albedo of ground surface can vary considerably and can be reduced by application of light absorbing surfactants, thus diminishing the amount of light reflected upward into the night sky.

8. Reduce dust production (e.g., by wetting the roads carrying traffic in the immediate drill site) to reduce light scattering to surrounding viewpoints. This might be most beneficial for astronomy applications. Some of the astronomical sites in Section 5.3.1 (notably Black Rock Desert) can experience significant airborne dust.

9. Limit vehicular traffic to drill sites at night; position equipment and materials at the drill site during daytime hours. Perhaps of most benefit to astronomy. Vehicle headlights, especially in newer vehicles, can be a significant source of horizontally directed short-wavelength (blue) light, which can be deleterious to astronomical viewing.

10. Control color of lighting (manage the spectral energy distribution (SED) of the light emitted by rig lights). Benefits all of the above applications; perhaps most astronomy and wildlife. This is a nuanced topic beyond the scope of this report. There are two relevant issues: 1) in the case of wildlife impacts it is known that excessively blue light (short wavelength LEDs) can have deleterious effects especially on nocturnal animal migrations, and 2) in the case of astronomical impacts there are optical filters that can in some instances help mitigate effects of bright sky backgrounds for some

types of astronomical observation. In the latter instance this involves matching rig light output to appropriate wavelength-blocking filters.

11. Limit drilling activity during peak bird migration periods either by season or not during the night during migration season. Principally provides potential benefits for the wildlife application.

5.4 Report Limitations

While quantitative measurement and analysis of the baseline data for the region of interest in this report is secure and repeatable, projections as to what a range of new field installations of drill rig lights will look like is subject to much greater uncertainty. Some of the sources of uncertainty are noted below:

- Projected simulations of ALAN sources are dependent upon empirical calibration curves. Those calibrations may introduce errors depending upon the comparative shielding of the lights used for calibration and those used on the proposed field installations. We addressed this issue by doing the simulations for a range of light output that is likely to bracket that which will be experienced for the actual installations. This approach can be validated by follow-up satellite radiance observation of the new field installations.

- Field installations of drill rig lighting can change on an *ad hoc* basis, depending upon specific needs of a given site, or the status of equipment maintenance and configuration. To the extent that such future installations differ from the specifications provided for this study the field results can manifest as a deviation from the projected radiance simulations. We note that follow-up satellite monitoring can readily detect such deviations and provide valuable information for implementation of simple mitigations.

- Satellite zenith angle measurements provide a simple validation of shielding protocols that can ensure minimal intrusion of ALAN into night sky brightness. However, because of their high zenith angle limitations they provide less useful information on emissions at ZA ~ 80-90°. Emissions in this range can be particularly deleterious to human night vision response, giving the impression of a much brighter sky than is actually present. This is especially problematical for people attempting to observe an otherwise dark sky while in close proximity to, and looking toward, the ALAN light source. This problem can be minimized by monitoring ZA brightness of the actual field installation and ensuring the most favorable shielding and pointing of the lights.

- While satellite radiance data are not a measure of sky brightness, they are, to first order, related to it. Numerous attempts have been made to provide high fidelity transformations of radiance data to sky brightness and NASA now offers access to the SET modeling software for accomplishing that goal. That tool has been used for this report to model the expected relative sky brightness arising from the proposed drill site operations, but it must be remembered that these are models that embody a number of approximations and assumptions and may deviate from the actual sky brightness. Interestingly, this can also be tested after the fact by actual sky brightness measurements.

LITERATURE CITED

1. Aubé M. (2015). Physical behaviour of anthropogenic light propagation into the nocturnal environment. Philosophical transactions of the Royal Society of London. Series B, Biological sciences, 370(1667), 20140117. https://doi.org/10.1098/rstb.2014.0117.
2. BLUE MOUNTAIN. (2021). Energy.Gov. https://www.energy.gov/lpo/blue-mountain
3. Craine, B.L. and Craine, E.R., "Light Emitting Diodes and Astronomical Environments: Results from in situ Field Measurements" Proc. SAS, 34, eds Warner, Bucheim, Foote, and Mais, 39 – 45 (2015).
4. Dark sky bill would protect stargazing for Nevada residents. (2021, February 23). Las Vegas Review-Journal. https://www.reviewjournal.com/news/politics-and-government/2021-legislature/dark-sky-bill-would-protect-stargazing-for-nevada-residents-2287001/
5. Empire, Nevada Population 2021 (Demographics, Maps, Graphs). (n.d.). World Population Review. Retrieved August 12, 2021, from https://worldpopulationreview.com/us-cities/empire-nv-population.
6. Falchi, Fabio; Cinzano, Pierantonio; Duriscoe, Dan; Kyba, Christopher C. M.; Elvidge, Christopher D.; Baugh, Kimberly; Portnov, Boris; Rybnikova, Nataliya A.; Furgoni, Riccardo (2016): Supplement to: The New World Atlas of Artificial Night Sky Brightness. V. 1.1. GFZ Data Services. https://doi.org/10.5880/GFZ.1.4.2016.001
7. Garstang, R. H. Model for Artificial Night-Sky Illumination. Publ. Astron. Soc. Pac. 98, 364 (1986).
8. Gerlach, Nevada Population 2021 (Demographics, Maps, Graphs). (n.d.). World Population Review. Retrieved August 12, 2021, from https://worldpopulationreview.com/us-cities/gerlach-nv-population.
9. Godin, R. Joint Polar Satellite System (JPSS) VIIRS cloud mask (VCM) algorithm theoretical basis document (ATBD). Joint Polar Satellite System (JPSS) Ground Project, Code 474, Doc. 474-00033. (2014).
10. Hammer projection - Wikipedia. (2021). Wikipedia. https://en.wikipedia.org/wiki/Hammer_projection.
11. Henderson, V., Storeygard, A., & Weil, D. N. (2011). Measuring Economic Growth from Outer Space. American Economic Review, 102 (2012), 994 – 1028.
12. http://www.bd-er.com/wp-content/uploads/2019/07/NLV_0119.pdf.
13. http://www.farnell.com/datasheets/1561590.pdf.
14. http://www.ofm.wa.gov/sites/default/files/public/dataresearch/pop/april1/ofm_april1_poptrends.pdf
15. https://nevadamagazine.com/issue/march-april-2019/9281/.
16. https://www.audubon.org/important-bird-areas/pyramid-lake
17. https://www.go-astronomy.com/astro-clubs-state.php?State=NV
18. https://www.go-astronomy.com/dark-sky-parks-stargazing-state.php?State=NV
19. https://www.westinghouselighting.com/pdfs/products/3707300_spec.pdf.
20. Hycroft Gold Mine Expansion Project, Nevada, USA. (2019, November 28). Mining Technology | Mining News and Views Updated Daily. https://www.mining-technology.com/projects/hycroft-mine-expansion-project-nevada/[Accessed 15 July. 2021].
21. IES TM-15-11. Luminaire Classification System for Outdoor Luminaires. Illuminating Engineering Society (2011)
22. Kocifaj M. (2017) Retrieval of angular emission function from whole-city light sources using night-sky brightness measurements, Optica 4, 255-262.
23. Luginbuhl C.B., et al (2009) From the Ground Up II: Sky Glow and Near-Ground Artificial Light Propagation in Flagstaff, Arizona, PASP 121 204
24. Massacre Rim (U.S.) | International Dark-Sky Association. (2019). Darksky.org. https://www.darksky.org/our-work/conservation/idsp/sanctuaries/massacre-rim-wilderness-study-area/
25. Mellander, C., Lobo, J., Stolarick, K., & Matheson, Z. (2015). Night-time light data: A good proxy measure for economic activity? PloS one, 10(10), e0139779.
26. Mills, S., Weiss, S. & Liang, C. VIIRS day/night band (DNB) stray light characterization and correction. in Earth Observing Systems XVIII 8866, 88661P (International Society for Optics and Photonics, 2013).
27. NASA software. (2021). NASA Technology Transfer Program. https://software.nasa.gov/software/LAR-19184-1. (Accessed 8 Jul 2021).
28. NOAA's Comprehensive Large Array-data Stewardship System. Available at: https://www.class.ncdc.noaa.gov/saa/products/welcome. (Accessed: 16th November 2017)

29. NPP Mission Overview | NASA. Available at: https://www.nasa.gov/mission_pages/NPP/mission_overview/index.html. [Accessed: 30th November 2017]
30. Ormat Technologies Inc. - Ormat Technologies Inc. - Global Projects. (2021). Ormat Technologies, Inc. https://www.ormat.com/en/projects/all/main/Default.aspx?Country=USA&Seg=0&Tech=6&pageNum=1[Accessed 15 July. 2021].
31. Rich, C., and T. Longcore (editors.). 2006. Ecological Consequences of Artificial Night Lighting. Island Press, Washington, DC.
32. The International Dark-Sky Association (IDA). International Dark-Sky Association, 2 Oct. 2018, darksky.org/our-work/conservation/idsp/communities/sedona/ [Accessed 26 Oct. 2018].
33. TIGER/Line® with Data. Available at: https://www.census.gov/geo/maps-data/data/tiger-data.html. (Accessed: 15th November 2017)
34. Van Doren, B.M., Horton, K.G., Dokter, A.M., Klinck, H., Elbin, S.B., and Farnsworth, A. 2017, Proc. Nat'l Acad. Sci., vol. 114, no. 42, 11175-11180.
35. Wilderness Connect. (1964, September 3). Wilderness Connect, from https://wilderness.net/learn-about-wilderness/key-laws/wilderness-act/default.php [Accessed August 28, 2021].

APPENDICES

APPENDICES FIGURES

APPENDICES TABLES

APPENDIX A. MAP OF REGIONS OF INTEREST.

Nighttime Lighting Overview

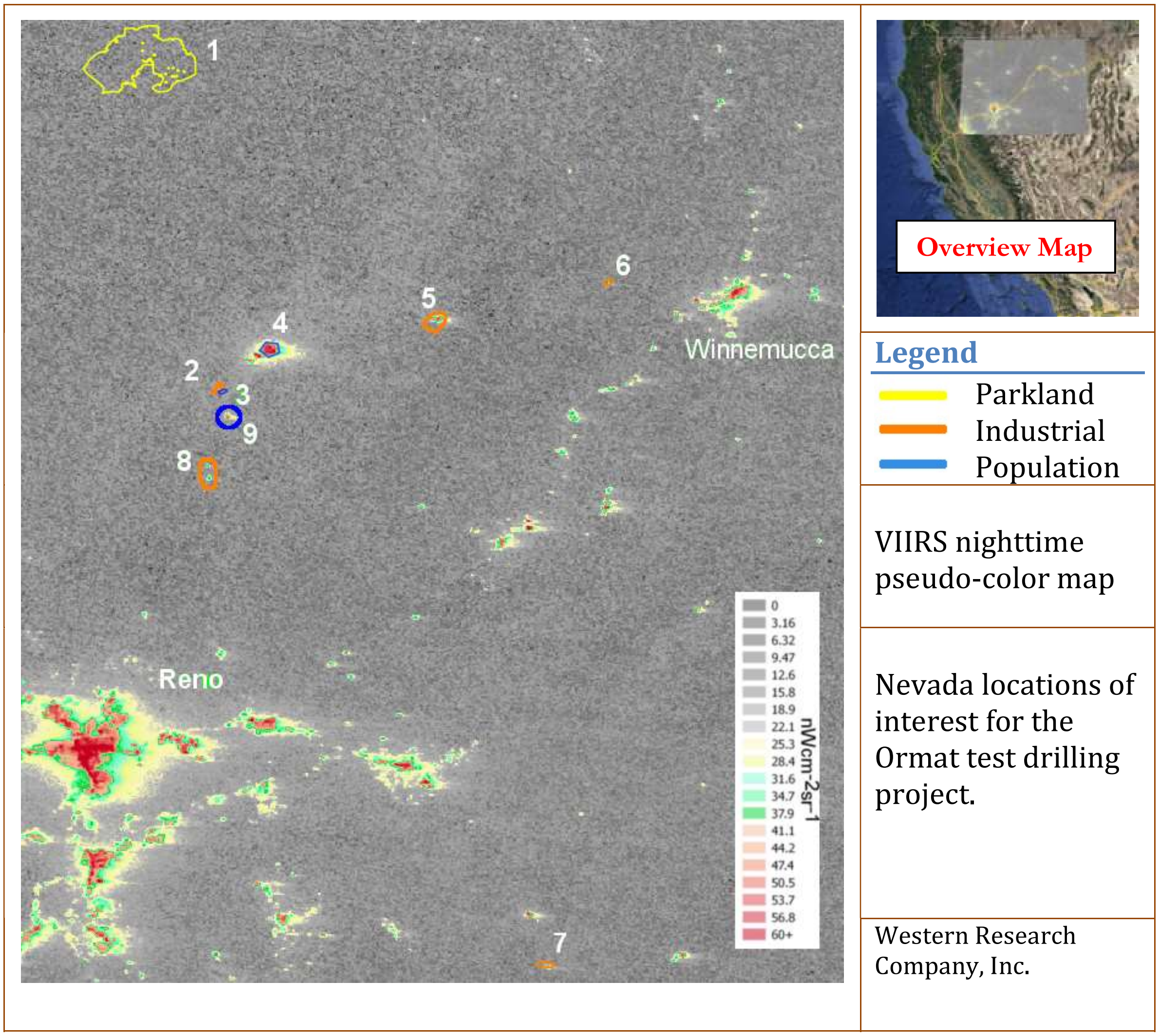

Figure A1. Overview map

ID	Location
1	Massacre rim WSA
2	Project area
3	Gerlach
4	Black Rock City
5	Hycroft Mine
6	Blue Mountain Geothermal
7	Don A. Campbell Geothermal
8	San Emidio Geothermal
9	Empire

Viewpoint Orientation

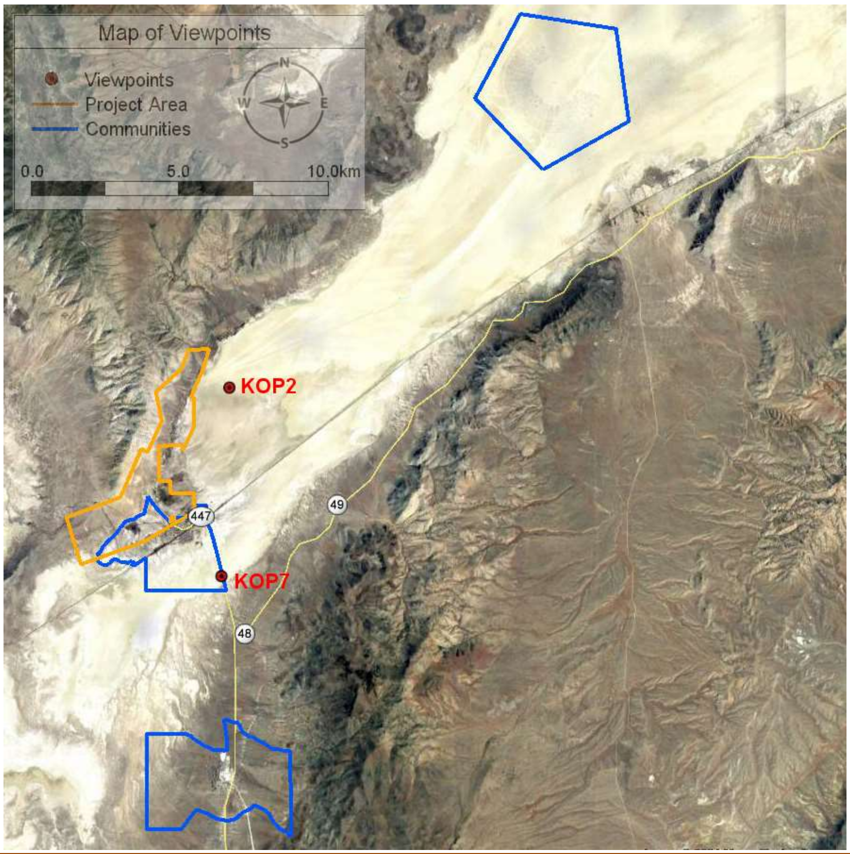

Terrain map

Location of selected viewpoints relative to Project area.

Western Research Company, Inc.

Figure A2. Key observing points map.

Gerlach Viewpoint Detail

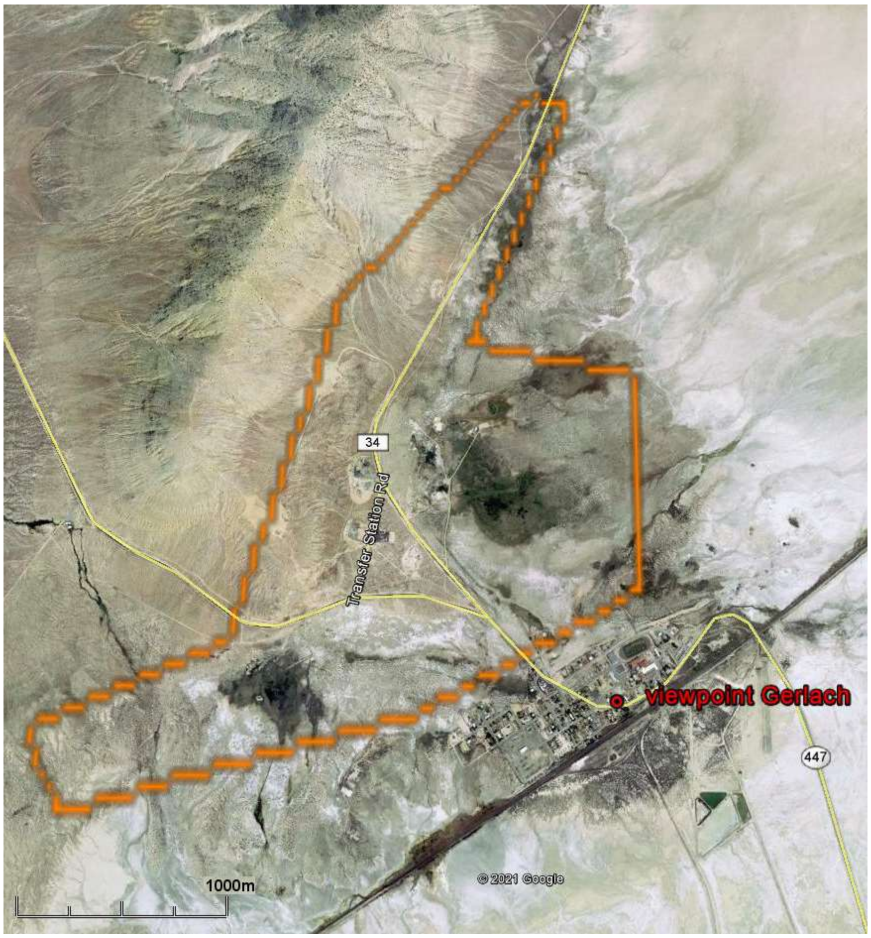

Legend

Viewpoint
Project area

Terrain map

Gerlach viewpoint detail map.

Western Research Company, Inc.

Figure A3. Gerlach, NV viewpoint.

Viewpoints and Drill Pad Locations

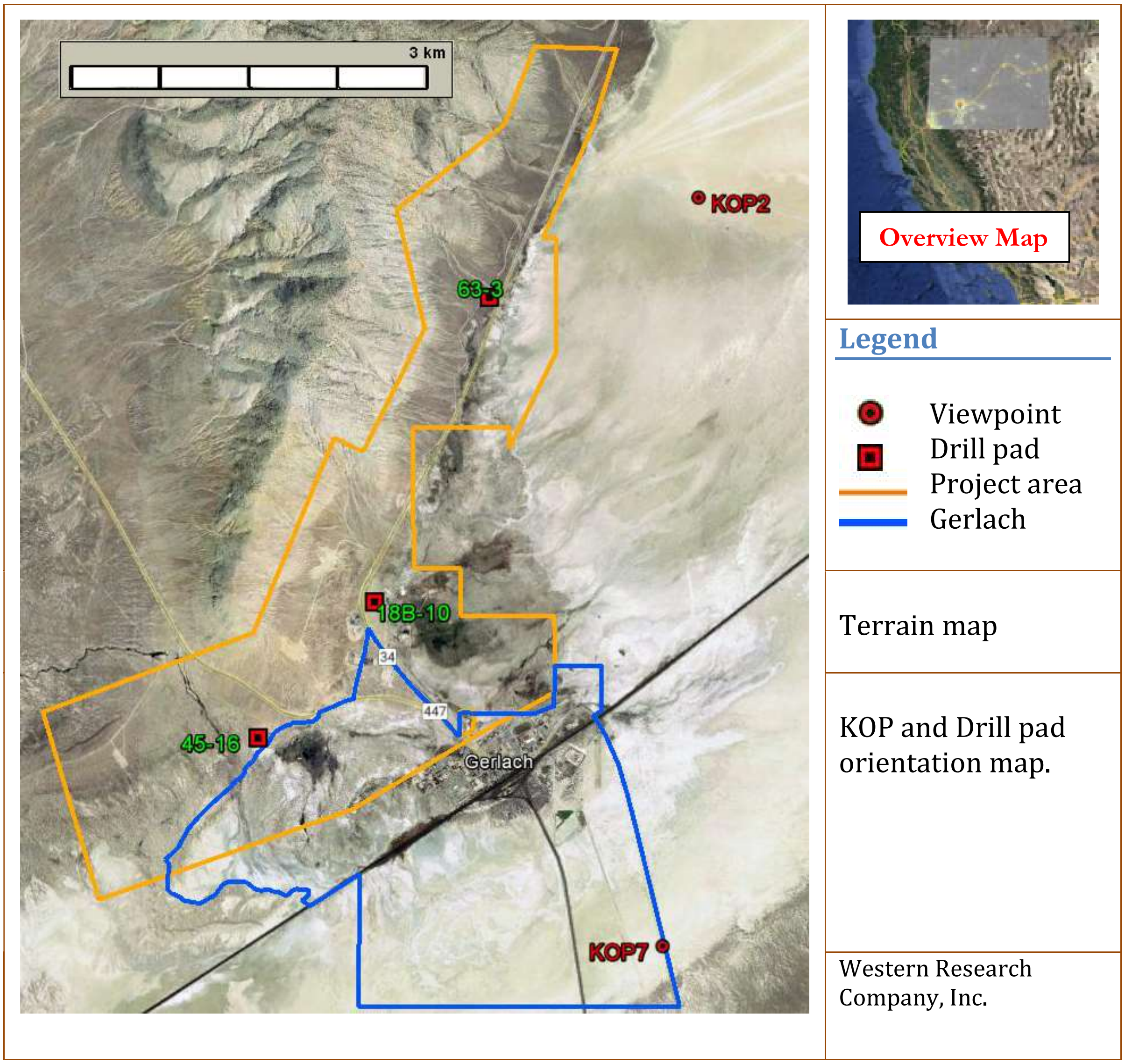

Figure A.4. Viewpoints and drill pad locations.

APPENDIX B. SIMULATED SATELLITE IMAGES WITH DRILL SITES.

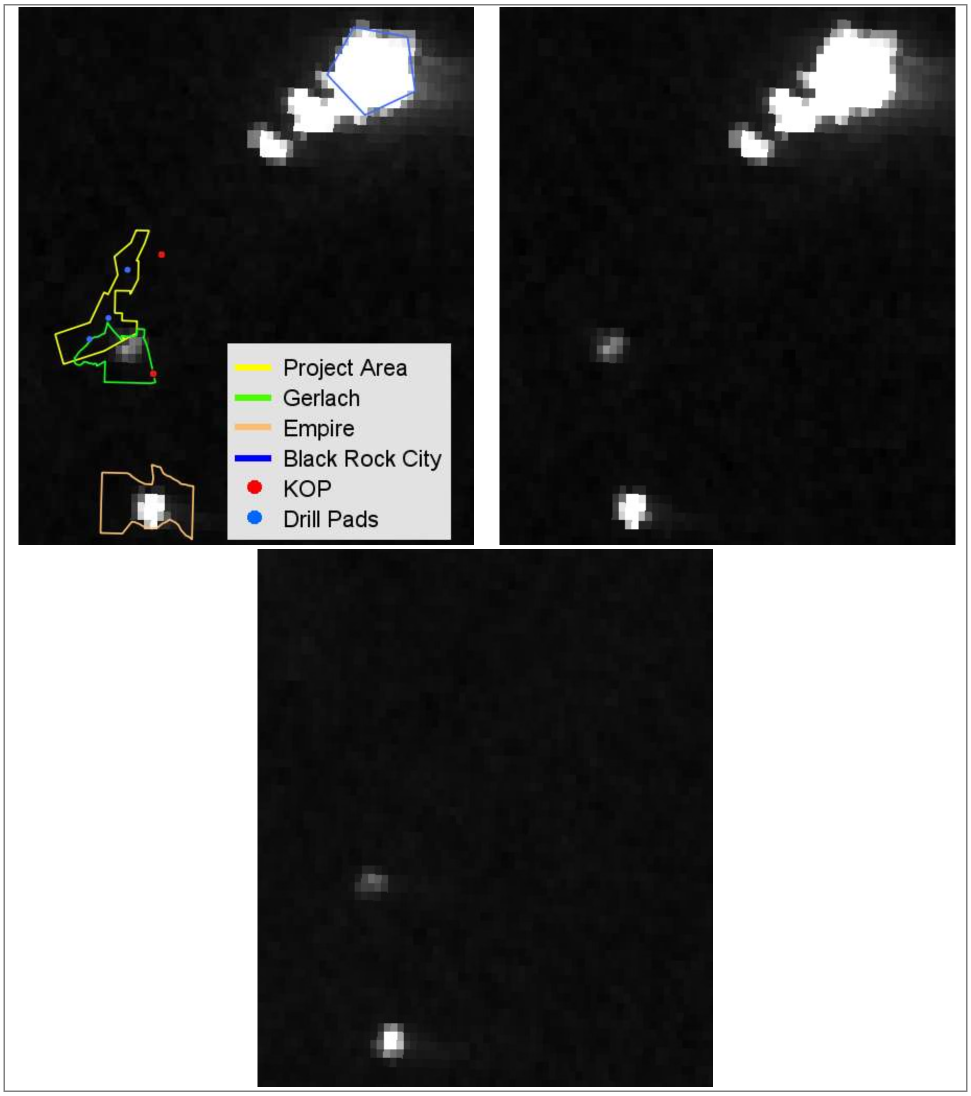

Figure A5. Satellite baseline image of Project area. The top left panel is an orientation image with key landmarks. The top right panel is a baseline image while Black Rock City is active (August 2019). The bottom panel is a recent image of the average nighttime lights during March 2021.

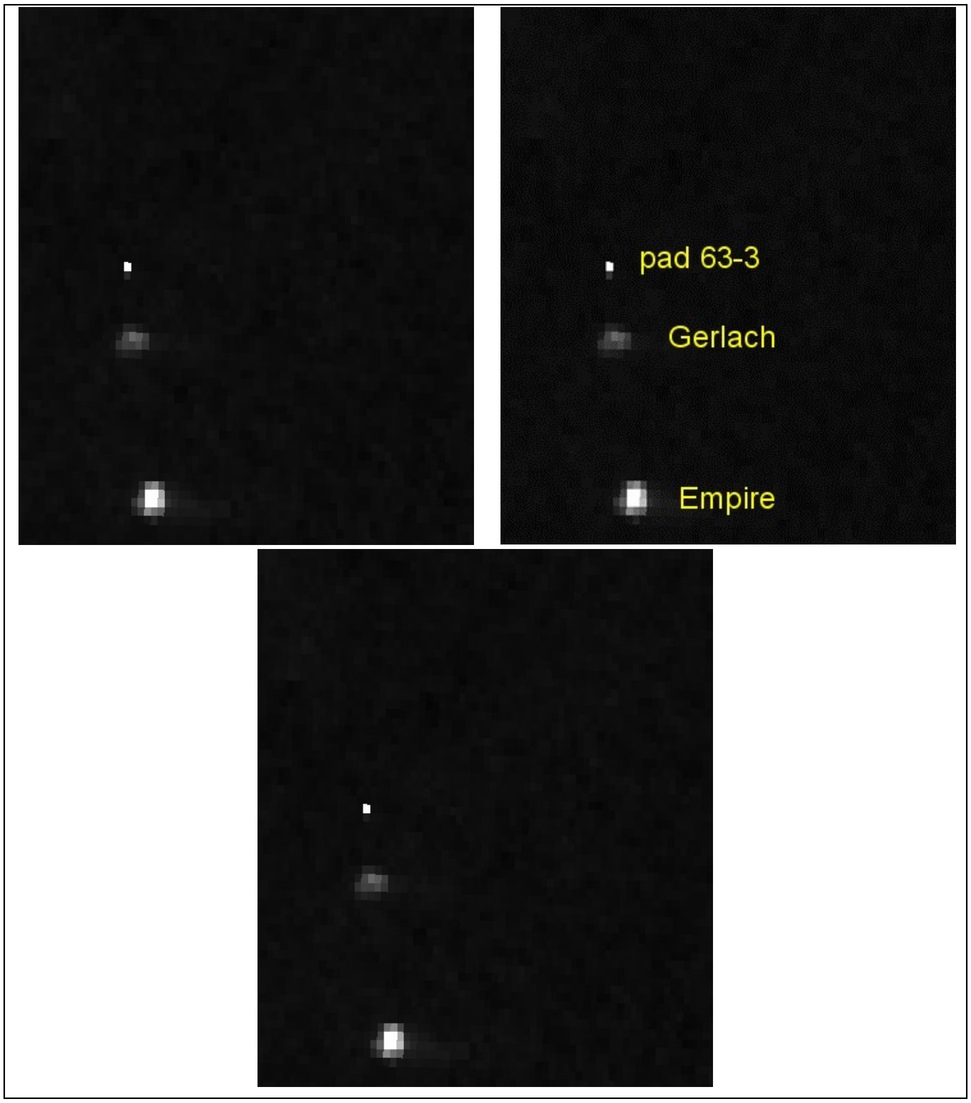

Figure A6. Simulated satellite images for an active pad 63-3. Top left panel is a simulation with the expected level of lighting. Top right panel is a simulation with 1.5x the expected level of lighting. Bottom panel is with LED substituted mobile lighting plants.

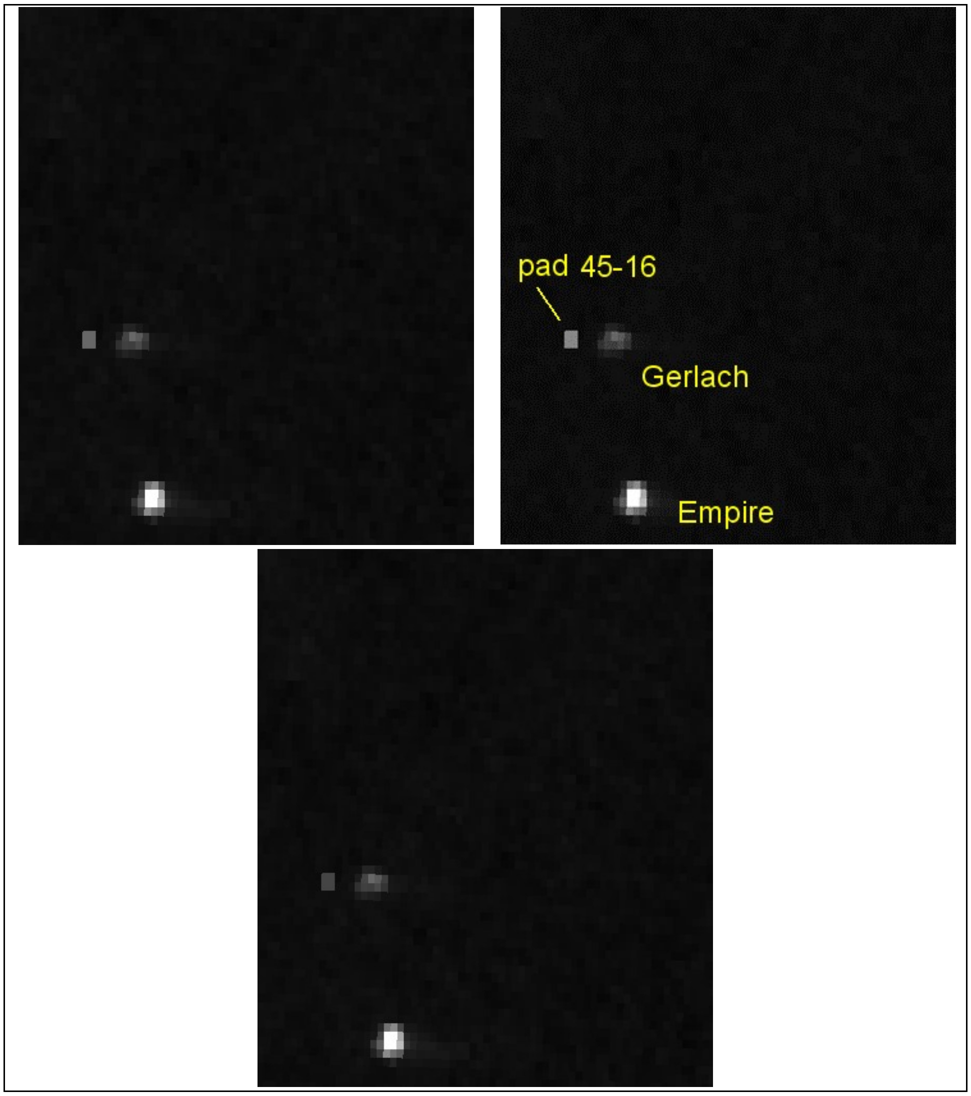

Figure A7. Simulated satellite images for an active pad 45-16. Top left panel is a simulation with the expected level of lighting. Top right panel is a simulation with 1.5x the expected level of lighting. Bottom panel is with LED substituted mobile lighting plants. [Note pad 45-16 was located at the vertex of 4 pixels which spreads the radiance among the 4 pixels. This accounts for the appearance of reduced intensity compared to the more concentrated radiance of pads 63-3 and 18B-10.]

Figure A8. Simulated satellite images for an active pad 18B-10. Top left panel is a simulation with the expected level of lighting. Top right panel is a simulation with 1.5x the expected level of lighting. Bottom panel is with LED substituted mobile lighting plants.

APPENDIX C. MODELLED SKY BRIGHTNESS

Baseline Models Viewed from KOP

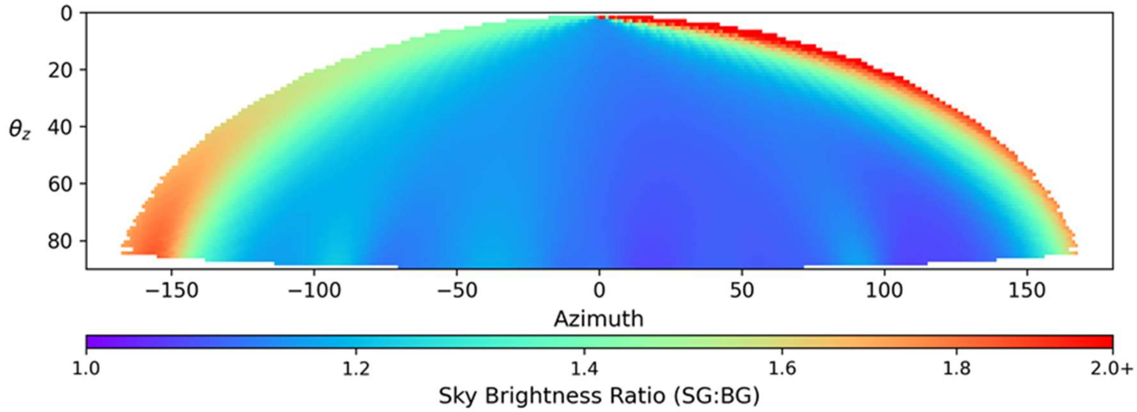

Figure A9. Modelling sky brightness from KOP7 near Gerlach, NV. Modelling based upon VIIRS satellite imagery from March 2021 as seen by an observer standing at KOP7 (119°20'24.2"W, 40°38'15.8"N). Azimuth 0 is north and positive values are to the East. θ_Z, is the zenith angle of view. The sky brightness is a logarithmic scale of the ratio of observed sky brightness to the background skyglow (i.e., the moonless brightness at the Massacre Rim WSA).

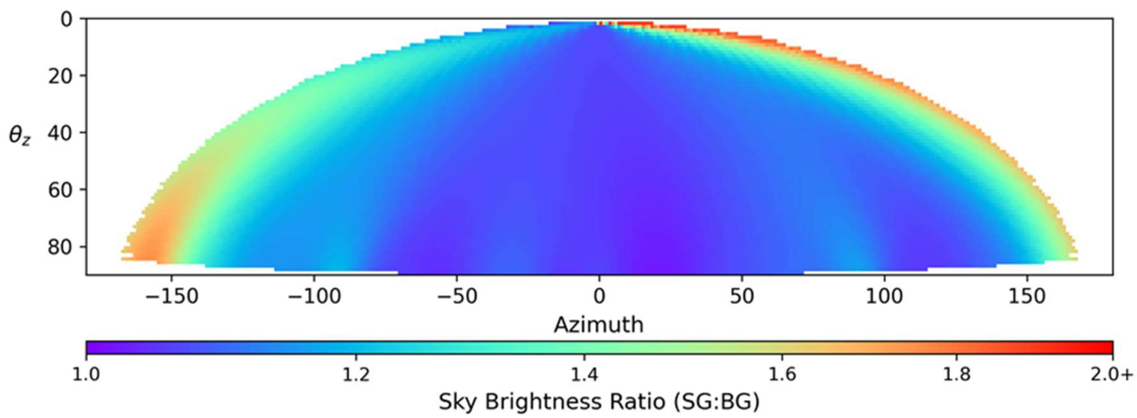

Figure A10. Modelling sky brightness from KOP2 northeast of Gerlach. Modelling based upon VIIRS satellite imagery from March 2021 as seen by an observer standing at KOP2 in the Black Rock Desert Playa (119°21'12.1"W, 40°41'41.3"N). Azimuth 0 is north and positive values are to the East. θ_Z, is the zenith angle of view. The sky brightness is a logarithmic scale of the ratio of observed sky brightness to the background skyglow (i.e., the moonless brightness at the Massacre Rim WSA).

<u>*Models with Simulated Drill Rigs from KOP*</u>

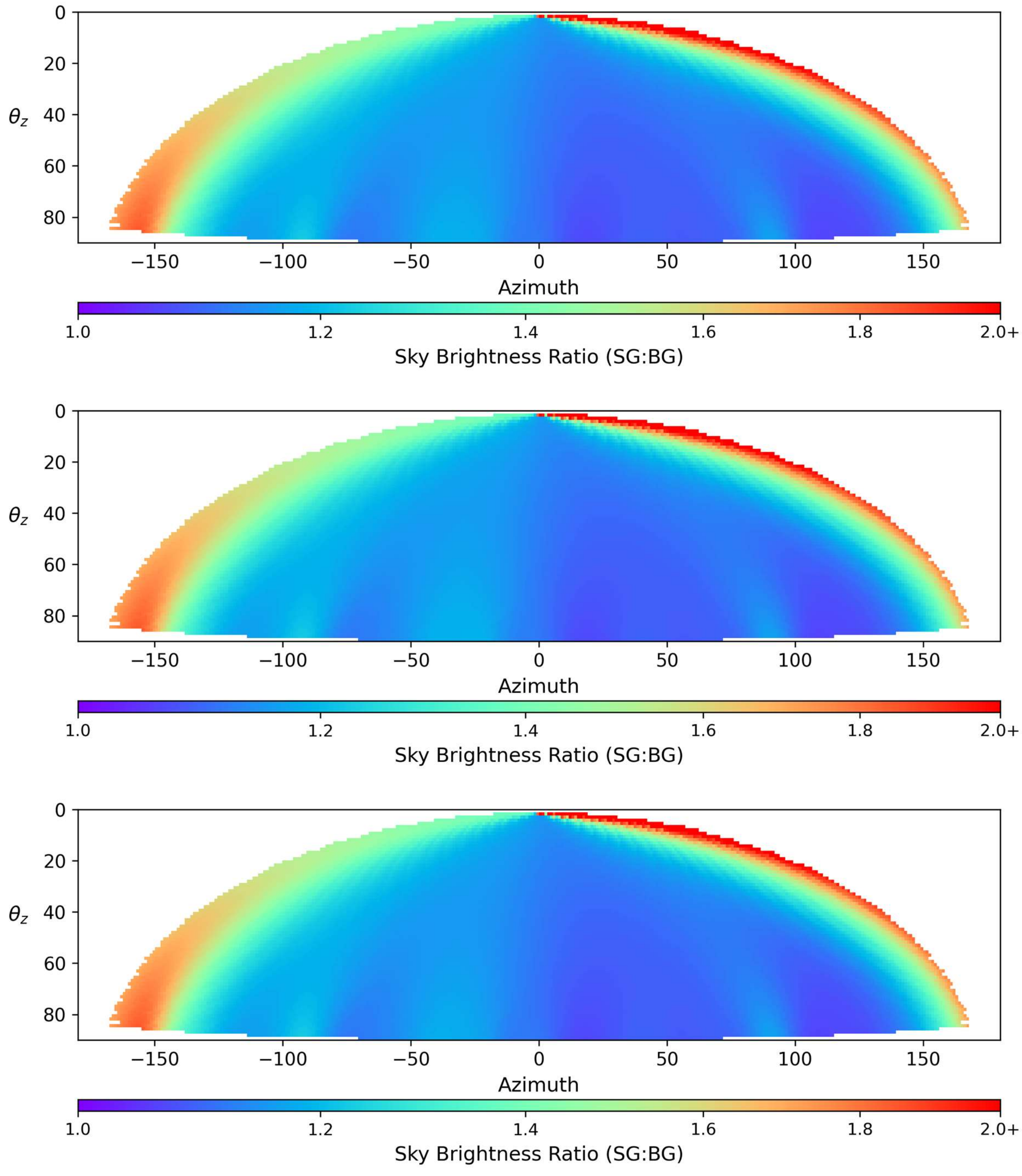

Figure A11. Modelling sky brightness of pad 63-3 from KOP7. Modelling based upon VIIRS satellite imagery from March 2021 as seen by an observer standing at the KOP7 (119°20'24.2"W, 40°38'15.8"N). Top panel models drilling pad 63-3 with the expected lighting of 1,776,000 lumens. The middle panel models pad 63-3 with 1.5 times excess (2,649,000) lumens. The bottom panel models an LED mobile plant substitution lit pad 63-3 with 602,000 lumens. Azimuth 0 is north and positive values are to the East. Bearing to drill pad from KOP7 is ~ -15°. θ_Z, is the zenith angle of view. The sky brightness is a logarithmic scale of the ratio of observed sky brightness to the background skyglow (i.e., the moonless brightness at the Massacre Rim WSA).

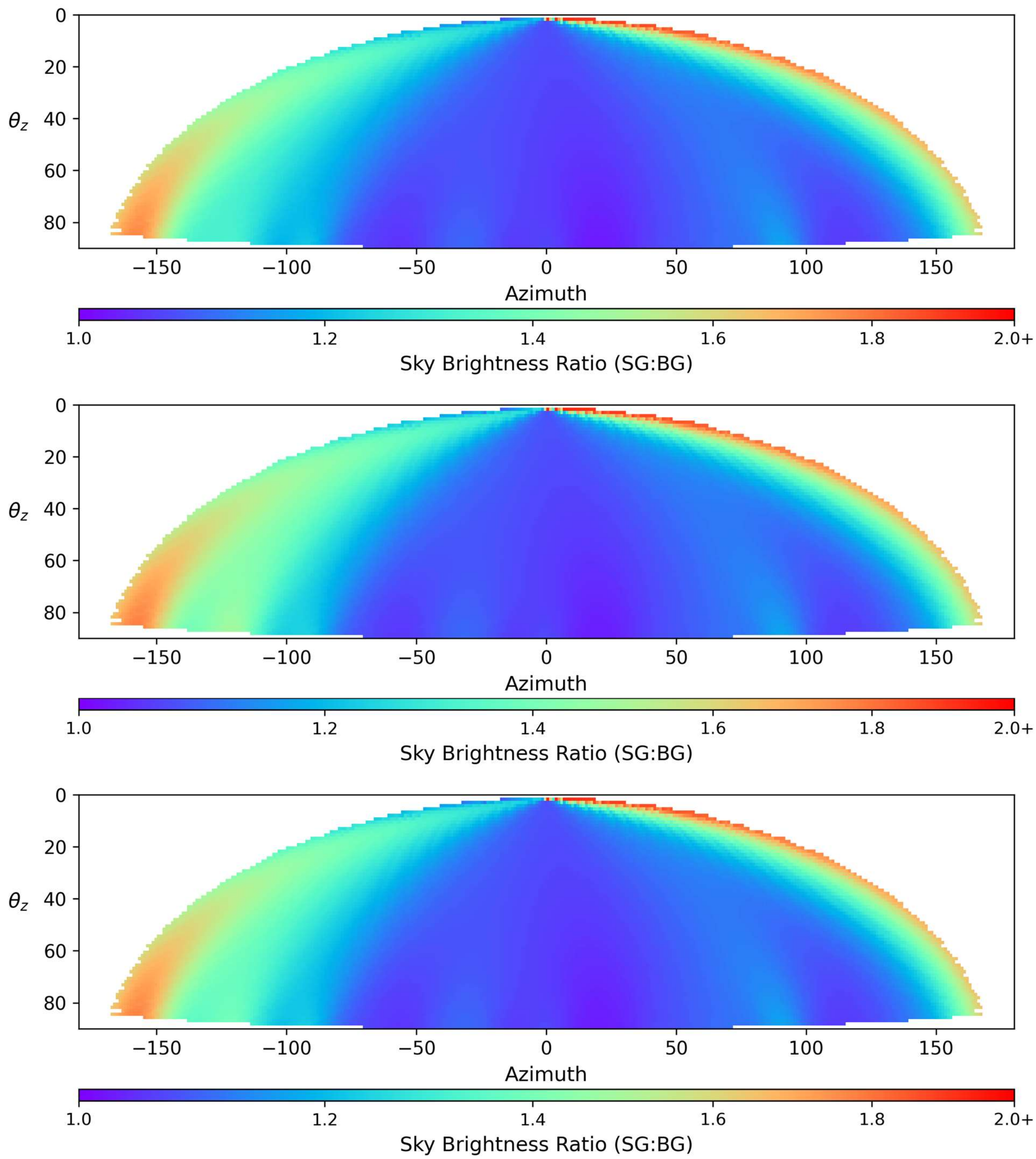

Figure A12. Modelling sky brightness of pad 63-3 from KOP2. Modelling based upon VIIRS satellite imagery from March 2021 as seen by an observer standing at the KOP2 (119°21'12.1"W, 40°41'41.3"N). Top panel models drilling pad 63-3 with the expected lighting of 1,776,000 lumens. The middle panel models pad 63-3 with 1.5 times excess (2,649,000) lumens. The bottom panel models an LED mobile plant substitution lit pad 63-3 with 602,000 lumens. Azimuth 0 is north and positive values are to the East. Bearing to drill pad from KOP2 is ~ -115°. θ_Z, is the zenith angle of view. The sky brightness is a logarithmic scale of the ratio of observed sky brightness to the background skyglow (i.e., the moonless brightness at the Massacre Rim WSA).

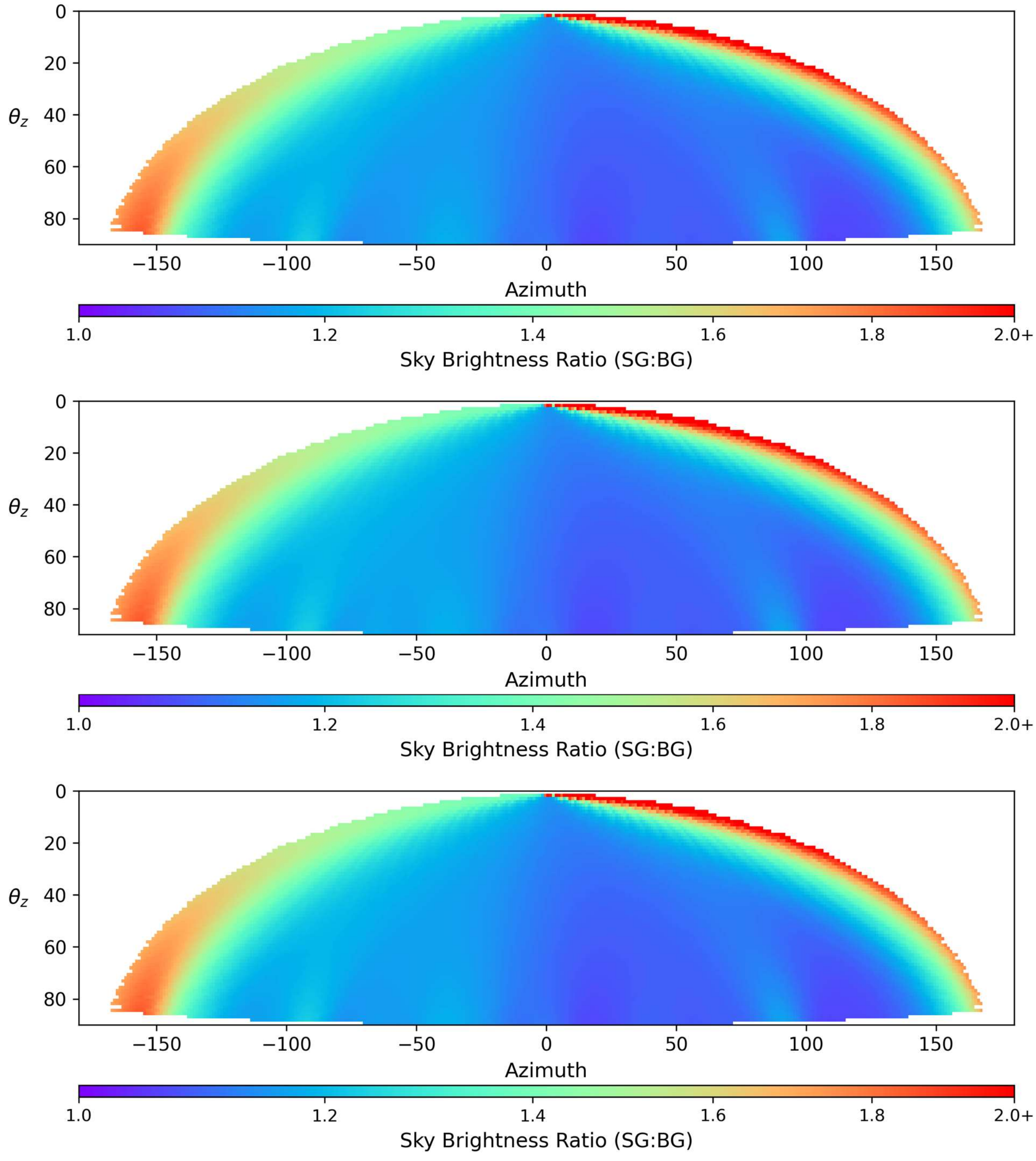

Figure A13. Modelling sky brightness of pad 45-16 from KOP7. Modelling based upon VIIRS satellite imagery from March 2021 as seen by an observer standing at the KOP7 (119°20'24.2"W, 40°38'15.8"N). Top panel models drilling pad 45-16 with the expected lighting of 1,776,000 lumens. The middle panel models pad 45-16 with 1.5 times excess (2,649,000) lumens. The bottom panel models an LED mobile plant substitution lit pad 63-3 with 602,000 lumens. Azimuth 0 is north and positive values are to the East. Bearing to drill pad from KOP7 is ~ -63°. θ_Z, is the zenith angle of view. The sky brightness is a logarithmic scale of the ratio of observed sky brightness to the background skyglow (i.e., the moonless brightness at the Massacre Rim WSA).

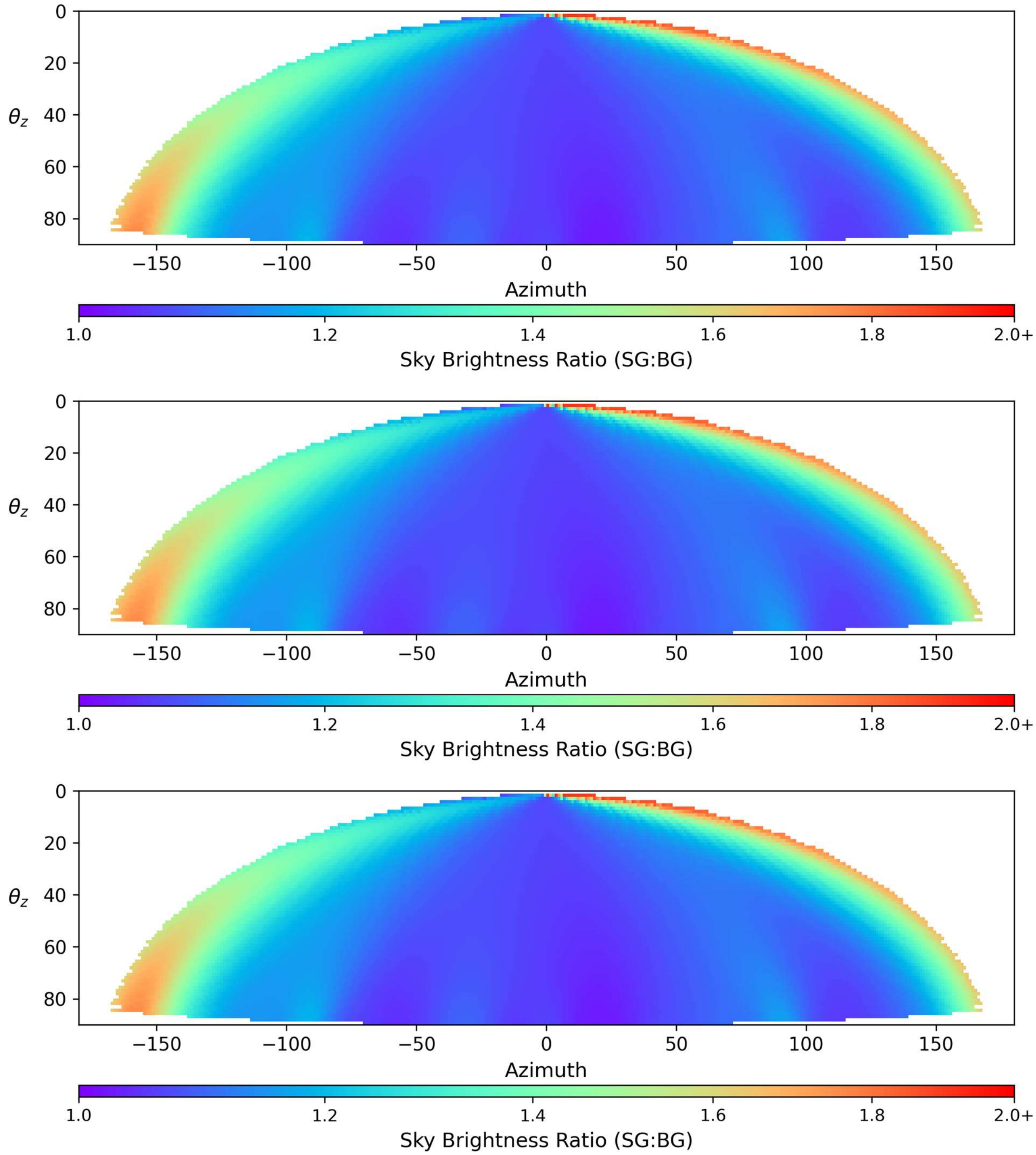

Figure A14. Modelling sky brightness of pad 45-16 from KOP2. Modelling based upon VIIRS satellite imagery from March 2021 as seen by an observer standing at the KOP2 (119°21'12.1"W, 40°41'41.3"N). Top panel models drilling pad 45-16 with the expected lighting of 1,776,000 lumens. The middle panel models pad 45-16 with 1.5 times excess (2,649,000) lumens. The bottom panel models an LED mobile plant substitution lit pad 45-16 with 602,000 lumens. Azimuth 0 is north and positive values are to the East. Bearing to drill pad from KOP2 is ~ -141°. θ_Z, is the zenith angle of view. The sky brightness is a logarithmic scale of the ratio of observed sky brightness to the background skyglow (i.e., the moonless brightness at the Massacre Rim WSA).

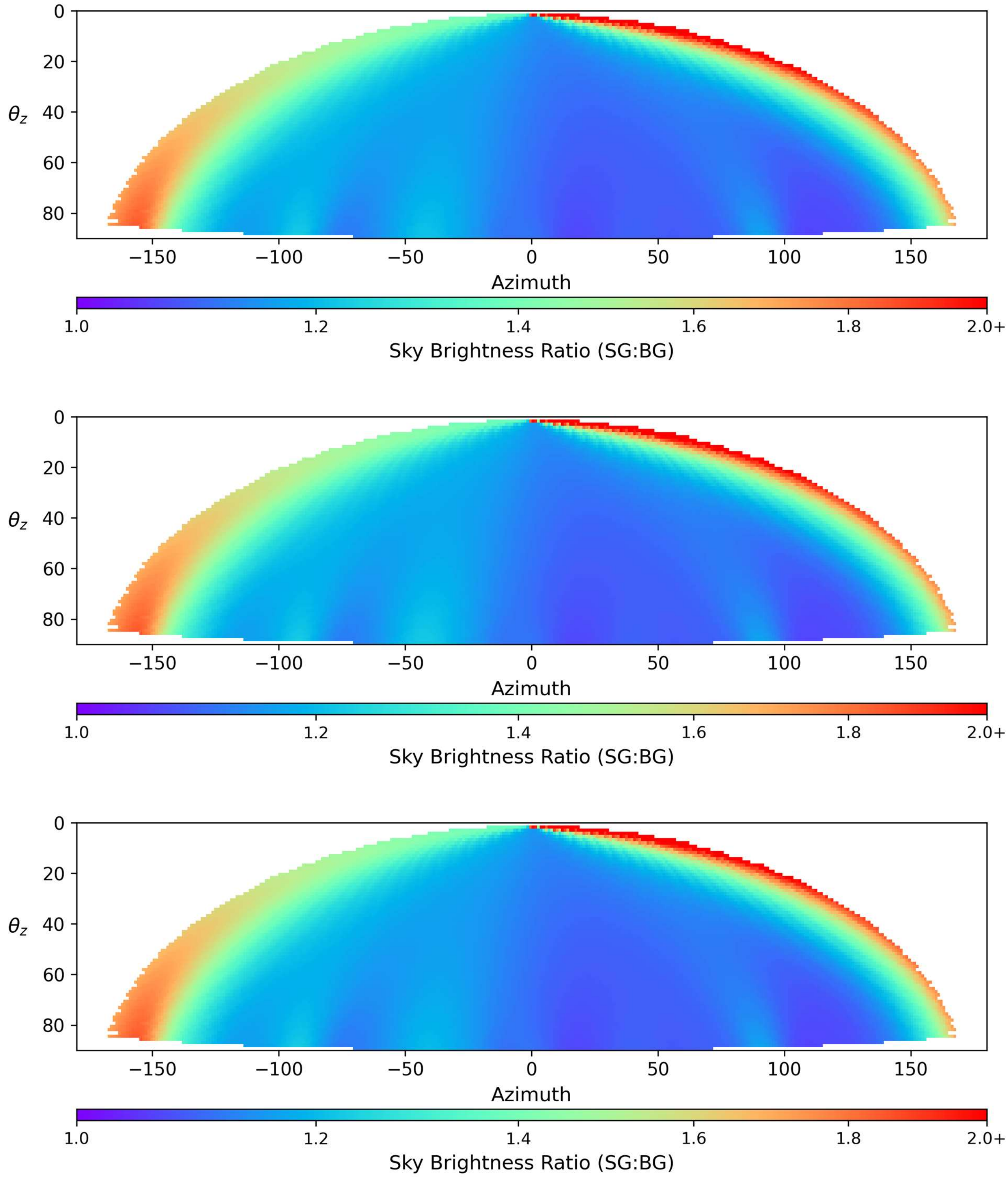

Figure A15. Modelling sky brightness of pad 18B-10 from KOP7. Modelling based upon VIIRS satellite imagery from March 2021 as seen by an observer standing at the KOP7 (119°20'24.2"W, 40°38'15.8"N). Top panel models drilling pad 18B-10 with the expected lighting of 1,776,000 lumens. The middle panel models pad 63-3 with 1.5 times excess (2,649,000) lumens. The bottom panel models an LED mobile plant substitution lit pad 18B-10 with 602,000 lumens. Azimuth 0 is north and positive values are to the East. Bearing to drill pad from KOP7 is ~ -40°. θ$_Z$, is the zenith angle of view. The sky brightness is a logarithmic scale of the ratio of observed sky brightness to the background skyglow (i.e., the moonless brightness at the Massacre Rim WSA).

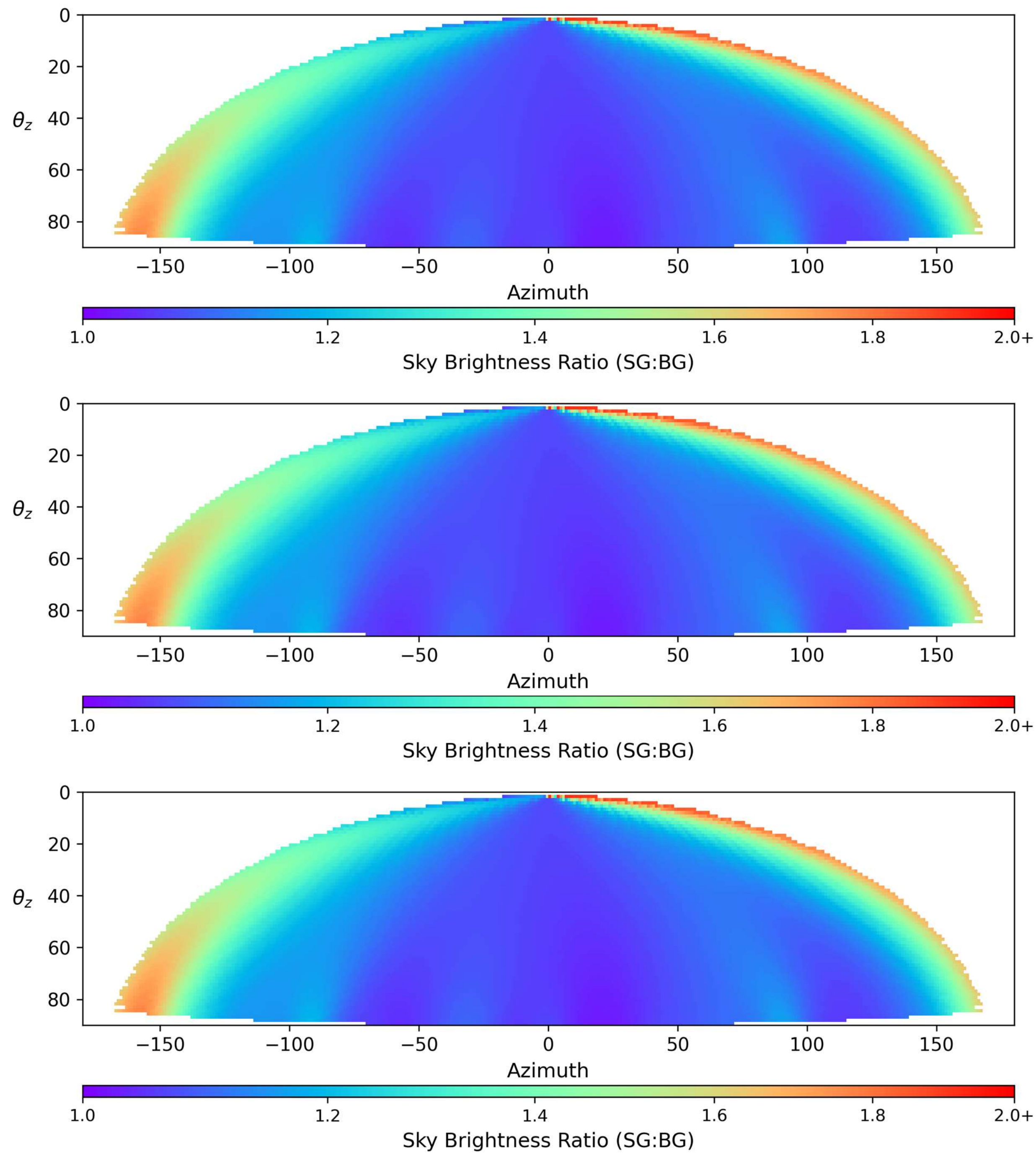

Figure A16. Modelling sky brightness of pad 18B-10 from KOP2. Modelling based upon VIIRS satellite imagery from March 2021 as seen by an observer standing at the KOP2 (119°21'12.1"W, 40°41'41.3"N). Top panel models drilling pad 18B-10 with the expected lighting of 1,776,000 lumens. The middle panel models pad 63-3 with 1.5 times excess (2,649,000) lumens. The bottom panel models an LED mobile plant substitution lit pad 18B-10 with 602,000 lumens. Azimuth 0 is north and positive values are to the East. Bearing to drill pad from KOP2 is ~ -142°. θ_Z, is the zenith angle of view. The sky brightness is a logarithmic scale of the ratio of observed sky brightness to the background skyglow (i.e., the moonless brightness at the Massacre Rim WSA).

APPENDIX D. TABLE OF EPOCHS OF PROJECT SATELLITE DATA.

Zenith Angle Satellite Data

Satellite imaging data obtained on moonless, cloud-free or partially cloud-free nights encompassing the region of Ormat Project Area used for calculation of the zenith angle functions and ZARI scores.

Table A1. Epochs of single night satellite data.

Satellite	Date	Time (UTC)	Orbit
Suomi-NPP	2021-06-14	10:12:08	49898
Suomi-NPP	2021-06-15	09:54:38	49912
Suomi-NPP	2021-06-16	09:31:26	49926
Suomi-NPP	2021-06-17	09:13:58	49940
Suomi-NPP	2021-06-19	10:15:41	49969
Suomi-NPP	2021-06-20	09:58:11	49983
NOAA-20	2021-06-14	09:20:56	18501
NOAA-20	2021-06-15	09:03:26	18515
NOAA-20	2021-06-15	10:40:10	18516
NOAA-20	2021-06-16	08:45:56	18529
NOAA-20	2021-06-16	10:22:39	18530
NOAA-20	2021-06-17	10:05:10	18544
NOAA-20	2021-06-19	09:30:09	18572
NOAA-20	2021-06-20	09:06:59	18586

APPENDIX E. LIGHTING SPECIFICATIONS.

Table A2. Luminance ratings for proposed test drill rigs. The expected satellite observed radiance in $nWcm^{-2}sr^{-1}$ are determined from empirical standard curves [3].

Lighting Source	Lumens/fixture	#Fixtures	Total Lumens	$nWcm^{-2}sr^{-1}$
canrig 4ft flourescent	3,000	8	24,000	1.65
rig 360° CFL	5,800	20	116,000	2.57
lighting plant (metal halide)	542,000	3	1,626,000	3.89
Pad Totals			1,766,000	8.12

Table A3. Luminance ratings for LED lamp substituted test drill rigs. The expected satellite observed radiance in $nWcm^{-2}sr^{-1}$ are determined from empirical standard curves [3].

Lighting Source	Lumens/fixture	#Fixtures	Total Lumens	$nWcm^{-2}sr^{-1}$
canrig 4ft flourescent	3,000	8	24,000	1.65
rig 360° CFL	5,800	20	116,000	2.57
lighting plant (LED)	154,000	3	462,000	1.26
Pad Totals			602,000	5.49

Figure A17. Specification for CFL bulbs. [19]

Westinghouse

Specification Sheet

High Wattage Twist Compact Fluorescent Lamp

Item Number **37073**

Specifications

Energy Used (Watts)	105
Incandescent Equivalent Wattage	400
Domestic Code	105TWIST/65
Brightness (Lumens)	5800
Average Rated Hours	8000
Life (in years)*	7.3
Light Appearance (Kelvin)	6500
CRI	82
CIE Chromaticity	x.313, y.337
Efficacy (LPW)	55
PF	≥0.5
Minimum Starting Temperature	-14°F/26°C
Estimated Yearly Energy Cost**	$12.65
Country of Origin	China

Physical Characteristics

Finish	Daylight
Base	Medium (E26)
MOL	12 5/8"

Lumen Maintenance

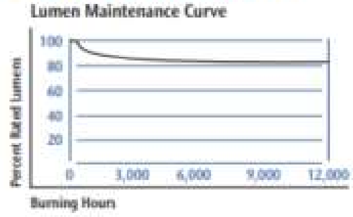

Spectral Distribution

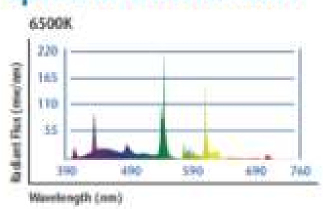

Limited Warranty

This lamp is warranted to be free from defects in material and workmanship for 2 years (based on using 3 hours per day). If the product fails during the warranty period, return defective product to retailer. Warranty terms and conditions of retailer apply. If replacement product is not available at retail store, please return product, original package and receipt to manufacturer at: 12401 McNulty Road, Philadelphia, PA 19154-1029.

Caution

Do not for use with emergency exit luminaires or lights, photocontrols or electric timers. DO NOT USE WITH DIMMERS. Enclosed luminaire is required for outdoor use. Not for use in totally enclosed non-vented luminaires. Not recommended for base up operation in recessed downlights. NOTE: Product may cause interference with radios, televisions, telephones, or remote controls. If interference occurs, move this product away from device or plug into another outlet.

* Based on 3 hrs./day

** Based on 3 hrs./day 11¢/kWh - Cost depends on rates and use.

Contains mercury. (Hg) For more on clean up and safe disposal, visit epa.gov/CFL.

Call 1-800-999-2226 or visit www.westinghouselighting.com

Figure A18. Specification for four-foot fluorescent tubes. [13]

Philips Lighting Company
200 Franklin Square Drive
P.O. Box 6800
Somerset, NJ 08875-6800
1-800-555-0050
A Division of Philips Electronics North America Corporation

www.philips.com

Philips Lighting
281 Hillmount Road
Markham, Ontario
Canada L6C 2S3
1-800-555-0050
A Division of Philips Electronics Ltd.

Printed in USA 6/05 P-1373-G

Philips 800 Series T12 Fluorescent Lamps Featuring ALTO® Lamp Technology

Electrical, Technical and Ordering Data (Subject to change without notice)

	Old Product: SPEC		**New Product:** Philips 800 Series Lamps								
Nominal Watts	Product Number	Ordering Code	Product Number	Ordering Code	Bulb	Length (In.)	Approx. Initial Lumens[1]	Design Lumens[2]	Rated Average Life (Hrs.)[3]	Color Temp. (Kelvin)	Color Rendering Index (CRI)
34	23775-0	F34/SPEC30/RS/EW/ALTO	14253-9	F34T12/830/EW/ALTO	T12	48	2800	2660	20,000	3000	82
34	23777-6	F34/SPEC35/RS/EW/ALTO	14254-7	F34T12/835/EW/ALTO	T12	48	2800	2660	20,000	3500	82
34	23779-2	F34/SPEC41/RS/EW/ALTO	14255-4	F34T12/841/EW/ALTO	T12	48	2800	2660	20,000	4100	82
34		Now Available >	14256-2	F34T12/850/EW/ALTO	T12	48	2650	2520	20,000	5000	82
40	27311-0	F40/SPEC30/ALTO	14261-2	F40T12/830/ALTO	T12	48	3200	3040	20,000	3000	82
40	27291-4	F40/SPEC35/ALTO	14262-0	F40T12/835/ALTO	T12	48	3200	3040	20,000	3500	82
40	27295-5	F40/SPEC41/ALTO	14263-8	F40T12/841/ALTO	T12	48	3200	3040	20,000	4100	82
40		Now Available >	14264-6	F40T12/850/ALTO	T12	48	3050	2900	20,000	5000	82

1) Approximate initial lumens. The lamp lumen output is based upon lamp performance after 100 hours of operating life when the output is measured during operation on a reference ballast under standard laboratory conditions. For expected lamp lumen output, commercial ballast manufacturers can advise the appropriate ballast factor for each of their ballasts when they are informed of the designated lamp. The ballast factor is a multiplier applied to the designated lamp lumen output.

2) Design lumens are the approximate lamp lumen output at 40% of the lamp's rated average life. This output is based upon measurements obtained during lamp operation on a reference ballast under standard laboratory conditions.

3) Average life under specified test conditions with lamps turned off and restarted no more frequently than once every 3 operating hours. Lamp life is appreciably longer if lamps are started less frequently.

† This fluorescent lamp is better for the environment because of its reduced mercury content. All fluorescent lamps contain mercury for effective operation; however, Philips lamps with ALTO® Lamp Technology average 70% less mercury than the 2001 industry average for fluorescent lamps up to sixty inches which are not TCLP-compliant.

Figure A19. Mobile lighting plant specifications.[12]

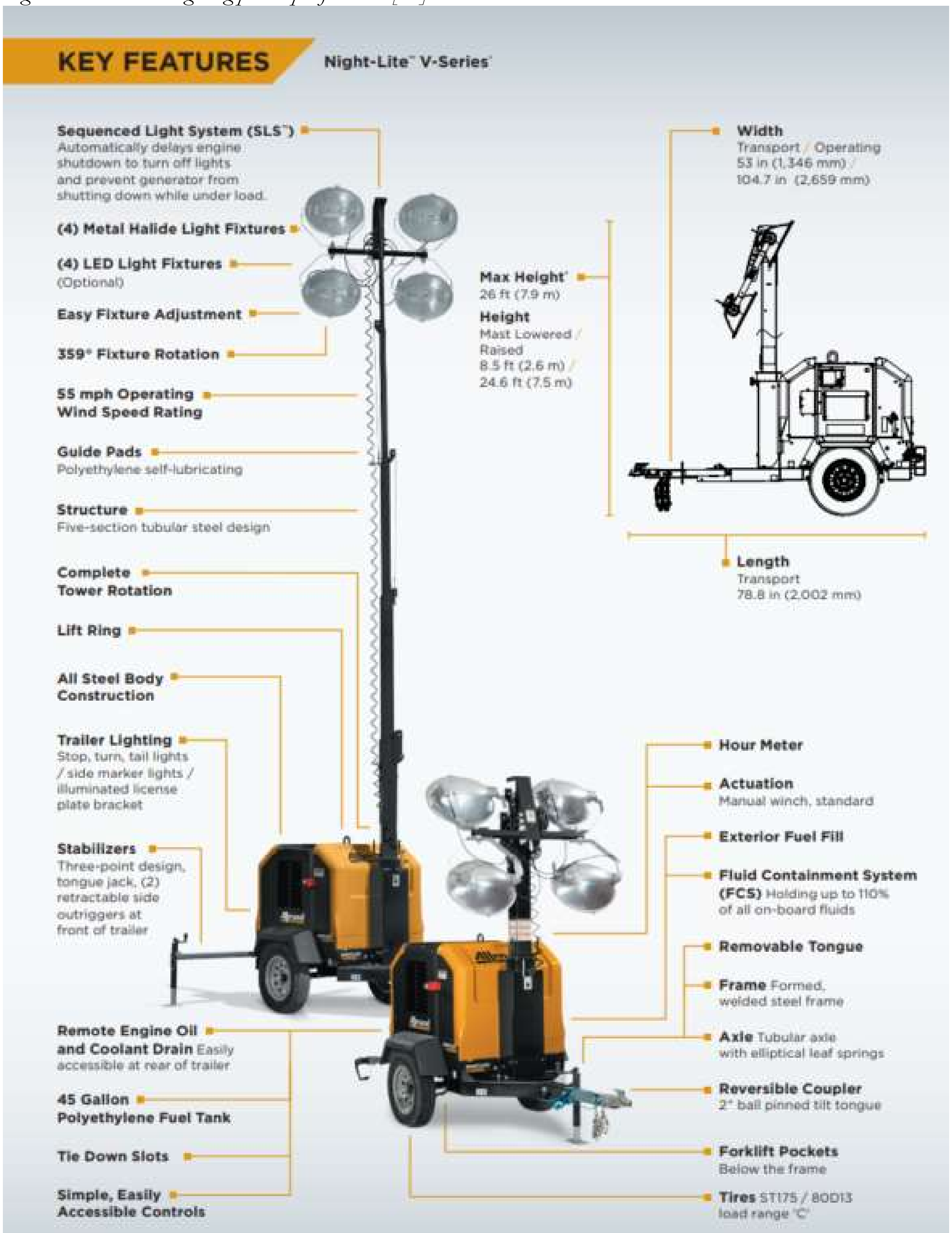

Night-Lite™ V-Series®

TECHNICAL SPECS

Model	NLV-ML3EC	NLV-K1005C	NLV-P11
Engine Brand / Model	Mitsubishi / L3E	Kubota / D1005	Perkins / 403D-11
Engine Prime Power (kW)**	6	7	8
Fuel Capacity gal (L)	45 (170.3)	45 (170.3)	45 (170)
Light Type - Metal Halide	(4) Metal Halide SHO-HD® fixture		
Metal Halide Wattage (per lamp)	1,250	1,250	1,250
Metal Halide Lumens (per lamp / total)	135,500 / 542,000	135,500 / 542,000	135,500 / 542,000
Operating Time (hrs)*** (Using four 1,250 W metal halide light fixtures)	75	72.6	75
Light Type - LED (Optional)	(4) Two LED, 5000°K color temperature		
LED Wattage (per lamp)	320	320	320
LED Lumens (per lamp / total)	38,500 / 154,000	38,500 / 154,000	38,500 / 154,000
Operating Time (hrs)*** (Using four 320 W LED light fixtures)	121.6	155.2	118.4
Features			
Outlets	**Standard** 20 A 120 VAC duplex GFCI / 30 A 240 VAC 4-Wire Twist Lock (NEMA L14-30R) / 30 A 120 VAC RV (NEMA TT-30R)		
Weights & Shipping			
Shipping Weight lbs (kg)	1,885 (855)		
Gross Vehicle Weight Rating (GVWR) lbs (kg)	2,200 (998)		
Shipping	18 units on a 48' flatbed trailer / 20 units on a 53' flatbed trailer		

LIGHT COVERAGE

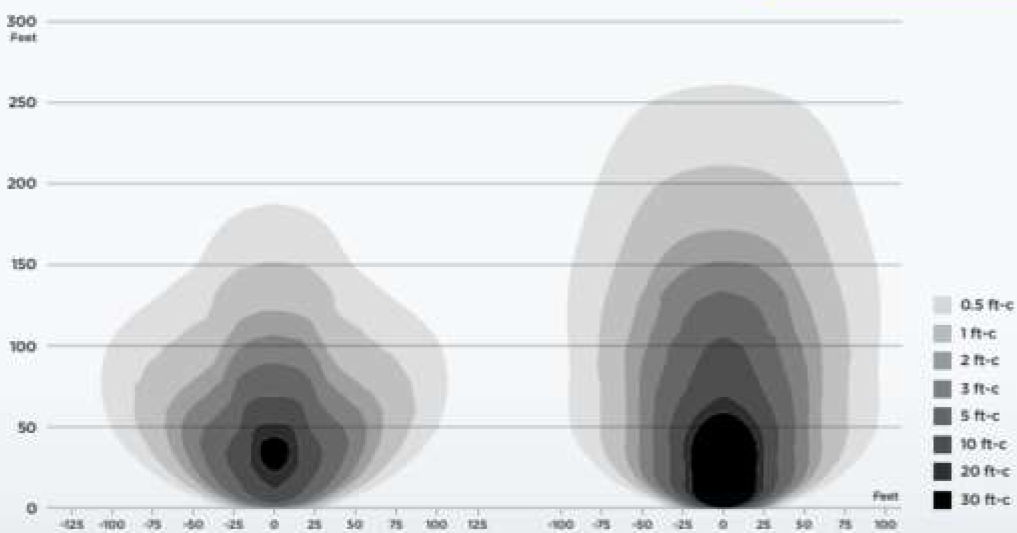

Night-Lite™ V-Series®
with 4 - 320 W Conssin LED Light Output
Area Lit to .5 Foot Candle (ft-c) or Higher: 28,449 ft²

Night-Lite™ V-Series®
with 4 - 1,250 W Metal Halide Light Output
Area Lit to .5 Foot Candle (ft-c) or Higher: 42,597 ft²

This page intentionally left blank.

Appendix B
Baseline Night Sky Photographs

This page intentionally left blank.

Appendix B. Baseline Night Sky Photographs

Baseline Night Sky Photographs

Baseline photos in this appendix document baseline night sky and ALAN conditions during bright moon and new moon phases as seen from the seven key observation points identified in Figure 4 of the baseline report. The camera used was a Nikon D3300 DSLR with a standard 18–55-millimeter lens. Each photo was taken with a 30-second exposure, f/3.5 aperture setting. Printed media and computer screens may display images and lighting differently. Individual computer screens may display images differently depending on the brightness, contrast, and make and model of the monitor. The images are a depiction of the baseline conditions.

Bright Moon

Bright moon photos were taken on August 19, 2021. The moon was in a waxing gibbous phase with an 89 percent illumination. The full moon (100 percent illumination) occurred on August 22, 2021. Photos were taken between 9:30 p.m. and 11:30 p.m. The estimated air quality index was between 55 and 80 with $PM_{2.5}$ as the primary pollutant.

KOP 1 (View from County Road 34 looking south toward Gerlach)

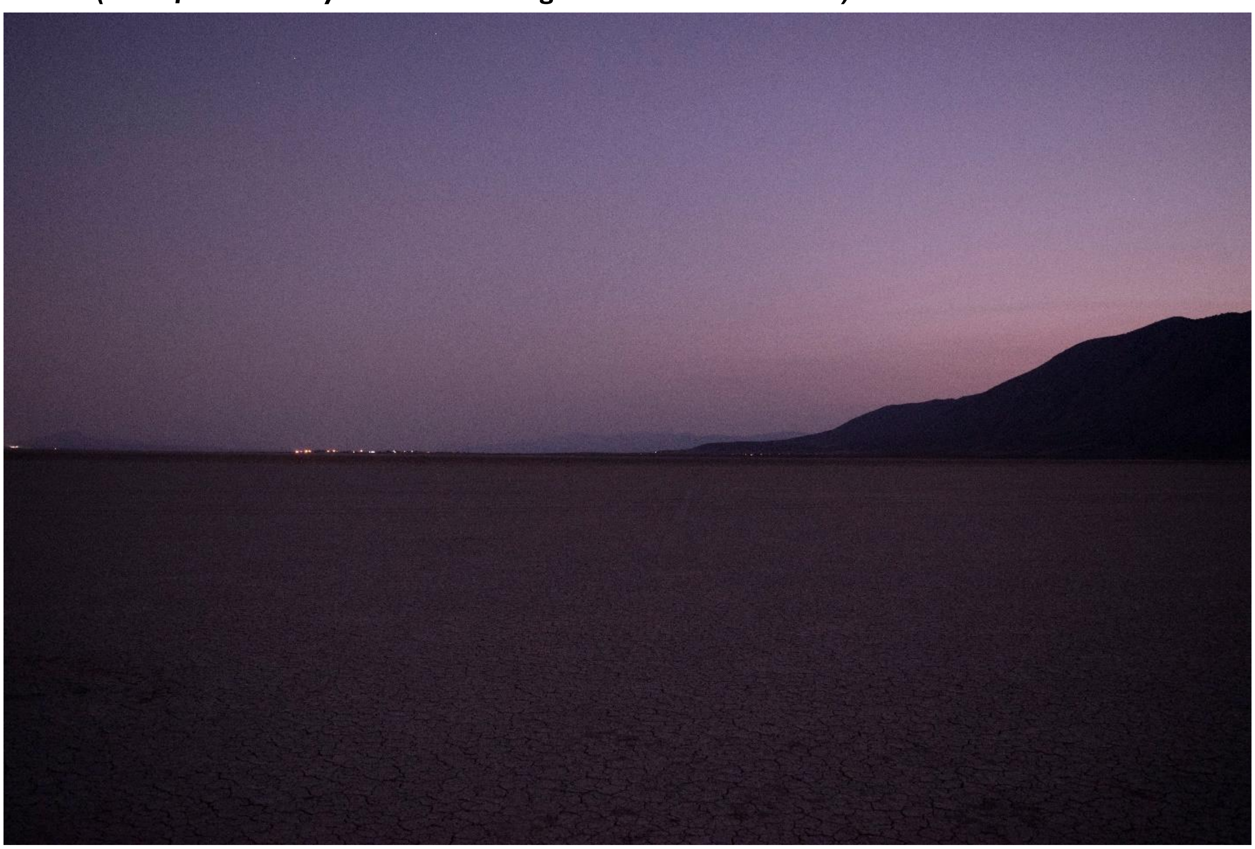

Photo note: Lights in the distance are from the community of Gerlach.

KOP 2 (View from the playa looking south toward Gerlach)

Photo note: Lights in the distance are from the community of Gerlach.

KOP 3 (Elevated view from north of Gerlach looking northeast)

Photo note: Lights in the middle, right portion of the frame are headlights on the playa. The lights on the left are on private property.

KOP 4 (View from the BLM Black Rock Station looking northeast)

KOP 5 (View from County Road 447 looking east)

KOP 6 (View from State Route 447 in Gerlach looking north)

There is no photo available for KOP 6. At the time of the photo inventory, access to KOP 6 was blocked by a line of trucks with the drivers gathered as a group in front of the trucks. All the trucks had their headlights on, which saturated the area with light.

KOP 7 (View from State Route 447 looking north toward Gerlach)

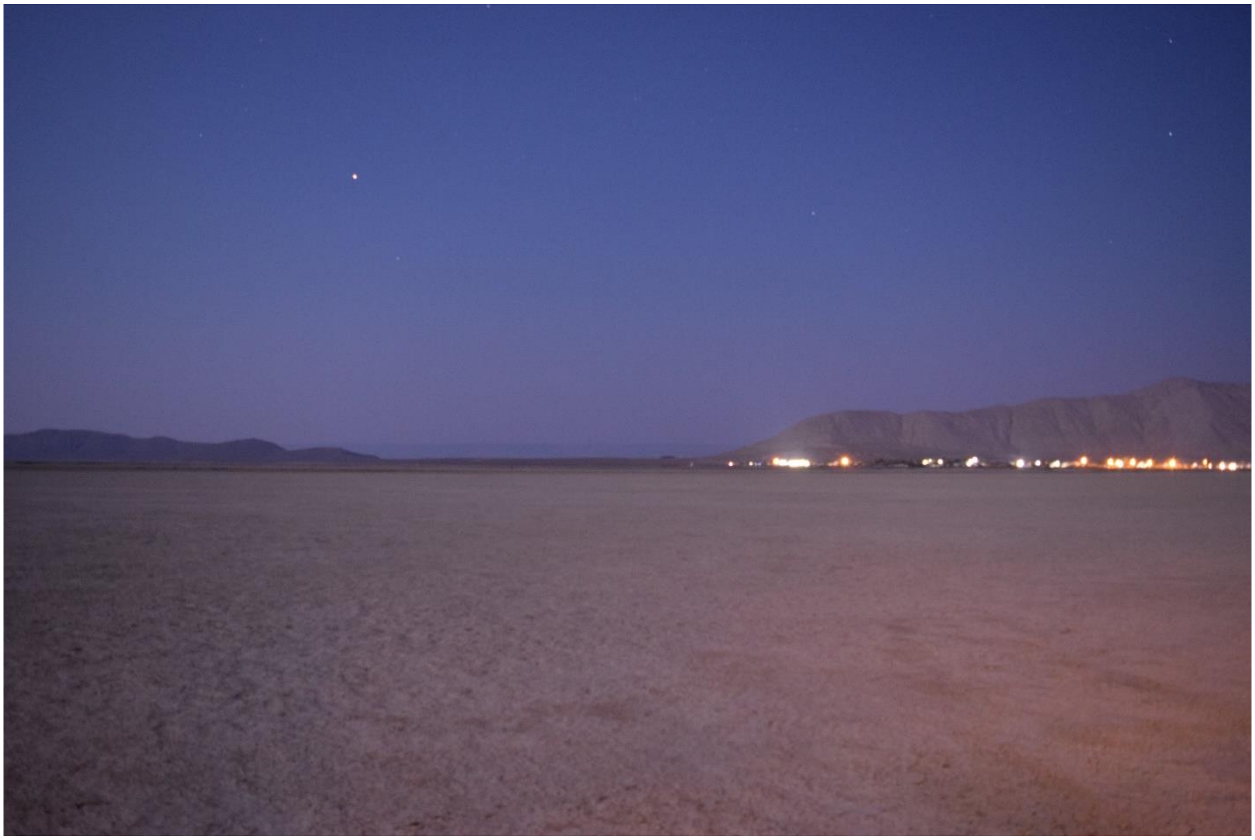

Photo note: Lights are from the community of Gerlach.

New Moon

New moon photos were taken on September 9, 2021. The moon was in a waxing crescent phase with an 8 percent illumination. The new moon (0 percent illumination) occurred on September 7, 2021. Photos were taken between 10 p.m. and 11:45 p.m. The estimated air quality index was between 30 and 75. Wind speed was estimated at less than 5 miles per hour.

KOP 1 (View from County Road 34 looking south toward Gerlach)

Photo note: The illumination in the foreground of this photo is from a portable information sign displaying the message "High Fire Danger." Lights in the distance are from the community of Gerlach.

KOP 2 (View from the playa looking south toward Gerlach)

Photo note: Lights in the distance are from the community of Gerlach.

KOP 3 (Elevated view from north of Gerlach looking northeast)

Photo note: Lights in the middle, right portion of the frame are headlights on the playa. Laser lights are from activity on the playa. Other lights are on private property.

KOP 4 (View from the BLM Black Rock Station looking northeast)

Photo note: Lights on the far right portion of the frame are headlights. The upward pointing lights on the right side of the image are laser lights from activity on the playa. Other lights in the middle of the frame are on private property.

KOP 5 (View from County Road 447 looking east)

KOP 6 (View from State Route 447 in Gerlach looking north)

Photo note: Observed lights are associated with activity on the playa.

KOP 7 (View from State Route 447 looking north toward Gerlach)

Photo note: Lights are from the community of Gerlach.

This page intentionally left blank.

Appendix C

Photographic Simulations

This page intentionally left blank.

Appendix C. Photographic Simulations

PHOTOGRAPHIC SIMULATIONS

Using the baseline new moon photographs taken on September 9, 2021, Wood Rodgers prepared photographic simulations of the proposed geothermal exploration project. The purpose of the images is to simulate the anticipated ALAN from the proposed project, which would include a single operational drill rig at one of the proposed well pads. As directed by the BLM, Wood Rodgers prepared photographic simulations for KOPs 2, 3, 5, 6, and 7. For each KOP, there are four images; each image depicts an operational drill rig at one of four proposed well pads. The BLM selected the following proposed well pads for the simulations: 18B-10, 45-16, 63-3, and 68-9 (see **Figure C-1**).

The camera used for the baseline photos was a Nikon D3300 DSLR with a standard 18–55-millimeter lens. Each photo was taken with a 30-second exposure, f/3.5 aperture setting. The moon was in a waxing crescent phase with an 8 percent illumination. The estimated air quality index was between 30 and 75. Wind speed was estimated at less than 5 miles per hour.

Wood Rodgers prepared the simulations using a three-dimensional model and inputs based on the proposed drill rig and ancillary lighting specifications provided by Ormat (see **Appendix D**). Angles of the proposed ground-based mobile lights were set to 45 degrees downward, per the specifications Ormat provided. Wood Rodgers assumed that the reflective dish behind each light causes the light to cast outward at a 170-degree cone. The images simulate $PM_{2.5}$ in the atmosphere equivalent to an air quality index of 5, which is less than the estimated average air quality index at the time of the baseline photos.

Printed media and computer screens may display images and lighting differently. Individual computer screens may display images differently depending on the brightness, contrast, and make and model of the monitor.

Figure C-1: KOPs and Well Pads Used in the Simulations

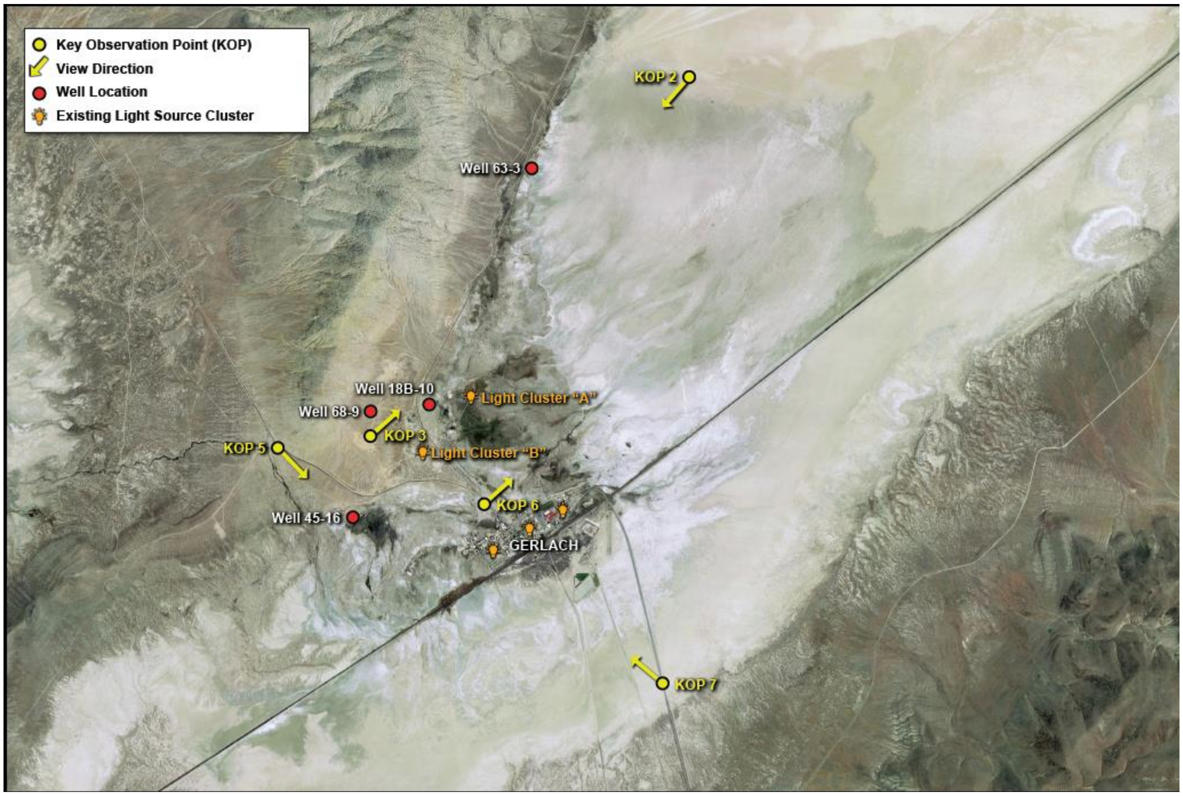

KOP 2 (View from the playa looking south toward Gerlach)

Composite Reference

Well Pad 18B-10

Well Pad 45-16

Well Pad 63-3

Well Pad 68-9

KOP 3 (Elevated view from north of Gerlach looking northeast)

Composite Reference

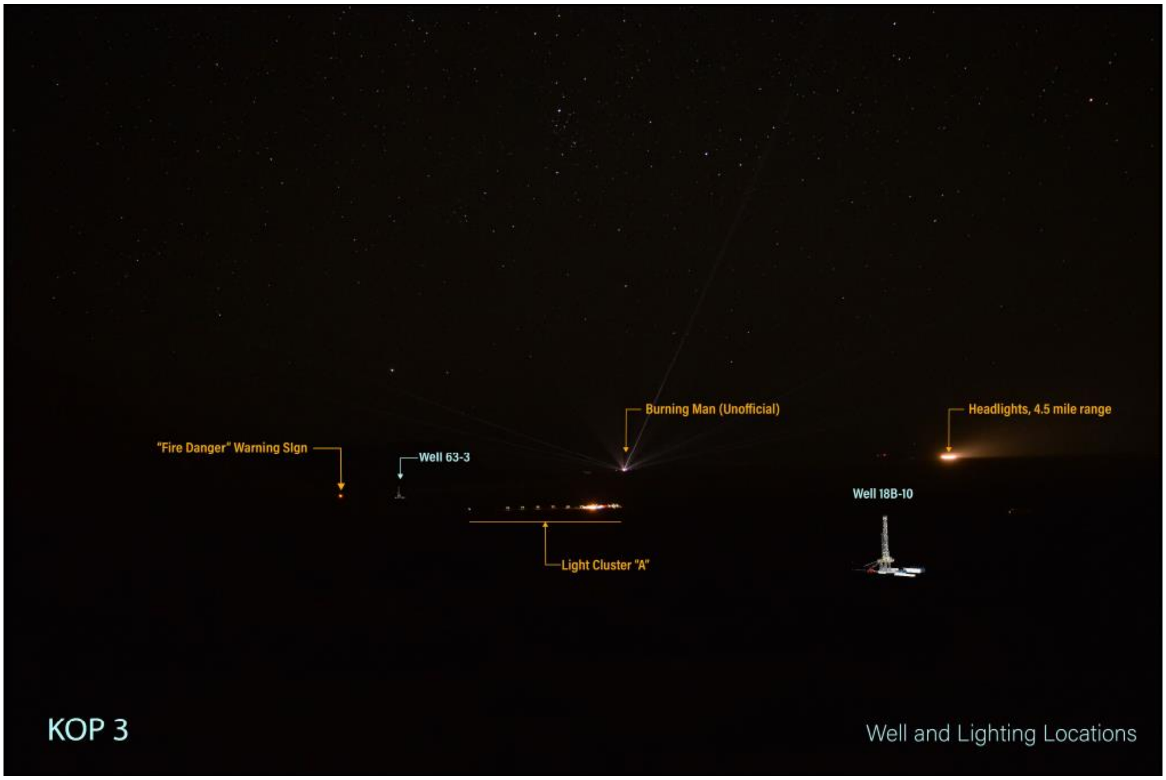

Well Pad 18B-10

Well Pad 45-16

Well Pad 63-3

Well Pad 68-9

KOP 5 (View from County Road 447 looking east)

Composite Reference

Well Pad 18B-10

Well Pad 45-16

Well Pad 63-3

Well Pad 68-9

KOP 6 (View from State Route 447 in Gerlach looking north)

Composite Reference

Well Pad 18B-10

Well Pad 45-16

Well Pad 63-3

Well Pad 68-9

KOP 7 (View from State Route 447 looking north toward Gerlach)

Composite Reference

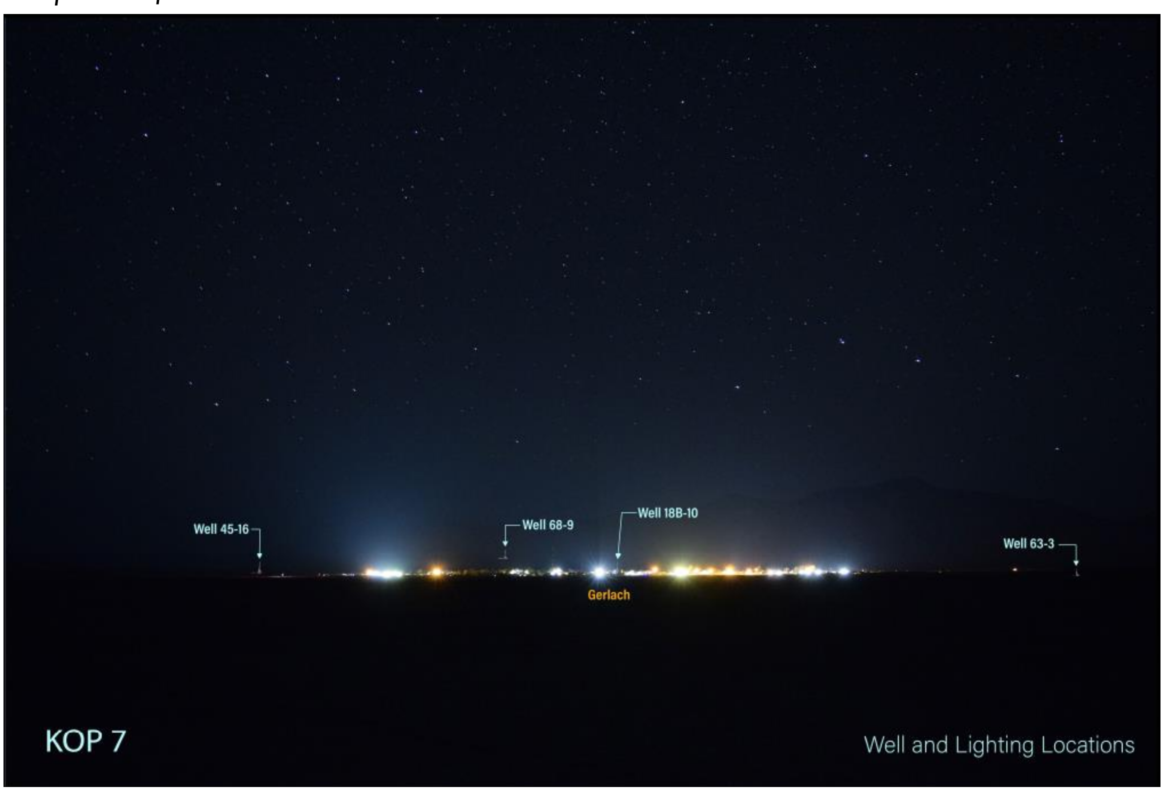

Well Pad 18B-10

Well Pad 45-16

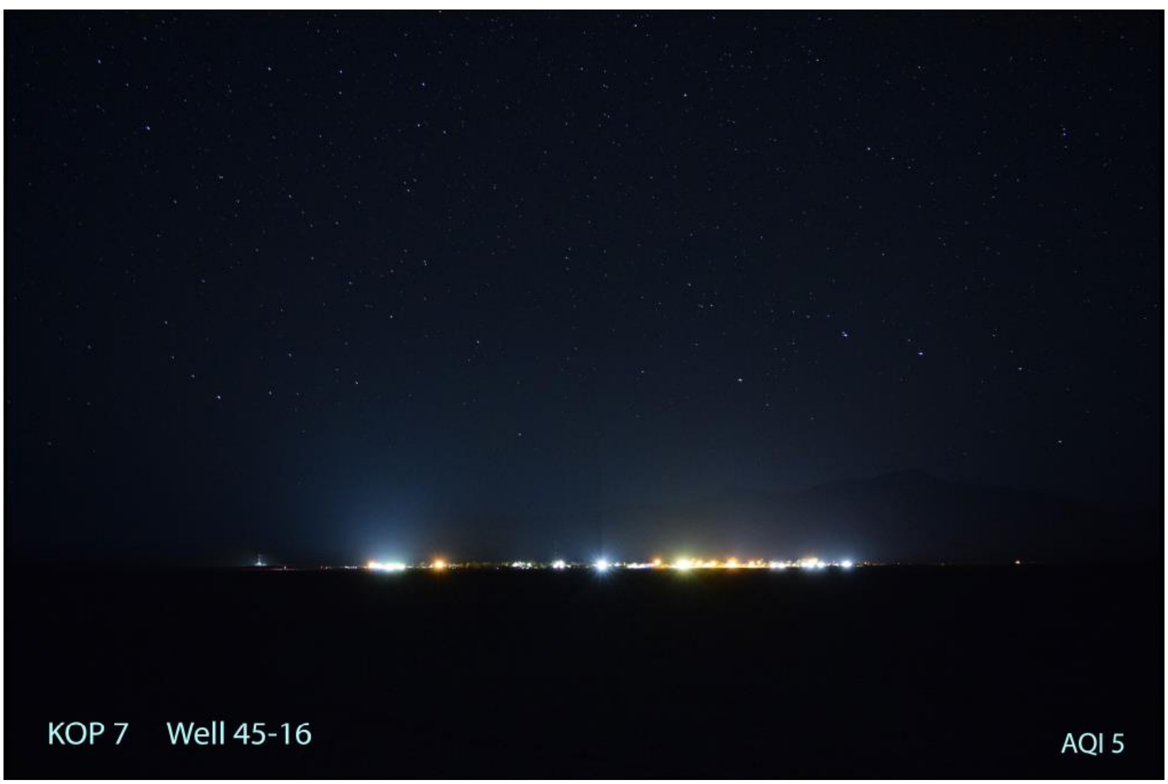

Well Pad 63-3

Well Pad 68-9

This page intentionally left blank.

Appendix D

Proposed Drill Rig and Lighting Specifications

This page intentionally left blank.

Appendix D. Proposed Drill Rig and Lighting Specifications

Drill Rig Profile

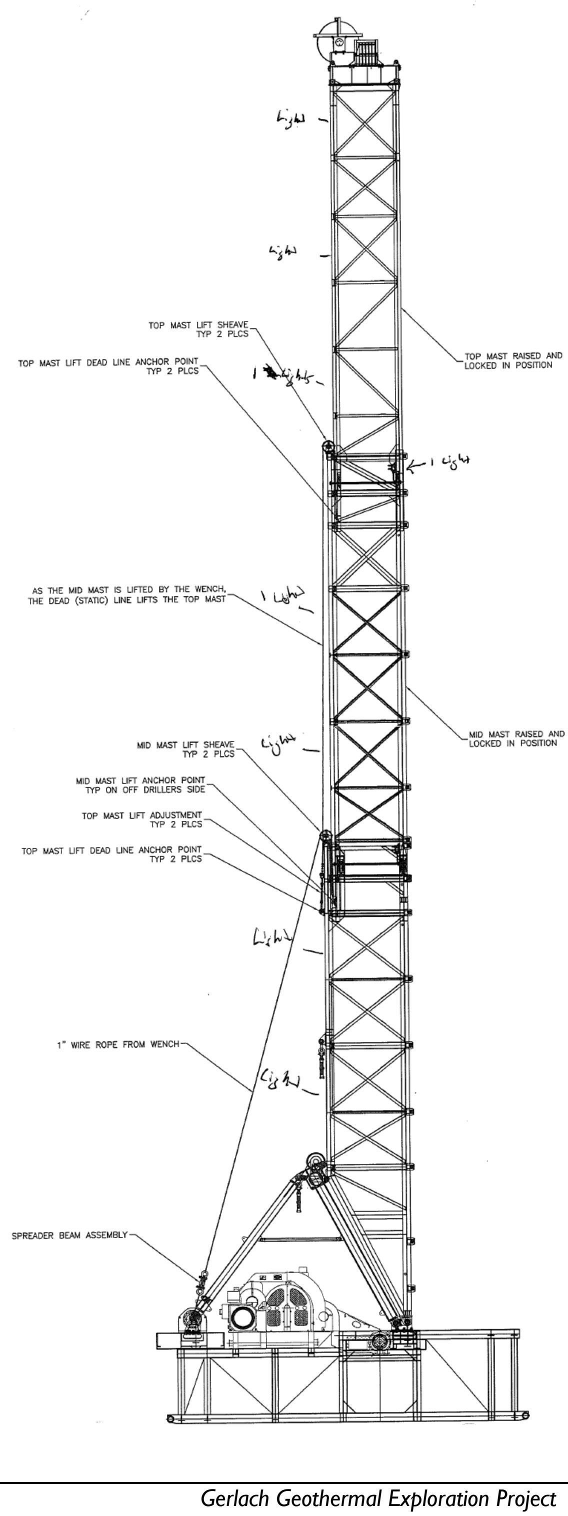

Drill Rig Layout

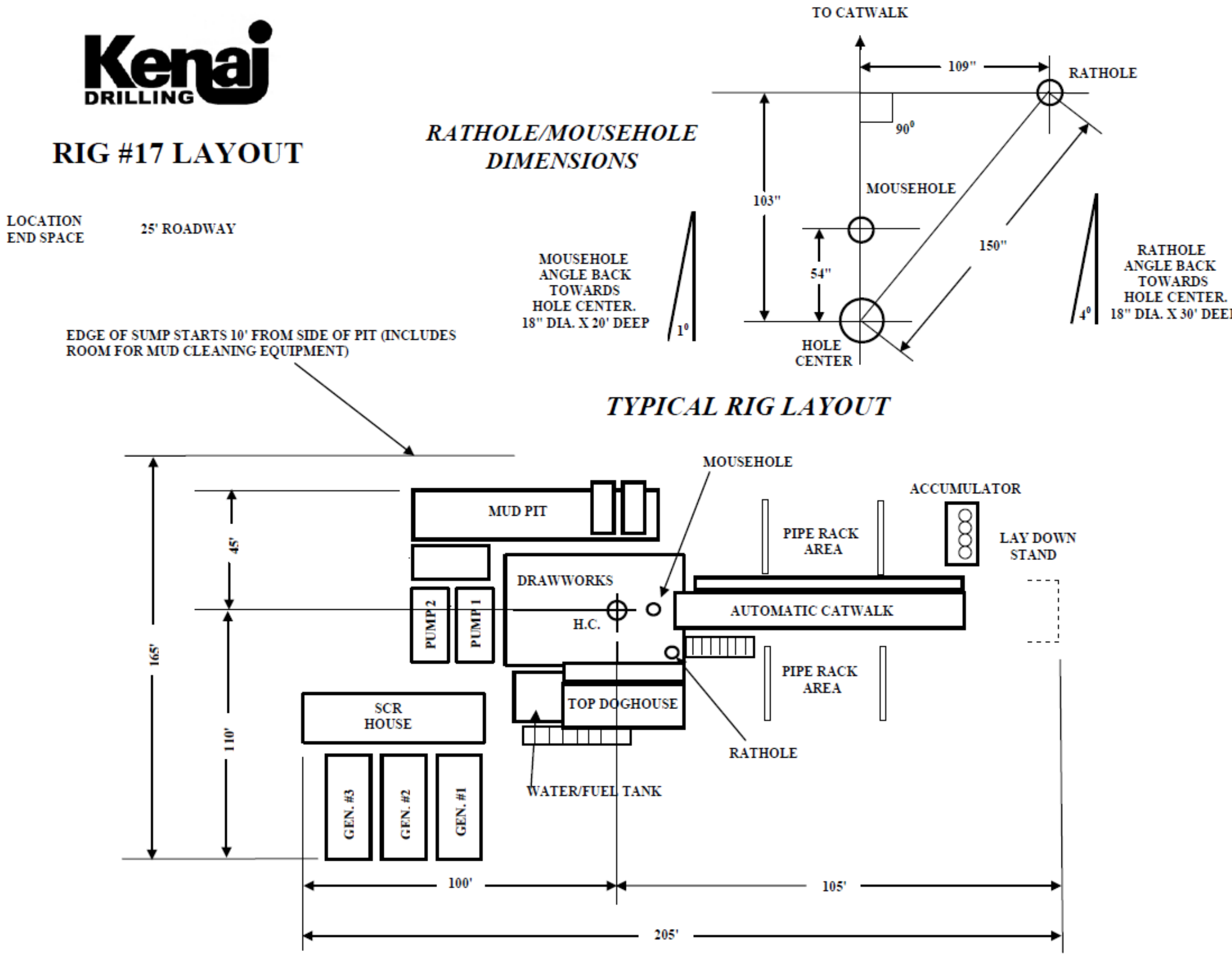

Drill Rig Specifications

Rig #17 Specifications

Drilling Range:	18,000' With 4½" Drill Pipe.
Drawworks:	TFI 1,500 HP Driven by (2)-1,000 HP General Electric 752 DC Traction Motors With An Eaton Disc Brake and Electrical Control Panel.
Mast:	Superior 136' High, Telescoping Mast Rated at 750,000# GNC, and 660,000# Static Hook Capacity.
Substructure:	Superior 20' High (10' Pony Available), With 750,000# Capacity.
Mud Pump #1:	Weatherford F-1,600, 7"x 12", 1,600 HP, Powered by (2)-1,000 HP General Electric 752 Traction Motors Charged by (1)-5x6 Centrifugal Pump.
Mud Pump #2:	Weatherford F-1,600, 7"x 12", 1,600 HP, Powered by (2)-1,000 HP General Electric 752 Traction Motors Charged by (1)-5x6 Centrifugal Pump.
Rotary Table:	TFI 27½".
Automatic Catwalk	Canrig Powercat Model 3000 Automatic Catwalk System.
Floorhand	Blohm + Voss Oil Tools GF 1100 Auto Floorhand Wrench & Spinner Combination.
Traveling Assembly:	TFI 350 Ton Block/Hook Combination.
Top Drive:	Canrig Model 1035, 350 Ton Top Drive Drilling System.
SCR /Power System:	(3)-Detroit Diesel, 16V2000 (1,400 BHP Each) Diesel Engines Driving (3)-Marathon 1,357 KW Generators With Ross Hill 4 Bridge SCR Unit and Ross Hill Electrical Control Unit.
Mud System:	400 Total Barrels, with Shaker, Volume, Mud Cleaning, Suction and Pill Mixing Compartments, (3)-Brandt Mud Agitators, and (2)–5x6 Centrifugal Pumps.
B.O.P.E.:	13-5/8", 5,000# Annular, 13-5/8", 5,000# D-Ram, 120 Gallon Accumulator and 5,000# Choke Manifold.
Water/Fuel Storage:	400 BBLS / 7,700 Gallons.
Auxiliary Equipment:	(2)-Hydraulic Winches, (2)-Screw Air compressors, Kelly Spinner & GOT Automatic Floorhand.

Rig Lighting Locations

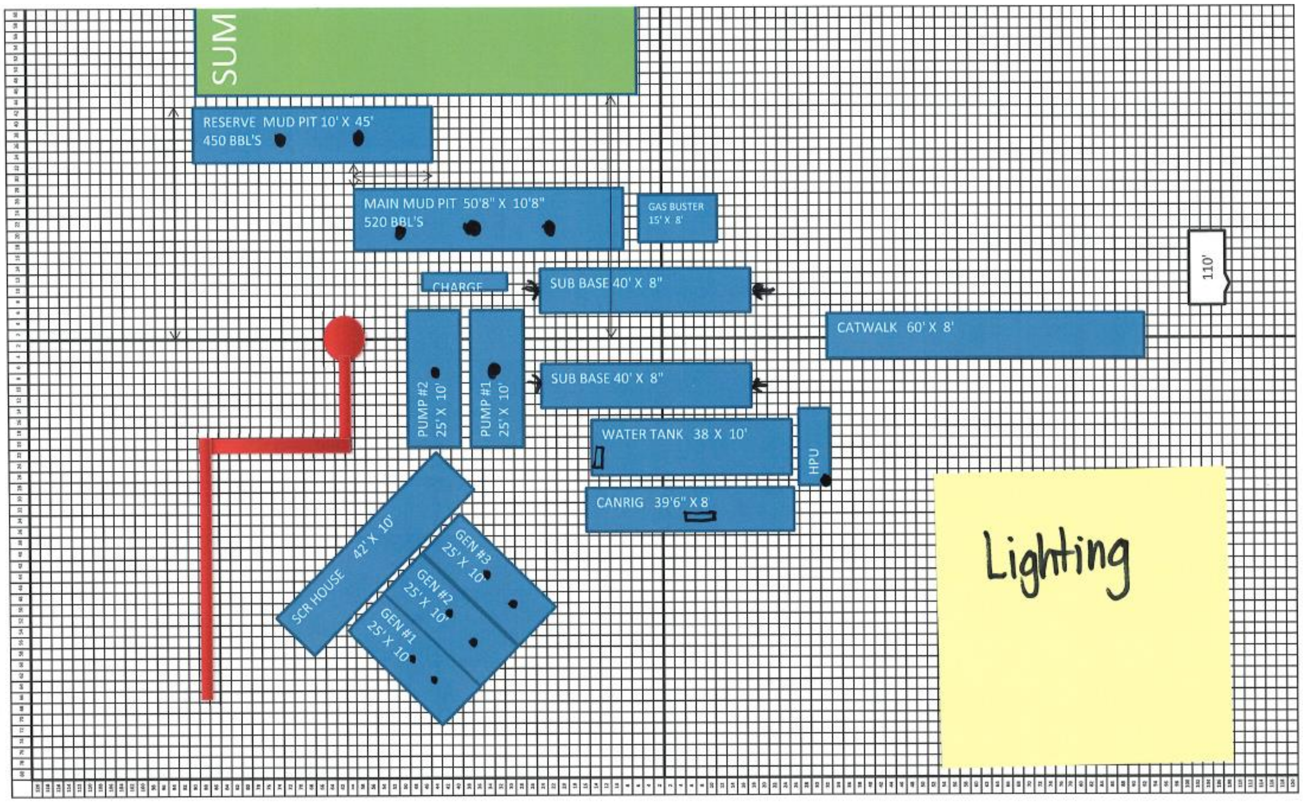

Ground-based Lighting Specifications

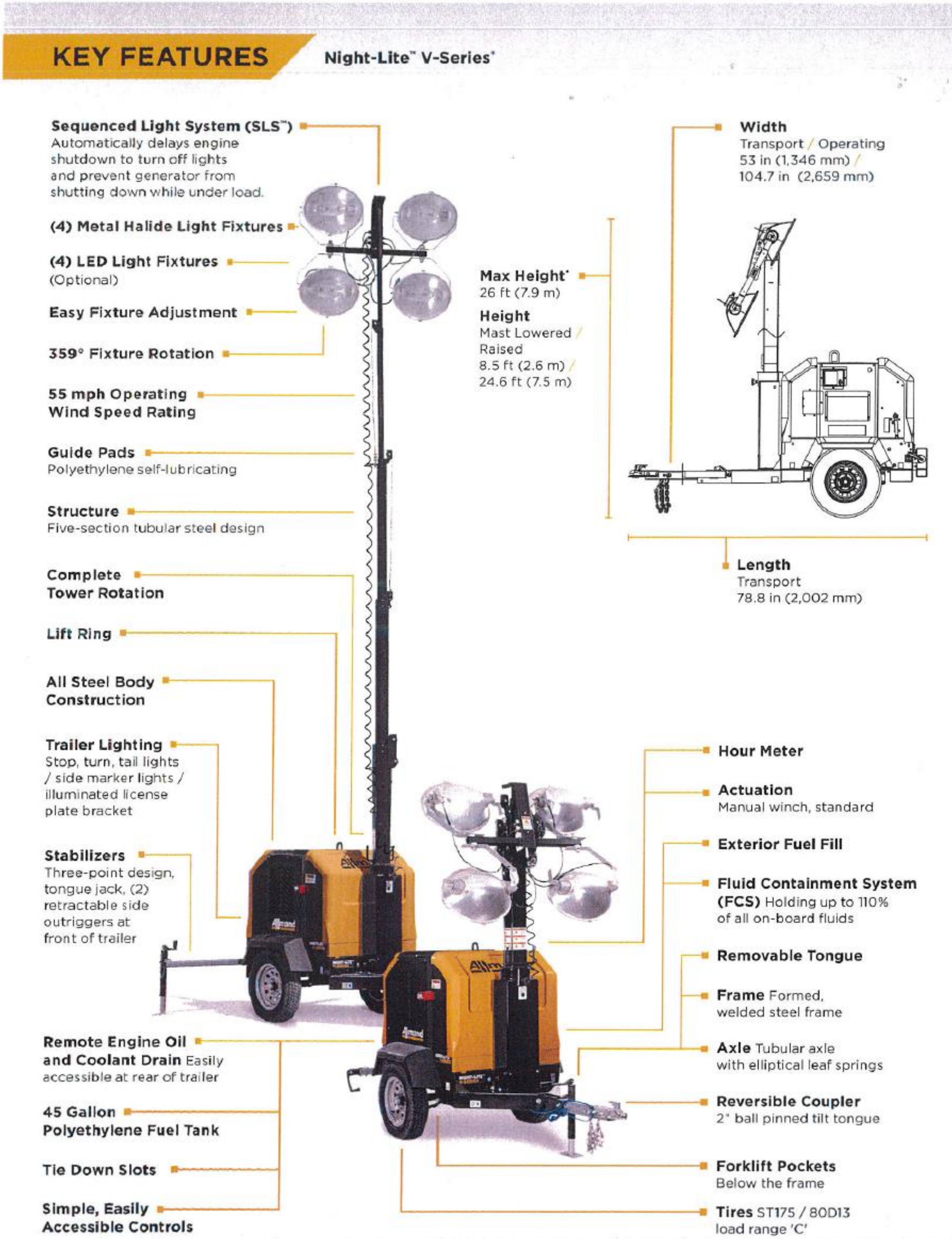

Night-Lite™ V-Series®

TECHNICAL SPECS

Model	~~NLV-ML3EC~~	NLV-K1005C	~~NLV-P11~~
Engine Brand / Model	~~Mitsubishi / L3E~~	Kubota / D1005	~~Perkins / 403D-11~~
Engine Prime Power (kW)**	~~6~~	7	~~8~~
Fuel Capacity gal (L)	~~45 (170.3)~~	45 (170.3)	~~45 (170)~~
Light Type - Metal Halide	(4) Metal Halide SHO-HD® fixture		
Metal Halide Wattage (per lamp)	~~1,250~~	1,250	~~1,250~~
Metal Halide Lumens (per lamp / total)	~~135,500 / 542,000~~	135,500 / 542,000	~~135,500 / 542,000~~
Operating Time (hrs)*** (Using four 1,250 W metal halide light fixtures)	~~75~~	72.6	~~75~~
Light Type - LED (Optional)	(4) Two LED, 5000°K color temperature		
LED Wattage (per lamp)	~~320~~	320	~~320~~
LED Lumens (per lamp / total)	~~38,500 / 154,000~~	38,500 / 154,000	~~38,500 / 154,000~~
Operating Time (hrs)*** (Using four 320 W LED light fixtures)	~~121.6~~	155.2	~~118.4~~
Features			
Outlets	Standard 20 A 120 VAC duplex GFCI / 30 A 240 VAC 4-Wire Twist Lock (NEMA L14-30R) / 30 A 120 VAC RV (NEMA TT-30R)		
Weights & Shipping			
Shipping Weight lbs (kg)	1,885 (855)		
Gross Vehicle Weight Rating (GVWR) lbs (kg)	2,200 (998)		
Shipping	18 units on a 48' flatbed trailer / 20 units on a 53' flatbed trailer		

LIGHT COVERAGE

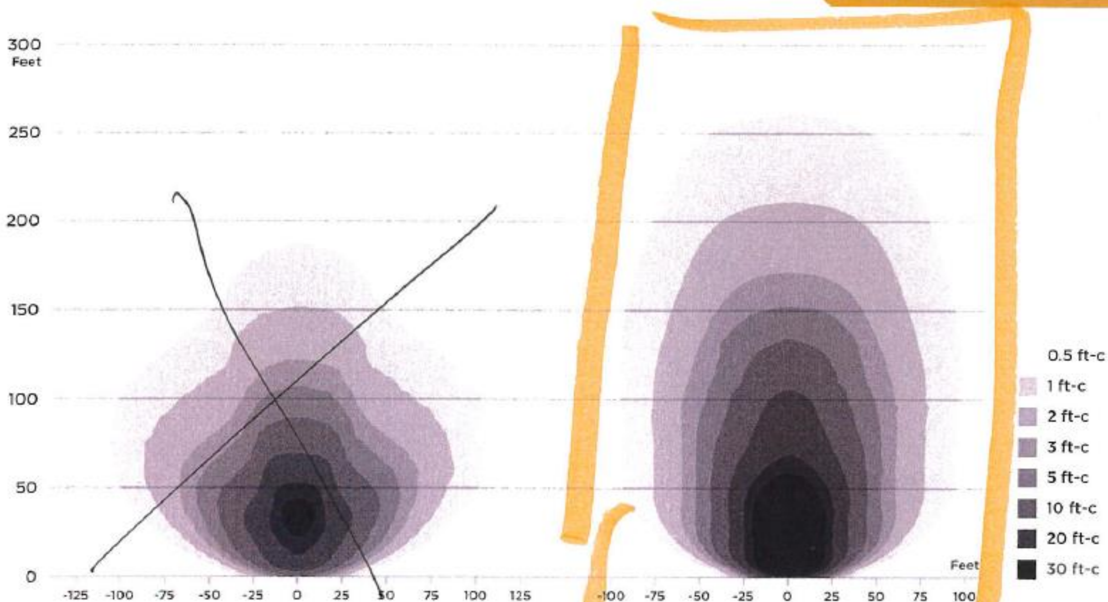

Night-Lite™ V-Series®
with 4 – 320 W Conssin LED Light Output
Area Lit to .5 Foot Candle (ft-c) or Higher: 28,449 ft²

Night-Lite™ V-Series®
with 4 – 1,250 W Metal Halide Light Output
Area Lit to .5 Foot Candle (ft-c) or Higher: 42,597 ft²

* Balloon light only included in raised dimension - balloon light is removed for transportation. ** Prime generator electrical output per Allmand® testing. *** Based on one hour run test full fuel tank consumption.
Allmand® has a policy of continuous product improvement and reserves the right to modify its specifications at any time and without prior notice. See operator's manual or www.allmand.com website for complete warranty details.